DOI:10.14753/SE.2014.1934

Examination of Thyrotropin-Releasing Hormone (TRH)-synthesizing System in the Rodent Hypothalamus

Ph.D. Thesis

Andrea Kádár

Semmelweis University
János Szentágothai Ph.D. School of Neuroscience

Tutor: Csaba Fekete D.Sc.

Opponents: Dóra Reglődi D.Sc.
Alán Alpár Ph.D.

Chairman of committee: György M. Nagy D.Sc.
Members of committee: Katalin Halasy D.Sc.
Zsuzsa Várnainé Tóth Ph.D.

Budapest
2014

DOI:10.14753/SE.2014.1934

I. Table of contents

DOI:10.14753/SE.2014.1934

DOI:10.14753/SE.2014.1934

DOI:10.14753/SE.2014.1934

II. List of abbreviations

α-MSH	- Alpha-melanocyte stimulating hormone
ABC	- Avidin-biotin-peroxidase complex
AGRP	- Agouti-related protein
ARC	- Arcuate nucleus
AVP	- Vasopressin
BAT	- Brown adipose tissue
BBB	- Blood-brain barrier
BSA	- Bovine serum albumin
BT	- Biotinylated tyramide
CART	- Cocaine- and amphetamine regulated transcript
CNS	- Central nervous system
CRE	- cAMP-response-element
CREB	- cAMP-response-element binding protein
CRH	- Corticotropin-releasing hormone
CSF	-Cerebrospinal fluid
D1	- Type 1 deiodinase
D2	- Type 2 deiodinase
D3	- Type 3 deiodinase
DAB	- Diaminobenzidine
DEPC	- Diethylpyrocarbonate
DMN	- Dorsomedial nucleus
EPSC	- Excitatory postsynaptic current
ERK	- Extracellular signal-regulated kinase
GFP	- Green fluorescent protein
GHRH	- Growth hormone-releasing hormone
GnRH	- Gonadotropin-releasing hormone
HPT axis	- Hypothalamus-pituitary-thyroid axis
icv.	- Intracerebroventricular
i.p.	- Intraperitoneal
IPSC	- Inhibitory postsynaptic current

IR	- Immunoreactive
KO	- Knock out
MC3-R	- Melanocortin receptor type 3
MC4-R	- Melanocortin receptor type 4
MCT8	- Monocarboxylate transporter type 8
MCT10	- Monocarboxylate transporter type 10
ME	- Median eminence
mTOR	- Mammalian target of rapamycin
NCoR1	- Nuclear receptor co-repressor 1
NHS	- Normal horse serum
NP	- Neurophysin
NPY	- Neuropeptide Y
OATP1C1	- Organic anion transporting polypeptide 1c1
OT	- Oxitocin
PBS	- Phosphate buffered saline
P-CREB	- Phosphorylated cAMP-response-element binding protein
PFA	- Paraformaldehyde
PI3K	- Phosphatidylinositol-3-kinase
PIF	- Prolactin-inhibiting factor
POMC	- Proopiomelanocortin
P-STAT3	- Phosphorylated signal transducer and activator of transcription 3
PVN	- Paraventricular nucleus
rT3	- Reverse triiodothyronin
RXR	- Retinoic X receptor
SCN	- Suprachiasmatic nucleus
SRC1	- Steroid receptor co-activator 1
SRIF	- Somatostatin
STAT3	- Signal transducer and activator of transcription 3
T2	- Diiodothyronin
T3	- Triiodothyronin
T4	- Thyroxine
TB	- Tris buffer

DOI:10.14753/SE.2014.1934

TH, THs	- Thyroid hormone, thyroid hormones
TR, TRs	- Thyroid hormone receptor, thyroid hormone receptors
TRα	- Thyroid hormone receptor alpha
TRα1	- Thyroid hormone receptor alpha type 1
TRβ	- Thyroid hormone receptor beta
TRβ1	- Thyroid hormone receptor beta type 1
TRβ2	- Thyroid hormone receptor beta type 2
TRE	- Thyroid hormone responsive element
TRH	- Thyrotropin-releasing hormone
TSH	- Thyroid stimulating hormone
UCP-1	- Uncoupling protein 1
VMN	- Ventromedial nucleus
vPVN	- Ventral paraventricular nucleus
WAT	- White adipose tissue
WT	- Wild type
Y1	- Neuropeptide Y receptor type 1
Y5	- Neuropeptide Y receptor type 5

DOI:10.14753/SE.2014.1934

III. Introduction

The hypophysiotropic TRH neurons are the main central regulators of the hypothalamus-pituitary-thyroid (HPT) axis [1]. These TRH neurons are located in the hypothalamic paraventricular nucleus (PVN) [2-4], integrate neuronal and humoral signals and serve as a final common pathway in the regulation of the hypothalamic-pituitary-thyroid axis [5]. The axons of the hypophysiotropic TRH neurons terminate outside the blood-brain-barrier (BBB) in the external zone of the median eminence (ME) where TRH is secreted to the portal capillary system of the anterior pituitary [6]. From these blood vessels, TRH enters to the extracellular space in the pituitary, and stimulates the synthesis and secretion of thyroid-stimulating hormone (TSH) [5], the hormone that regulates the hormone production of thyroid gland. Thyroid hormones (THs) have widespread biological actions including the regulation of energy metabolism through influencing the basal metabolic rate, adaptive thermogenesis and feeding behavior and regulation of the development and normal functioning of the central nervous system (CNS) [7-11].

1.Thyroid hormones: metabolism, signaling and effects

1.1. The metabolism of THs

Thyroid hormones - 3,3',5-triiodothyronin (T3) and thyroxine (T4) - are synthesized in the follicles of thyroid gland by iodination of tyrosine residues of thyroglobulin [12]. Although T4 is the predominant product of the thyroid gland, T3 is the form of thyroid hormones that can bind to thyroid hormone receptors with high affinity [13]. The activation of thyroid hormones by conversion of T4 to T3 and the degradation of these hormones are catalyzed by deiodinase enzymes [13, 14]. These enzymes are critical for the regulation of thyroid hormone levels in the circulating blood, but also for the tissue specific, local regulation of thyroid hormone availability [15].

All three known deiodinase enzymes (D1-3) are selenoproteins containing selenocysteine residue in their active site [16].

Type 1 deiodinase (D1) can remove iodine from both the inner and outer rings of THs, forming either T3 or the inactive reverse T3 (rT3) from T4 or convert T3 to the inactive diiodothyronin (T2) [14, 16]. Since this enzyme can both activate and inactivate thyroid

hormones, it has the least clear physiological role in the deiodinase protein family. Because D1 is able to convert T4 to the considerably active T3, initially it was thought to be the main source of extra-thyroidal T3 [16, 17]. Recently, however, increasing evidence indicates that D1 contributes significantly to the circulating T3 concentration only in hyperthyroid patients, but not in healthy subjects [18, 19]. Therefore, currently D1 is considered a thyroid hormone inactivating enzyme in euthyroid conditions by producing inactive rT3 or T2 [14]. The liver and kidney, where D1 participates in the clearance of TH derivatives, contains a relatively large concentration of this enzyme, but D1 is also present in the anterior pituitary, intestine, placenta and thyroid gland [16, 20]. In rats, D1 is also present in the cerebral cortex with relatively low activity, but in humans, D1 is absent from the CNS [21, 22].

The main source of extra-thyroidal T3 is type 2 deiodinase (D2) that converts T4 to T3 by 5'-monodeiodination of the outer ring of the molecule [14, 18]. In addition to regulating circulating T3 concentration, this deiodinase enzyme also plays critical role in the organ specific regulation of T3 availability [15]. Although the adequate level of T3 is essential for the sufficient neuronal activity, T3 can be transported through the BBB remarkably less efficiently than T4 [23]. More than 75% of T3 in the cortex is generated locally by D2 catalyzed conversion of T4 to T3 [24]. In human D2 is the only 5' deiodinase in the brain [15]. In accordance with this cardinal role, D2 has a widespread expression in the brain [15, 16]. D2 is expressed predominantly in glial elements of the neuronal tissue, such as tanycytes and astrocytes [25]. These glial cells have crucial role in the maintenance of the adequate T3 level in the CNS [25]. Tanycytes are specialized ependymal cells located in the basal and lateral walls of the third ventricle in the hypothalamus [26]. Hypothalamic D2 expression is concentrated in the median eminence and arcuate nucleus, where D2 is expressed primarily in tanycytes [14]. D2 activity is absent from most hypothalamic regions including the PVN where the hypophysiotropic TRH neurons reside [27]. This distribution of D2 is in contrast with the homogenous D2 expression of astrocytes in other brain regions [27-29]. D2 can also be found at high levels in the pituitary, brown adipose tissue (BAT) and placenta and also occurs in the gonads, pineal gland, thymus, mammary gland, coronary artery and smooth muscle cells of the aorta [15, 16].

In contrast to the role of D2, the primarily function of the type 3 deiodinase (D3) is the local inhibition of TH signalization by inactivation of THs. D3 performs inner ring deiodination converting T4 to rT3 and T3 to T2 [15, 16]. This deiodinase enzyme is primarily expressed in neurons in the CNS where D3 plays an important role by protecting neurons from the excess of T3 [14, 30]. In the brain, D3 mRNA can be observed widely in the cerebral cortex, hippocampal pyramidal cells, granule cells of the dentate and pyriform cortex. In addition, lower level of D3 expression can be found in hypothalamic neurons [15, 16, 31]. Although the main function of D3 is to protect tissues from excess THs, the systemic administration of thyrotoxic doses of T3 induces a surprisingly modest increase in D3 expression of the hypothalamus. This finding is in contrast with observations in other brain regions such as the cortex, the hippocampus and the olfactory bulb [31]. Hence, hypothalamic deiodinase enzymes appear to convert the changes of peripheral THs to changes of hypothalamic T3 concentration allowing T3 to serve as a regulatory signal for neuroendocrine functions [14]. Besides its presence in the CNS, a remarkable amount of D3 is also expressed in most of the fetal organs and placenta, confirming the essential role of this enzyme in the precise regulation of the TH level during embryonic development [32].

1.2. The transport of THs

Although THs are lipid soluble molecules, their passage through the cell membranes and the BBB requires specific transporter molecules [33]. The transport of THs is facilitated by at least three transporter molecules: organic anion transporting polypeptide 1c1 (OATP1C1), monocarboxylate transporter 8 (MCT8) and 10 (MCT10) [34].

OATP1C1, a member of the organic anion transporting family, is highly specific for T4, rT3 and T4 sulfate [35, 36]. It binds T3 with much lower affinity [35, 36]. The presence of OATP1C1 has been described in Leydig cells of the testis and in the capillaries of the brain [37-39]. In the rodent brain, OATP1C1 is highly expressed in cerebral microvessels underlining its cardinal role in the TH transport through the BBB [40]. OATP1C1 is also expressed in hypothalamic tanycytes [40].

The most studied TH transporter is MCT8, a member of the monocarboxylate transporter family with 12 helical transmembrane domains [34]. This transporter molecule has strong affinity for T3, T4 and rT3 [41]. MCT8 is expressed in various

tissues including heart, liver, kidney, adrenal and thyroid gland [42, 43]. MCT8 is also present in most areas of the CNS, such as hypothalamus, choroid plexus, amygdala, hippocampus, olfactory bulb and cortex [40, 44-46]. Although MCT8 is the main TH transporter of neurons it can also be found in tanycytes [45]. The importance of MCT8 in normal neurological function is underlined by the demonstration of the mutation of this gene in families with inherited mental retardation and underdevelopment [47, 48]. The syndrome caused by this mutation is called Allan-Herndon-Dudley syndrome, which has typical endocrine abnormalities in addition to the strong neurological phenotype: elevated serum T3 and reduced T4 and rT3 levels [49]. Although Mct8 knock out (KO) mice have the same alteration in the level of THs, interestingly no major neurological abnormalities were found in these animals [50, 51] that suggests species-specific differences in the neuronal transport of THs and raises the possibility that in rodents, MCT8 is not the only neuronal thyroid hormone transporter.

The amino acid sequence of MCT10 shows great degree of homology with MCT8 [34]. Although data about its physiological function is limited, cell culture studies demonstrate that MCT10 prefers T3 instead of T4 [52]. This TH transporter molecule is expressed in the intestine, kidney, liver, muscle and placenta, but there is no data that confirms its presence in the CNS [53-56].

1.3. TH receptors and signalization

The thyroid hormone receptors (TRs) are located in the nucleus of cells and act on thyroid hormone response elements (TRE) of DNA as ligand-dependent or independent transcription factors [57, 58]. All the known types of TRs are encoded by two genes: *THRA* and *THRB* [58]. Alternative splicing of the *THRA* transcript results in different TRα isoforms, but only TRα1 acts as a functional receptor [59]. The other TRα variants seem to have inhibitory effect on TH induced gene expression in *in vitro* studies [59]. The THRB gene also has two products: TRβ1 and TRβ2 [58]. Both of these receptors are functional receptors and differ in the transcription initiation site, which results in different amino end of the two TRβ isoforms [60]. The distribution of TRα1 and TRβ1 is widespread, whereas TRβ2 is expressed predominantly in TRH neurons of the PVN and in thyrothrop cells in the anterior pituitary [60-63]. Examination of TRβ KO and TRβ2

KO animals confirms that the TRβ2 receptor plays a crucial role in mediating the negative feedback effect of THs on TRH and TSH synthesis [64, 65].

The thyroid hormone regulated genes can be divided into two main categories: positively and negatively regulated genes. The mechanisms of positive and negative regulation of thyroid hormone responsive genes is markedly different. The effect of T3 on the positively regulated genes is mainly mediated by the heterodimer complex of a TR and retinoic X receptor (RXR) [66]. The TR-RXR complex is fully active when not only T3 binds to TR, but 9-cis retinoic acid also binds to the RXR component of the heterodimer [67]. The transcriptional initiation of positively regulated genes is facilitated by the recruitment of co-activator molecules to the ligand bound TR-RXR complex [58, 60]. In the absence of T3, the unliganded TR-RXR heterodimer complex is also associated with TRE, however, in the absence of T3, TRs recruit co-repressor proteins mediating the basal, ligand independent repression of the target genes [68, 69].

In contrast, the transcriptional activity of genes negatively regulated by T3 is stimulated by the complex of the unliganded receptor and the co-repressor molecules, while the liganded receptor-co-activator complex suppresses these genes [65]. Although, it was debated for years, the action of TRs on the negatively regulated genes also appears to require direct binding of the receptor to the TRE of genes [70-72]. The typical co-activator molecule, steroid receptor co-activator 1 (SRC1) has inhibitory effect on the HPT axis [73] while the co-repressor molecule, nuclear receptor co-repressor 1 (NCoR1) is required for the ligand independent activation of the HPT axis [74, 75].

1.4. Effects of THs

Thyroid hormones can influence a variety of tissue types. They regulate the embryonic neurogenesis, the migration of pyramidal cells in the cerebral cortex [11, 76-79], granule cells in the hippocampal gyrus dentatus [80-82] and Purkinje cells in the cerebellum [83, 84]. Furthermore, they have effects affect on axonal growth [85] and dendritic arborization [86, 87]. THs also influence learning and memory in adults [88, 89] and influence wakefulness [90] and mood [91]. In addition, THs influence energy homeostasis via increasing the basal metabolic rate [10], stimulating the diet-induced [92] and adaptive thermogenesis [93], facilitating lipogenesis [94, 95] and increasing food intake [95].

One of the major effects of THs on energy expenditure is the stimulation of basal metabolic rate. In cells regulated by THs, the basal metabolic activity is stimulated by the increased number and size of the mitochondria, the increased expression of the respiratory chain components, and the increased membrane permeability for Na^+ and K^+, and the increased concentration of the Na^+/K^+ ATP-ase in the membrane [96].

Thyroid hormones also increase the energy expenditure by stimulating the thermogenesis in the BAT [97, 98]. The heat production of BAT requires sympathetic activation [97, 98], thyroid hormones [93] and local activation of T4 by D2 [99]. The synergistic effect of the adrenergic stimulation via β adrenergic receptors and the locally generated T3 result in increased uncoupling protein 1 (UCP-1) synthesis and thermogenesis [99, 100]. Without thyroid hormones or D2, sympathetic activity is unable to increase UCP-1 synthesis and thermogenesis [99]. During cold exposure, the marked increase of D2 expression also plays a critical role in the local increase of T3 concentration in the BAT. This virtually saturates all TRs in this tissue, allowing thus the cold induced thermogenesis of the BAT to be fully active even if circulating thyroid hormone levels are slightly above normal [99]. The increased UCP-1 level interrupts the connection between the respiratory chain and ATP synthesis. This way, most of the energy released by substrate oxidation dissipates as heat [8].

2. Hypophysiotropic TRH neurons

The primary central regulator molecule of thyroid hormone synthesis is TRH, a tripeptide amide (pGlu-His-ProNH2) [1]. In the anterior pituitary, TRH stimulates the synthesis and release of TSH by acting on the G protein coupled type 1 TRH receptor [101]. In addition, TRH increases the posttranslational glycosylation of TSH, which has an important effect on the biological activity of the molecule [102, 103]. The secreted TSH then acts on the thyroid gland and regulates its hormone production [104]. Neutralization of endogenous TRH by administration of anti-TRH serum induces transient reduction of circulating level of TSH and THs [105, 106]. In newborn TRH KO mice, no difference can be observed neither in the morphology of anterior pituitary nor in the synthesis of THs at birth compared to wild type (WT) mice [107, 108]. However, the gradual increase of the TH levels observed during the first postnatal days in WT animals is absent in the TRH KO mice [107, 108]. Furthermore, the lack of TRH causes a

dramatic decrease in the number of the TSH-immunoreactive (-IR) cells in the anterior pituitary and also in the TH levels after the 10th postnatal day [107, 108]. These observations suggest that TRH has an essential role in the early postnatal development of the HPT axis and also in the maintenance of the activity of this neuroendocrine axis in adult animals. The critical importance of TRH in the regulation of the HPT axis is also demonstrated in some human patients with idiopathic central hypothyroidism [109]. In these patients the release of biologically inactive TSH is accompanied by low circulating levels of THs [109]. This clinical picture can be cured with chronic intravenous TRH administration [109], further demonstrating the key role of TRH in the central regulation of the HPT axis.

TRH is widely synthesized throughout the CNS [5], but only the so called hypophysiotropic TRH neurons that project to the external zone of the median eminence and secret the TRH into the portal capillary are involved in the regulation of HPT axis [3, 6]. These neurons are located in the PVN, a bilateral triangle-shaped nucleus in the dorsal margin of the third ventricle. The PVN can be divided into two main divisions named based on the size of their neurons: the parvocellular and magnocellular divisions. In rats, the parvocellular division can be further divided into six subdivisions: the anterior, medial, dorsal, periventricular, ventral and lateral subdivisions (fig.1.) [110]. TRH-synthesizing neurons can be found in all parvocellular subdivisions in rats [111], but the hypophysiotropic TRH neurons are located exclusively in the periventricular and medial parvocellular subdivisions (fig.1.) [2, 3, 6, 111]. In rats, a distinctive feature of the hypophysiotrophic TRH neurons is their cocaine- and amphetamine regulated transcript (CART) expression; this peptide has not been identified in any other TRH-expressing neuron population of the brain [2, 3, 6, 111]. Although the localization of the hypophysiotropic TRH neurons is precisely determined in rats, limited information is available currently about the distribution of these neurons in mice, the most frequently used animal model of the current days.

3. The negative feedback regulation of the hypophysiotropic TRH neurons by THs

Since the maintenance of normal thyroid hormone levels is critical for the appropriate functioning of the organism, the activity of both the hypophysiotropic TRH-producing neurons and the TSH-expressing cells of the anterior pituitary are tightly regulated by the

negative feedback effect of THs [60] (fig.2.). Hence, under basal conditions the rise of TH levels inhibits TRH and TSH expression. In contrast, the fall in circulating TH levels has stimulatory effect on TRH and TSH secretion. [112]. In the CNS, the TRH gene expression is controlled by the negative feedback effect of thyroid hormones only in the hypophysiotropic TRH neurons [113]. The observation that T3 administration to the PVN of hypothyroid animals results in a decrease of the TRH expression exclusively in the side of the implantation verifies that THs have direct effect on TRH neurons [114]. The negative feedback effect of THs on TRH expression is mainly mediated by TRβ2 [64], although results of studies using siRNA mediated TRβ1 gene silencing suggest that TRβ1 also contributes to the ligand independent activation of TRH gene expression [115]. Interestingly, hypophysiotropic TRH neurons also express TRα1 which has stimulatory effect on TRH expression in the presence of T3 [65]. However, this TRα1-mediated effect is masked by the inhibitory effect of TRβ receptors in adult animals [65, 116]. In addition to the direct effect of THs on the TRH gene, THs also modulate TRH production by the downregulation of prohormone convertases type 1/3 and 2, resulting in accumulation of immature proTRH derivatives and a decrease in the production of mature TRH molecules [117].

DOI:10.14753/SE.2014.1934

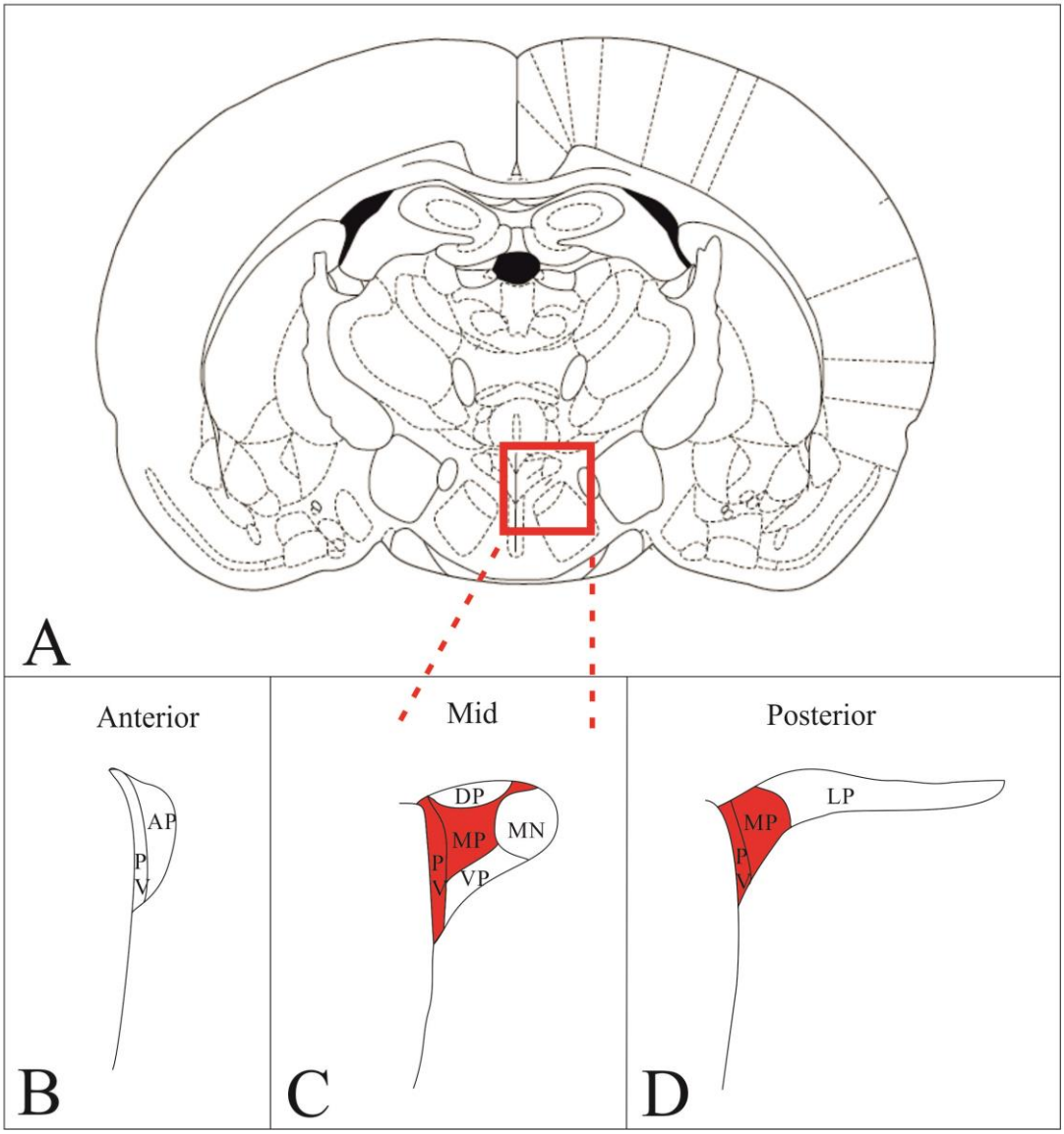

Figure 1. Schematic drawing illustrates the organization of the PVN in rats and the localization of the hypophysiotropic TRH neurons. The higher magnification maps based on the figures of Fekete et al. [112] show the subdivisions of rat PVN in three different antero-posterior levels (B-D). Red areas indicate the presence of hypophysiotropic TRH neurons. TRH neurons with hypophysiotropic function are absent from the anterior level (B), but present in the medial and periventricular subdivisions of the mid (C) and posterior (D) levels of PVN.

MN – magnocellular division

Parvocellular subdivisions:

PV – periventricular; AP – anterior; VP – ventral; MP – medial; DP – dorsal; LP - lateral

DOI:10.14753/SE.2014.1934

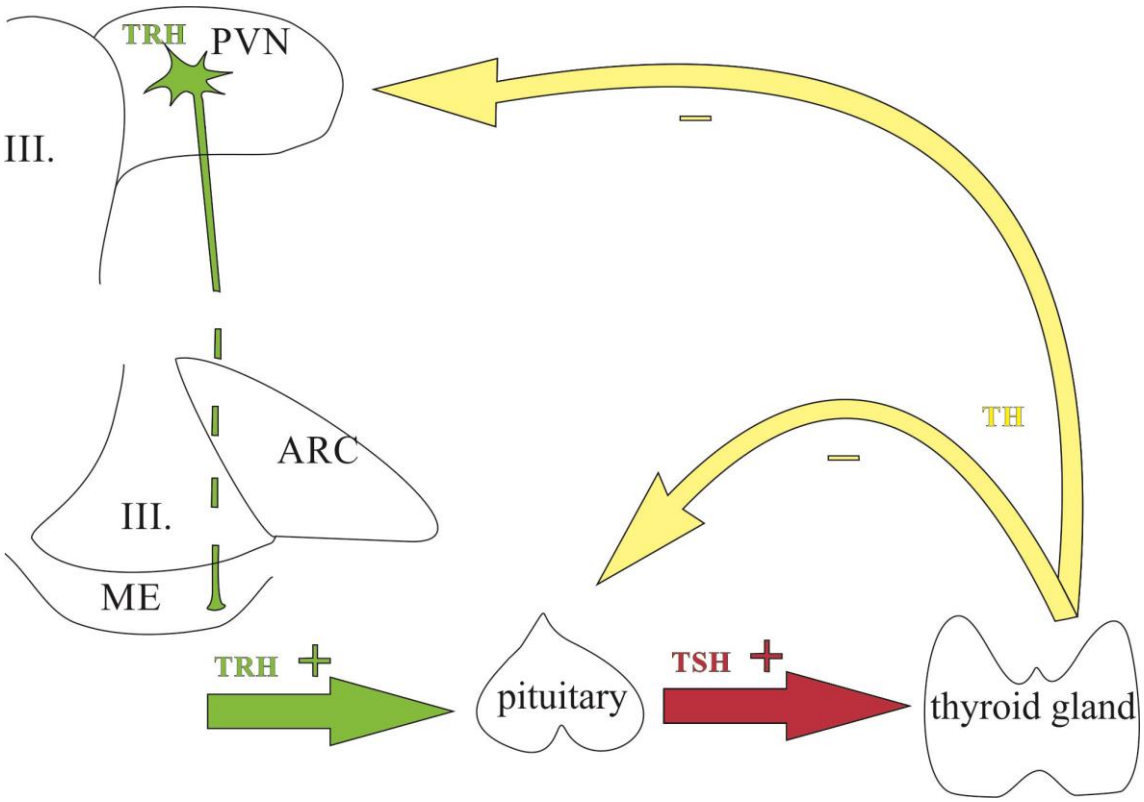

Figure 2. Schematic illustration of the hypothalamus-pituitary-thyroid axis.
Cell bodies of the hypophysiotropic TRH neurons are located in the PVN and their axons terminate in the ME where TRH is released to the circulation. TRH reaches the anterior pituitary through the hypophysial portal system and stimulates the TSH secretion. TSH stimulates the T3/T4 production of the thyroid gland. THs exert negative feedback effect both on the hypophysiotropic TRH neurons and the thyrotrop cells of the anterior pituitary.

4. Tanycytes: location in the ME and role in the regulation of the HPT axis

4.1. The structure of the ME

The release of the hypophysiotropic hormones into the circulation occurs in the BBB-free ME, where the axons of the hypophysiotropic neurons terminate [118]. The ME can be divided into three parts: ependymal layer, internal and external zones [119]. Hypophysiotropic neurosecretory cells, such as TRH-, corticotropin-releasing hormone (CRH)-, gonadotropin-releasing hormone (GnRH)-, prolactin-inhibiting factor- or dopamine (PIF)-, growth hormone-releasing hormone (GHRH)- and somatostatin

(SRIF)-producing neurons release their substances in the densely vascularized external zone of the ME [3, 6, 118, 120-124]. The hormones secreted by hypophysiotropic neurons to the capillary loops are transported directly to the anterior pituitary by its long portal vascular system [125]. The internal zone of the ME contains the axons of the magnocellular neurosecretory cells, these vasopressin (AVP)- and oxytocin (OT)-containing axons pass through the ME and terminate in the posterior pituitary where the hormones are secreted to the circulation [126, 127]. The ependymal layer that forms the floor and ventrolateral walls of the third ventricle contains the cell bodies of specialized glial cells called tanycytes [26]. These glial cells has essential role in the regulation of HPT axis [5].

4.2. Tanycytes

Tanycytes are elongated glial cells with cell body located in the ependymal layer [26]. Tanycytes contact the cerebrospinal fluid (CSF) with their surface covered with microvilli and has a long basal process to the median eminence or to discrete hypothalamic areas [26].

Four subtypes of tanycytes (α1-2, β1-2) can be distinguished based on their location, morphology and function [26, 128].

α-tanycytes line the lateral walls of the third ventricle [26, 128]. The basal process of α1-tanycytes project to the hypothalamic ventromedial (VMN) and dorsomedial nuclei (DMN) where they terminate on neurons while α2-tanycytes send their process to the neurons and/or capillaries of the arcuate nucleus (ARC) and the lateral part of the tuberoinfundibular sulcus [26, 128].

β-tanycytes line the floor of the third ventricle; β1-tanycytes are located in the lateral envaginations of the third ventricle and project to the tuberoinfundibular sulcus terminating on the surface of the pars tuberalis of the pituitary [26, 128]. β2-tanycytes which form the ventral wall of the third ventricle send their basal process to the portal capillary system in the median eminence [26, 128] where the axons of the hypophysiotropic neurons terminate to release their neurohormones into the hypophysial portal circulation [118] (fig. 3.).

A characteristic property of β-tanycytes is their involvement in barrier formation. β1-tanycytes form a barrier between the arcuate nucleus and the BBB free median eminence

[129] while β2-tanycytes establish a barrier between CSF and the neuropil of the median eminence [26]. β1-tanycytes are linked together by zonulae adherentes and maculae adherentes, whereas β2-tanycytes are joined together by tight junctions and zonulae adherentes [26].

An important feature of tanycytes is that they establish connection with the CSF and also with blood vessels [26]. Therefore, the tanycytes are in the anatomical position to sense the alterations in the composition of the CSF, but also the changes in the level of blood-born substances [26].

4.3. The role of tanycytes in the regulation of hypothalamic T3 homeostasis

Increasing amount of data suggest that the tanycytes are not only supportive and BBB forming cells, but they also play a major role in the regulation of neuroendocrine axes [26]. The β2 tanycytes can inhibit the secretion of neuroendocrine hormones by blocking the access of hypophysiotropic terminals to the fenestrated capillaries of the median eminence [130]. The coverage of the portal capillaries by the end feet of β2-tanycyte processes is variable and depends on the physiological conditions [130, 131]. By this plasticity tanycytes can separate the axon terminals from the capillaries or, to the opposite, they can allow access of the terminals to the surface of blood vessels [130]. The most studied example for the tanycyte remodeling is the regulation of the access of GnRH nerve terminals to the portal capillaries during the different phases of the estrous cycle. In proestrus, GnRH axons terminate in the pericapillary space, resulting in massive GnRH release [130]. In contrast, in diestrus, tanycyte end feet separate the GnRH axon terminals from the portal capillaries, contributing to a decreased secretion of GnRH [130]. Changes in peripheral TH levels also induce remodeling of the end feet of tanycyte processes around the capillaries [131]. This observation suggests that tanycytes may also regulate the access of the hypophysiotropic TRH neurons to the capillaries and the release of TRH to the circulation.

The importance of tanycytes in the regulation of the HPT axis is further supported by the data that these glial cells express a number of proteins which are involved in the hypothalamic TH metabolism and signaling and have regulatory effect on the HPT axis. These proteins include TRβ2 [132], the TH transporter OATP1c1 and MCT8 [40, 133], D2 that has capability to convert T4 to the active TH form [27, 29, 134], T3, and D2

inactivating WSB-1 and reactivating USP-33 enzymes [135]. The role of D2 in the regulation of HPT axis is underlined by the fact that the restoration of peripheral T3 level in hypothyroid rats by administration of T3 without addition of T4 is unable to decrease TRH gene expression to euthyroid level [136], although T3 is the predominant form of THs that acts on TRs [13]. This observation can be explained by the fact that T3 is poorly transported to the brain [35, 36], and the majority of hypothalamic T3 is produced locally from T4 by D2 [16]. Although the main hypothalamic sources of D2 are tanycytes, D2 can also be found in some hypothalamic astrocytes [25]. Interestingly, astrocyte specific D2 knock out mice show no disturbance in the negative feedback regulation of TRH, suggesting that astrocytes do not play a role in the negative feedback effect of THs on TRH neurons [25]. In addition, in the hypothalamus, hypothyroidism induces only slight increase of D2 expression and no rise of D2 activity [27, 137], suggesting that hypothalamic D2 does not compensate the changes in the circulating level of THs. Therefore, the changes of peripheral T4 levels are converted into changes of hypothalamic T3 concentration that is critical for the feedback regulation of TRH neurons. [14]. Although it is clear that the D2-containing tanycytes are the principal source of T3 acting on hypophysiotrophic TRH neurons [14], it has not been clarified yet how T3 is transported from the tanycytes to the nucleus of the hypophysiotropic neurons in the PVN. The perikarya of hypophysiotropic TRH neurons are located far from the tanycytes; therefore, volume transmission between the tanycytes and the TRH neurons would be a relatively slow process. In contrast, the tanycyte end feet and the terminals of the TRH neurons are closely associated in the external zone of the ME [26]. We have recently hypothesized that T3 produced by tanycytes may be taken up by axon terminals of these neurosecretory neurons in the ME and transported retrogradely to the nucleus of these cells.

DOI:10.14753/SE.2014.1934

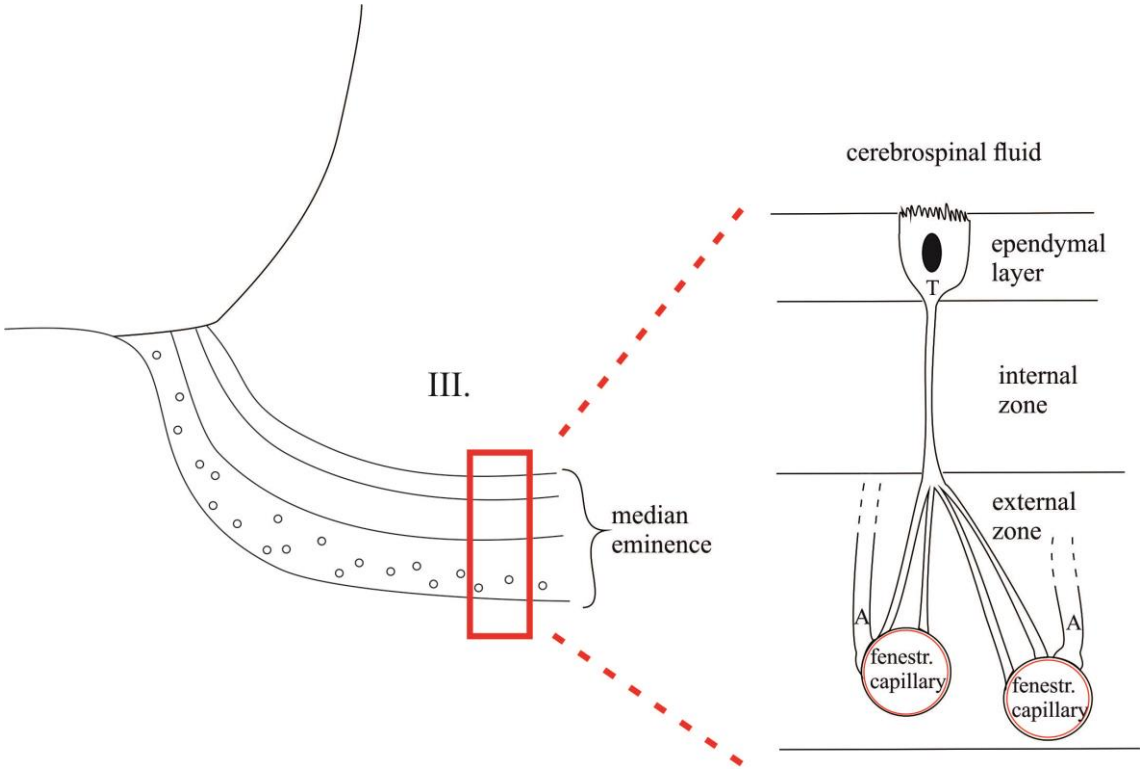

Figure 3. Schematic drawing presents the location of β2-tanycytes in the median eminence.

The cell bodies of β2-tanycytes can be found in the ventral and ventro-lateral walls of the third ventricle, but they send processes to the capillary loops in the external zone of median eminence. Tanycytes are able to take up substances from both the blood flow and the CSF and actively influence the composition of the CSF.

III – third ventricle; T – β2-tanycyte; A – axon terminal of hypophysiotropic neurons.

5. Neuronal inputs of hypophysiotropic TRH neurons

In addition to receiving humoral inputs, the TRH expression of hypophysiotrophic neurons is also regulated by neuronal inputs to adapt the HPT axis to the changing internal and external milieu. The hypophysiotropic TRH neurons integrate neuronal inputs from various areas of the central nervous system [5]. The most extensively studied and best-known sources of this innervation are the catecholaminergic cell groups of the brainstem, the hypothalamic arcuate nucleus (ARC) and the DMN [5].

5.1. Catecholaminergic neurons of the brainstem

Approximately 20% of the synapses on TRH neurons originate from the catecholaminergic neurons of the brainstem [138], indicating the critical importance of this input in the regulation of HPT axis. These axons mainly form asymmetric synapses on the surface of hypophysiotropic TRH neurons which is indicative of the excitatory function of these inputs [139]. Two types of catecholaminergic neurons innervate the hypophysiotropic TRH neurons which can be distinguished by their neurotransmitter content: adrenergic and noradrenergic neurons [140]. Approximately two thirds of the catecholaminergic innervation is adrenergic and one third is noradrenergic [140]. Adrenergic inputs originates from the C1-3 regions of the medulla whereas the noradrenergic innervation of TRH neurons arrives primarily from the A1 and A6 areas of the brainstem [141]. The catecholaminergic input of TRH neurons has been shown to mediate the cold induced upregulation of the HPT axis [5]. In cold environment, TRH gene expression is rapidly and transiently increased in the PVN, which, in turn, causes increased peripheral TSH and TH levels [142]. This activation of the HPT axis can be important in the stimulation of thermogenesis in the brown adipose tissue to prevent the drop of body temperature [5]. The cold induced activation of the hypophysiotropic TRH neurons is mediated by the catecholaminergic neurons of the medulla, as it can be inhibited by intraventricular administration of α-adrenergic antagonists [143]. Furthermore, the cold induced activation of the HPT axis is absent in rats during the first ten postnatal days when the catecholaminergic innervation of TRH neurons is immature [144]. The activation of the catecholaminergic inputs results in a shift in the set point of the negative feedback regulation of the hypophysiotropic TRH neurons in a way that higher thyroid hormone levels are necessary to suppress the TRH gene expression [5]. These changes lead to the development of central hyperthyroidism in cold environment.

5.2. Arcuate nucleus

At least two separate neuron populations of the ARC send projections to TRH neurons to mediate metabolic signals from the blood to the PVN (fig.4). These two neuron populations can be distinguished by their neuropeptide content: while one of these neuronal populations synthesizes α-melanocyte stimulating hormone (α-MSH) and cocaine- and amphetamine regulated transcript (CART), the other neuronal group

produces agouti-related protein (AGRP) and neuropeptide Y (NPY) [5, 145]. While both cell groups are capable of detecting satiety signals, they are regulated oppositely by these signals and they exert antagonistic effects on the hypophysiotropic TRH neurons [5, 145].

5.2.1. The anorexigenic neuronal population of the ARC

One of the feeding related neuronal groups of the arcuate nucleus synthesizes two anorexigenic peptides, α-MSH and CART [146, 147]. These neurons are primarily located in the lateral part of the arcuate nucleus and have crucial role in the regulation of energy homeostasis [145]. Intracerebroventricular (icv.) administration of α-MSH or CART markedly inhibit food intake and stimulate energy expenditure [148, 149]. α-MSH exerts its central effects on the energy homeostasis via two G protein coupled receptors, the melanocortin 3 and 4 receptors (MC3-R and MC4-R) [150, 151]. Binding of α-MSH to either MC3-R or MC4-R induces cAMP mediated signaling [152] which results in rapid phosphorylation of the cAMP-response-element binding protein (CREB) [153]. The phosphorylated CREB (P-CREB) binds to the cAMP response element (CRE) in the promoter of the regulated genes [153].

The signaling pathway of CART is less understood, because of the failure of previous studies to identify the CART receptor. However, several second messenger systems were identified that might mediate the effects of CART on the target cells. In CRH neurons, CART can induce CREB phosphorylation [154]. In the hippocampus, CART inhibits voltage-dependent intracellular Ca^{2+} signaling probably through the inhibition of L-type voltage-gated Ca^{2+} channel activity via a G protein dependent pathway [155]. In addition, in cell culture of AtT20 and PC12 cells, CART induces the phosphorylation of Extracellular Signal-Regulated Kinase (ERK) [156, 157]. It seems possible that CART also acts via a G-protein coupled signaling pathway.

In addition to the anorexigenic effect of the centrally administered peptides, the role of α-MSH and CART in the regulation of energy homeostasis is also supported by the phenotype of transgenic animals. The lack of α-MSH caused by the mutation of its precursor proopiomelanocortin (POMC) gene results in hyperphagia and morbid obesity in transgenic mice [158, 159]. This phenotype is caused by the combined effect of the increased food intake and the decreased energy expenditure of these animals [158, 159]. A highly similar phenotype was also discovered in humans due to the mutation of the

POMC gene [160]. Mutation of the MC4-R also results in morbid obesity in both mice and humans [161]. Indeed, the most frequent monogenic cause of morbid obesity is the mutation of this receptor [162]. The absence of CART in KO mice results in less profound phenotype in young animals, but these animals also develop obesity when they are older [163]. The importance of the α-MSH/CART neurons in body weight regulation gains further support from the observation of obesity following the ablation of POMC neurons in adult animals [164].

The α-MSH/CART neurons express receptors for circulating metabolic signals including glucose, insulin and leptin, and the activity of these neurons is regulated by nutritional conditions [165]. The activity of the α-MSH/CART neurons and the synthesis of α-MSH in these cells are markedly stimulated by both insulin and leptin [165]. Leptin also increases the synthesis of CART [165]. During fasting, when circulating levels of leptin and insulin fall, α-MSH neurons are inhibited and the α-MSH and CART synthesis is repressed [165]. In contrast, leptin administration can prevent this fasting induced inhibition of the α-MSH/CART neurons [165].

In the rat PVN, about 70% of TRH neurons in the periventricular parvocellular subdivision and 34% in the medial parvocellular subdivision are innervated by α-MSH/CART neurons [166]. The axon terminals of anorexigenic neurons of the ARC typically form asymmetric synapses on the surface of TRH neurons, suggesting that these neurons have stimulatory effect on the TRH neurons [2]. Indeed, central administration of both α-MSH and CART have stimulatory effect on the TRH gene expression in the PVN [2, 149, 166, 167]. Icv. administration of α-MSH or CART to fasted rats stimulates TRH synthesis [2, 166].

In the hypophysiotropic TRH neurons, α-MSH acts predominantly on type 4 melanocortin receptor (MC4-R) [168] and induces a cascade that results in P-CREB binding to the CREB response element (CRE) of the TRH gene promoter [169]. This P-CREB binding contributes to the stimulation of TRH gene expression in hypophysiotropic neurons [169, 170]. Indeed, mutation of the CRE element in the TRH promoter can block the stimulatory effect of α-MSH on this promoter [170].

CART has a very similar stimulatory effect on hypophysiotropic TRH neurons [2]. However, the effect of CART seems to be mediated by different second messenger

pathway as central CART administration does not induce CREB phosphorylation in hypophysiotropic TRH neurons [154].

5.2.2. The orexigenic neuronal population of the ARC

The medially located feeding related neuron population of the ARC expresses two orexigenic peptides, neuropeptide Y (NPY) and agouti-related protein (AGRP) [5]. This neuron population stimulates food intake and decreases energy expenditure [171]. The central administration of AGRP or NPY has potent orexigenic effect [171]. In the hypothalamus NPY acts on Y1 and Y5 receptors [172] which have G_i-protein mediated inhibitory effect on adenylyl-cyclase and converges with α-MSH induced signalization [173]. AGRP is an endogenous antagonist of α-MSH on the MC3-R and MC4-R [174, 175] therefore, AGRP can also influence the cAMP-dependent pathway in the target cells.

Toxin-mediated elimination of the AGRP/NPY neuron population in adult transgenic mice produces dramatically hypophagic animals with increased energy expenditure [164]. Interestingly, neither AGRP- and NPY-KO animals nor the double KO mice have abnormally hypophagic feeding behavior [176-178], suggesting the development of compensatory mechanisms.

Similarly to the anorexigenic neuronal group, the orexigenic cell population also expresses receptors for leptin, insulin and glucose [165], which confirms that these cells also play role in the detection of metabolic signals. Leptin, insulin and glucose inhibit the gene expression of NPY, though AGRP synthesis is only influenced by leptin and not by insulin or glucose [165]. All these metabolic signals inhibit the activity of these cells [165]. During fasting when the circulating level of leptin is low the AGRP/NPY neurons are active and the level of both AGRP and NPY expression is elevated [165]. Leptin administration to fasted rats can decrease the AGRP and NPY synthesis to fed levels, indicating that leptin is a key regulator of the activity of AGRP/NPY neurons [165].

The AGRP/NPY neurons densely innervate the hypophysiotropic TRH neurons of the PVN, but as opposed to α-MSH/CART neurons, they form inhibitory synapses [179]. In addition, the chronic icv. administration of either NPY or AGRP to fed rats can markedly decrease TRH gene expression, similarly to the effect of fasting [180, 181].

In MC4-R KO mice AGRP has no effect on TRH gene expression, which confirms that the predominant melanocortin receptor for the regulation of hypophysiotropic TRH

neurons is MC4-R [182]. NPY can influence the TRH gene expression via both the Y1 and Y5 receptors [183].

5.3. The hypothalamic dorsomedial nucleus

The hypothalamic dorsomedial nucleus (DMN) also innervates densely the hypophysiotropic TRH neurons of the PVN [5]. Neurons of the DMN predominantly form symmetric type synapses on the surface of TRH neurons, suggesting an inhibitory effect [184]. However, the DMN seems to contain both orexigenic and anorexigenic neuron populations [185]. While neurons of the DMN can directly detect metabolic signals such as leptin, insulin, ghrelin and glucose [185-188], they also receive massive innervation from both α-MSH- and AGRP- producing neurons of the ARC, indicating that the DMN may also relay indirect metabolic information sensed by the ARC neurons to the TRH system [189, 190]. Since the chemical ablation of the ARC results in the lack of the regulation of TRH neurons by fasting or leptin [191], it is likely that the regulatory effect of the DMN on the hypophysiotropic TRH neurons is not independent from the ARC inputs. Therefore, the ARC-DMN-PVN pathway may serve as an alternative pathway in the mediation of metabolic signals to hypophysiotropic TRH neurons.

In addition, the DMN also receives input from the suprachiasmatic nucleus (SCN), the key regulator of the circadian rhythms [112]. Lesions of the DMN reduces circadian rhythms of wakefulness, locomotor activity, feeding and serum corticosteroid levels [192]. The DMN has also been shown to play critical role in the food entrainable circadian regulation of endocrine functions [193]. These observations suggest that the DMN may integrate the ARC and SCN inputs and contribute to the synchronization of light- and energy homeostasis mediated regulation of the HPT axis.

DOI:10.14753/SE.2014.1934

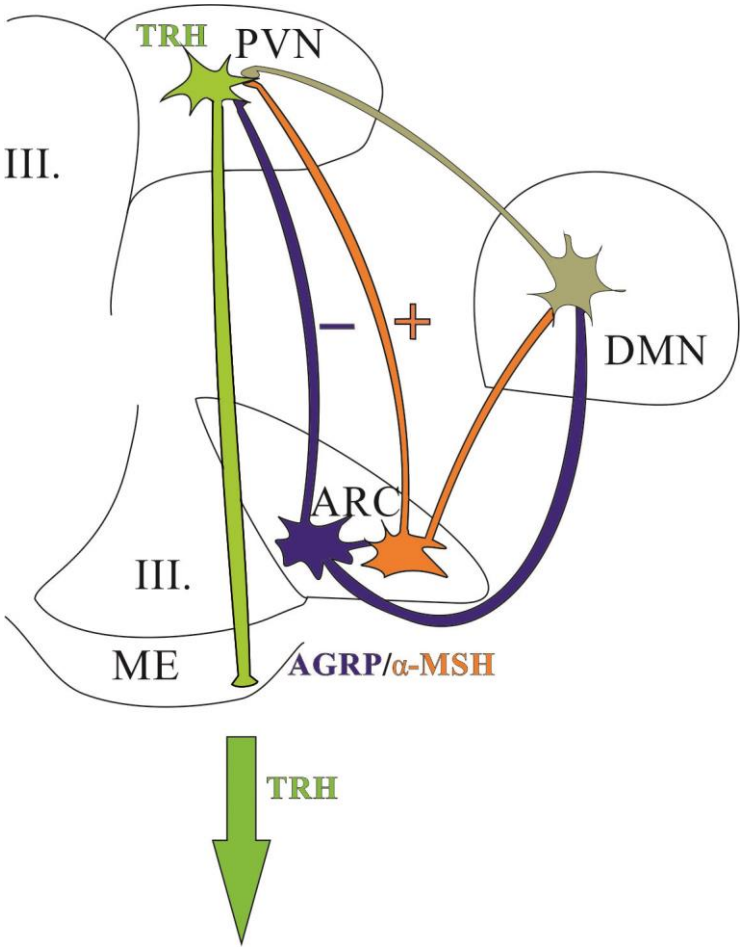

Figure 4. Schematic drawing illustrates the connection between the neuron populations of the ARC and the hypophysiotropic TRH neurons of the PVN.
The ARC contains two antagonistic neuron populations that project to the TRH neurons in the PVN. α-MSH-immunoreactive neurons form excitatory synapses on the surface of TRH neurons and also stimulate the TRH expression by at least two neuropeptides: α-MSH and CART. To the opposite, AGRP neurons form inhibitory synapses on TRH neurons and these neurons inhibit the TRH expression by AGRP and NPY release. DMN receives robust innervation from both α-MSH and AGRP neurons and project to TRH neurons in the PVN.

6. Regulation of the HPT axis during fasting and refeeding

During longer periods of restricted access to environmental resources, the rapid and precise adaptation to energy availability has a critical role in survival. Fasting induces a marked decrease in circulating levels of TH which is accompanied by lower TSH levels and a significant reduction of TRH gene expression [194-196]. This status referred to as

central hypothyroidism promotes energy conservation by decreasing basal metabolic rate and reducing thermogenesis [5]. The fasting induced central hypothyroidism can be prevented by the chemical ablation of the ARC [191]. Furthermore the lack of ARC inhibits the stimulatory effect of leptin on TRH gene expression, and also on TSH and TH release in fasting animals [191]. After 24 hours of starvation when the mass of white adipose tissue (WAT) is still not reduced significantly, the circulating level of leptin already falls because of its decreased release from the pool stored in adipocytes [197]. The low circulating level of leptin causes the loss of the activation of α-MSH/CART neurons which results in decreased stimulatory tone on TRH gene expression [165]. To the opposite, during fasting the decreased blood-level of leptin stimulates NPY and AGRP gene expression and the activity of these cells, which, in turn, inhibit TRH neurons in the PVN [165] (fig.5.).

Leptin administered icv. to rats can induce the phosphorylation of signal transducer and activator of transcription 3 (STAT3), an intracellular component of leptin receptor mediated signalization machinery, in the TRH neurons in the PVN [198]. This suggests that leptin can directly act on TRH neurons. Although the distribution of phosphorylated STAT3 (P-STAT3)-IR TRH neurons regulated directly by leptin and the pattern TRH neurons that are activated by α-MSH after leptin administration overlap only partially. This observation suggests that TRH neurons which are directly regulated by leptin differs from the ones receiving information about leptin concentration indirectly from the ARC [198]. The relevance of the ARC-independent leptin signalization pathway is unclear yet, but the role of this direct leptin signaling pathway seems to be insignificant during fasting as the inhibitory effect of fasting on the HPT axis is absent in ARC ablated rats [191] and also in double-transgenic mice lacking both melanocortin and NPY signaling [199].

7. Melanocortin resistance of the hypophysiotropic TRH neurons during the early phase of refeeding

When animals are refed after fasting, they are satiated 2h after the onset of food intake [200], but their energy expenditure is increased only after 24h coincidently with the normalization of TRH gene expression [201]. A quick satiety response of the animals is accompanied by the presence of c-Fos, a member of the immediate early gene family and a marker of neuronal activation, in 90% of the α-MSH neurons in the ARC and in the α-

MSH activated neurons of the ventral parvocellular subdivision of the PVN [200]. In contrast, only a modest increase in the presence of c-Fos can be observed in TRH neurons and accordingly, TRH gene, TSH and TH levels are not influenced by this short period of refeeding [201]. The TRH mRNA expression in the PVN returned to fed level only 24 hours after the start of refeeding [201]. However, the activation of the α-MSH neurons of the ARC plays critical role in the determination of meal size during the first two hours of refeeding. During this early phase of refeeding the hypophysiotropic TRH neurons seem to be resistant to the stimulatory effect of these ARC neurons [201]. The background of the melanocortin resistance of TRH neurons during the early phase of refeeding is still unidentified.

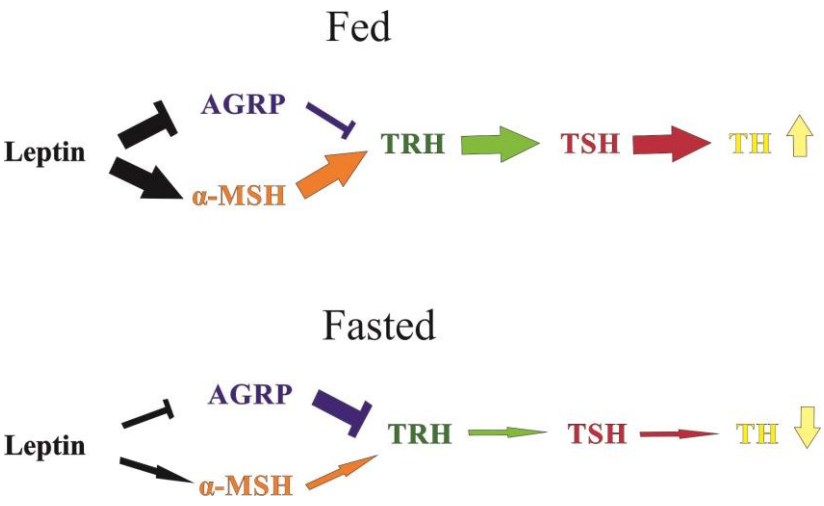

Figure 5. Schematic illustration of the regulatory effect of leptin on the HPT axis.
In fed animals the high circulating level of leptin facilitates the stimulatory effect of α-MSH neurons on TRH synthesis and represses the inhibitory effect of AGRP neurons on TRH neurons. These actions result in the release of THs. During fasting reduced circulating levels of leptin induce the inactivation of α-MSH neurons and cancel the inhibition of AGRP neurons. The altered activity of neuron populations of ARC results in the repression of TRH-synthesis which causes the fall of circulating TH levels.

8. Leptin-induced synaptic rearrangement in the regulation of feeding-related hypothalamic neuronal groups

Increasing evidence suggests that leptin can induce the synaptic rearrangement of the hypothalamic feeding-related neuronal circuitry. In the ARC, leptin-related alteration has been described in the innervation of both feeding related neuron populations that regulate the TRH neurons [202]. In leptin deficient ob/ob mice, a significant increase in the number of excitatory postsynaptic currents (EPSC) can be observed onto NPY neurons compared to WT mice, while the frequency of inhibitory postsynaptic currents (IPSC) onto the α-MSH-producing POMC neurons was significantly higher in ob/ob mice than in WT animals [202]. These observations were confirmed by the electron microscopical comparison of ob/ob and WT mice, which revealed alterations in the total number and the ratio of excitatory and inhibitory synapses on the surface of both NPY and POMC neurons in ob/ob mice compared to WT mice [202]. The lack of leptin increases the total number of synapses on the perikarya of NPY neurons [202]. Although a slight fall can be observed in the number of inhibitory synapses in ob/ob mice, the dominant effect of the lack of leptin is the marked increase of excitatory synapses on these cells when compared to WT animals [202]. In contrast, when studying the perikaryal surface of α-MSH neurons in ob/ob mice, a remarkable decrease can be observed in the number of excitatory synapses and a slight, but not significant reduction in the number of inhibitory connections [202]. In addition, leptin seems to induce changes not only in the incidence of synaptic inputs to α-MSH/CART and AGRP/NPY neurons but it also contributes to altered axonal growth of these neurons during development [203]. In the PVN of 10-day-old ob/ob mice, 10 times less fibers of ARC origin can be observed compared to WT littermates [203]. Although this disruption in the fiber density decreases in adult mice, a 3 to 4 fold lower density of axons originating from the ARC can still be detected in the medial parvocellular subdivision of the PVN of leptin deficient mice [203]. The chronic intraperitoneal (i.p.) leptin injection to 4-days-old ob/ob mice can prevent the disruption of axonal growth from the ARC to the PVN, corroborating the essential role of leptin in the stimulation of the development of the hypothalamic feeding-related neuronal network [203]. Although leptin treatment of adult ob/ob mice does not reverse the decreased ARC innervation of the PVN [203], transcriptional-profiling studies suggest that in the PVN of adult mice leptin regulates genes like basigin (*Bsg*), apolipoproteinE (*ApoE*), growth

associated protein 43 (*Gap43*), synuclein-γ and $GABA_A$ receptor associated protein (*Gabarap*); these genes are involved in synapse formation and neuronal growth [204]. These data about role of leptin in the regulation of hypothalamic synaptic plasticity suggest that leptin may also regulate TRH gene expression by influencing the synaptic plasticity of the arcuato-paraventricular pathway.

9. Non-hypophysiotropic TRH neurons

Although the first described and most studied role of TRH is its hypophysiotropic function, TRH is also released as a neurotransmitter modulating synaptic transmission within the central nervous system. TRH synthesizing neurons are located in many areas of the CNS, such as the olfactory bulb [205], septum [206], brainstem [207], amygdala [208], cerebellum [209], cortex [210] and the hypothalamic PVN [5, 211], periventricular nucleus [111, 211], DMN [111, 211], perifornical area [111] and the lateral hypothalamus [211]. The function of the non-hypophysiotropic TRH-expressing neuron populations is less well understood although TRH is known to have wide non-hypophysiotropic effects, like analgesia, anticonvulsant activity, increase of arousal, memory facilitation, increase of locomotor activity, organ specific increase of blood flow and intensified gastrointestinal activity [5]. In addition, increasing evidence indicates that some of the non-hypophysiotropic TRH neuron populations in the hypothalamus may also play role in the regulation of energy homeostasis; non-hypophysiotropic TRH-synthesizing neurons of the anterior PVN and perifornical area seem to be involved in the appetite regulation [212, 213].

Examination of TRH knock out (TRH-KO) mice indicates that the lack of TRH induces several alterations that are related to the non-hypophysiotropic roles of TRH [108]. In these mice behavioral abnormalities like depressive mood and alcohol intolerance can be observed [108]. In accordance, TRH expression is often altered in psychiatric disorders [214]. Although centrally administered TRH has well known anorexigenic effect [215], the data about the body weight and development of the TRH-KO animals is controversial. Interestingly, at the age of 4 weeks the TRH-KO mice were smaller than WT animals, but no significant difference was observed between the two groups at postnatal week 8 [107].

10. Identification of the activated elements of neuronal networks

In the studies applying c-Fos immunolabeling for the identification of the activated neurons, the question of the neuronal input of identified cells is always difficult. Generally, double labeling immunohistochemical methods are used for the visualization of the connection between axons and perikarya [166]. Although the observation of axon varicosities on the surface of a neuronal cell body cannot verify the synaptic communication, but it indicates, at least, the anatomical connectivity of the two neuronal structures. Therefore, analyses of the presence of immunoreactive boutons on the surface of perikarya at light microscopic level can be helpful to estimate the extent of the interaction of the two systems, if the presence of synapses is validated by electron microscopy [166].

Althought c-Fos labeling can identify the activated neurons, the analysis of their inputs is not possible with this technique in the absence of cytoplasmic labeling in the activated neurons.

The Nissl-staining method is a widely used counterstaining method which labels the cytoplasm of neurons based on the interaction of basic dyes and the nucleic acid content of the cells [216, 217]. These dyes, such as cresyl violet, toluidine blue, anylin, methylen blue and thionine bind to the DNA with strong affinity and visualize primarily the cell nuclei, but also label the cytoplasmic RNA content of the cells [216]. Since remarkable amount of protein is continuously synthesized in neurons, a high concentration of rough endoplasmatic reticulum can be observed in the cytoplasm of these cells [218, 219]. Nissl-staining is often used in combination with immunohistochemical methods as a counterstaining approach to facilitate the mapping of the labeled cell populations [220-222]. Unfortunately, after the immunolabeling procedure Nissl-dyes often visualize only the cell nuclei, but not the cytoplasm, making the counterstaining less valuable [220-222]. In this case the individual determination of the contacts of the c-Fos labeled neurons is not possible. We hypothesized that the lack of cytoplasmic labeling after immohistochemical processes is caused by the digestion of the RNA content of the neurons by RNase enzyme contamination and that the application of RNase-free conditions and RNase inhibitors during the immunohistochemical processes could improve the labeling of cytoplasm by the subsequent Nissl-staining.

DOI:10.14753/SE.2014.1934

IV. Specific aims

1. To map the distribution of hypophysiotropic TRH neurons in the mouse hypothalamus

2. To determine the route of T3 transport between the thyroid hormone activating tanycytes and the hypophysiotropic TRH neurons

3. To clarify the mechanism of the melanocortin resistance of the hypophysiotropic TRH neurons during refeeding

4. To develop an improved method for the combined use of immunocytochemistry and Nissl-staining

DOI:10.14753/SE.2014.1934

V. Materials and methods

1. Animals

The rodent species and strains used for the studies of the thesis are summarized in *Table 1*. The animals were housed under standard environmental conditions (light between 6:00 A.M. and 6:00 P.M., temperature 22°C, food and water *ad libitum*) in the animal facility of the Institute of Experimental Medicine of the Hungarian Academy of Sciences. All experimental protocols were reviewed and approved by the Animal Welfare Committee at the Institute of Experimental Medicine of the Hungarian Academy of Sciences and carried out in accordance with legal requirements of the European Community.

Table 1. Summary of animals used in different experiments

Study	**Species**	**Strain**	**Sex**	**Weight**
Mapping the distribution of hypophysiotropic TRH neurons in the mouse hypothalamus	Mouse	CD1	Male	28-30g
Identification of the transport route between the thyroid hormone activating tanycytes and hypophysiotropic TRH neurons	Rat	Wistar	Male	220-250g
	Mouse	CD1	Male	28-30g
Deciphering the mechanism of the melanocortin resistance of hypophysiotropic TRH neurons during refeeding	Mouse	TRH/Cre-Z/EG	Male	28-30g
Development of an improved method for combined use of immunocytochemistry and Nissl-staining	Rat	Wistar	Male	300-310g

2. Tissue preparation and labeling

2.1. Methods used for mapping the distribution of hypophysiotropic TRH neurons in the PVN of mice

2.1.1. Flouro-Gold injection and tissue preparation for immunocytochemistry

To detect hypophysiotropic neurons, 4 mice received intravenous injection of Fluoro-Gold (15μg/g BW in 100μl 0.9% saline, Fluorochrome. Llc., Denver, CO., USA). Two days later, the mice were injected intraperitoneally with the same dose of Fluoro-Gold to further enhance the labeling in the hypophysiotropic cell bodies. Fluoro-Gold is a retrograde tracer which is not able to pass through the BBB. Therefore, only the axons terminating outside of the BBB, including the axon terminals of hypophysiotropic TRH neurons in the median eminence can take up Fluoro-Gold from the circulation and transport it to their perikarya where the accumulation of this tracer can be detected. Since non-hypophysiotropic TRH neurons have no direct connection with the circulation, they are not able to concentrate Fluoro-Gold. Therefore, the presence of Fluoro-Gold uptake in TRH-IR perikarya is indicative of the hypophysiothropic nature.

Five days after the second tracer injection, the deeply anesthetized animals (ketamine: 50 μg/g; xylazine: 10 μg/g body weight, i.p.) were icv. treated with colchicine, an inhibitor of axonal transport (1 μg/g body weight) by injection through a 26 G needle placed into the lateral ventricle under stereotaxic control (coordinates from Bregma: antero-posterior –0.2 mm, lateral –1mm, dorsoventral -2.5mm) [223]. The colchicine treatment was applied to facilitate the detection of TRH-IR perikarya. In intact animals, only a few TRH-IR perikarya are detectable with immunocytochemistry in the PVN, because TRH is rapidly transported to the axons. In contrast, the colchicine induced inhibition of axonal transport markedly increases the TRH-content of cell bodies and therefore, the detectability of the perikara of TRH neurons. Control animals were not injected with Fluoro-Gold, but received icv. colchicine treatment as described above. Twenty hours after the colchicine treatment, the animals were deeply anesthetized with ketamine-xylazine and perfused through the ascending aorta with 10 ml phosphate buffered saline (PBS; pH 7.4), followed by 30 ml 1% acrolein + 3% paraformaldehyde (PFA) in PBS, and finally 20 ml 3% PFA in PBS. Both PFA and acrolein form irreversible cross-links between the primary amino groups of proteins, resulting in the fixation of tissues. PFA is used in most routine immunocytochemical detections. However, TRH is

a very small peptide and the antibody used for the detection of TRH was produced against TRH conjugated to bovine serum albumin (BSA) with acrolein, which markedly modifies the structure of TRH. Therefore, the antiserum raised this way can only recognize TRH if the tissue is also perfused with an acrolein-containing tissue fixative.

After perfusion, the brains were removed and cryoprotected in 20% sucrose containing PBS at 4°C overnight, to prevent frezeing artefacts, and then, frozen on dry ice. Twenty-five micrometer thick, coronal sections through the rostro-caudal extent of the PVN were cut on freezing microtome (Leica Microsystems, Weltzar, Germany), collected in four identical sets in cryoprotective solution (30% ethylene-glycol; 25% glycerol; 0.05 M phosphate buffer) and stored at -20°C until used.

2.1.2. Pretreatment for single-, double- and triple labeling immunocytochemistry

The sections were treated with the strong reducing agent sodium borohydride (1% in distilled water for 30 min) to extinguish the free aldehyde activity of acrolein by reducing it to hydroxyl group. Then the sections were incubated in a mixture of 0.5% Triton X-100, a detergent applied to increase the permeability of cell membranes, and 0.5% H_2O_2 to inhibit the endogenous peroxidase activity (in PBS for 15 min). Nonspecific antibody binding was blocked with 2% normal horse serum (NHS) in PBS for 15 min. The sections were then processed for single-, double- or triple labeling immunocytochemistry as described below.

2.1.3. Single-labeling immunocytochemistry for TRH

The sections were incubated in sheep anti-TRH serum (1:4000, generated in our laboratory, # 08W2) in serum diluent (2% NHS, 0.2% PhotoFlo, 0.2% sodium azide in PBS) for two days at 4°C, followed by incubation in biotinylated donkey anti-sheep IgG (1:500, Jackson ImmunoResearch Laboratories, West Grove, PA, USA) for two hours at room temperature. Then the sections were immersed in Avidin-Biotin-Peroxidase complex (ABC) (1:1000 Vector Laboratories Inc., Burlingame, CA, USA) in 0.05 M Tris buffer (TB) (pH 7.6) for 1 hour. The peroxidase activity of the antibody-ABC complex was visualized by Ni-DAB developer [mixture of 0.05% diaminobenzidine (DAB), 0.15% Nickel-ammonium-sulfate, 0.005% H_2O_2 in 0.05 M Tris buffer] that resulted a dark blue precipitate in the TRH-IR neurons. Then the sections were mounted onto glass

microscope slides from 0,3% polyvinyl alcohol disolved in distilled water (Elvanol). After dehydrating the sections in ascending series of ethanol and xilene, they were coverslipped with DPX mounting medium (Sigma-Aldrich Inc., St. Louis, MO, USA)

2.1.4. Triple-immunofluorescent labeling to detect Fluoro-Gold, TRH and vasopressin or oxytocin

Triple immunofluorescent labeling was performed for Fluoro-Gold, TRH and the secreted peptide hormone of one of the two magnocellular neuron population: AVP or OT, to map the hypophysiotropic TRH neurons in the PVN of mice and determine their relationship with the magnocellular neurons. Although Fluoro-Gold shows autofluorescence, the detection of the hypophysiotropic neurons was facilitated with immunofluorescencent labeling of the tracer resulting in brighter and more stable fluorescent signal.

The sections were pretreated as described above and incubated in a mixture of rabbit anti-Fluoro-Gold serum (1: 24,000, Chemicon, EMD Millipore Corp., Billerica, MA, USA), sheep anti-TRH serum (1:4000) and mouse anti-AVP-neurophysin (AVP-NP) antibody (1:500, PS-41; gift from Dr H.Gainer, NIH, Bethesda, MD, USA) or mouse anti-oxytocin-neurophysin (OT-NP) (1:500, PS-38; 1/1000, kindly provided by Dr. Sharon Key, Public Health Service, NIH, Bethesda, MD, USA) in serum diluent for two days at 4°C. Then, the sections were incubated in the following mixture of secondary antibodies: biotinylated donkey anti-rabbit IgG for detection of Fluoro-Gold (1:500, Jackson ImmunoResearch Laboratories, West Grove, PA, USA), Alexa 555-conjugated donkey anti-sheep IgG for detection of TRH (1:500, Invitrogen, Life Technoligies Corp., Grand Island, NY, USA) and FITC-conjugated donkey anti-mouse IgG for identification of AVP-NP or OT-NP (1:50, Jackson ImmunoResearch Laboratories, West Grove, PA, USA) in serum diluent at room temperature for 2 hours. This was followed by an incubation in ABC reagent at 1:1,000 dilution in 0.05 M TB for 1 hour. The immunoreaction detecting Fluoro-Gold was further amplified using the biotinylated tyramide (BT) TSA amplification kit (Perkin Elmer Life and Analytical Sciences, Waltham, MA, USA) according to the manufacturer's instructions. Finally, the sections were incubated in Cy5-conjugated streptavidin (1:200, Jackson ImmunoResearch Laboratories, West Grove, PA, USA) diluted in serum diluent, for 1.5 h. The sections

were mounted onto glass microscope slides from TB and coverslipped with Vectashield mounting medium containing DAPI fluorescent counterstain (Vector Laboratories Inc., Burlingame, CA, USA).

2.1.5. Double-labeling immunofluorescence for TRH and CART

The sections were incubated in sheep anti-TRH serum (1:4000) and mouse anti-CART antibody (1:1500, gift from Dr. Jes Thorn Clausen, Novo Nordisk A/S, Denmark) for 2 days at 4°C. Then, the sections were treated with a mixture of Alexa 555-conjugated donkey anti-sheep IgG for labeling the antibodies against TRH (1:500, Invitrogen, Life Technologies Corp., Grand Island, NY, USA) and FITC-conjugated donkey anti-mouse IgG for the visualisation of anti-CART IgGs (1:300, Jackson ImmunoResearch Laboratories, West Grove, PA, USA) for 2 hours at room temperature. After the immunocytochemistry the sections were mounted onto glass microscope slides from TB and coverslipped with Vectashield mounting medium containing DAPI.

2.1.6. Nissl-counterstaining

To study the organisation of the PVN in mice, Nissl-counterstaining was performed in sections from different levels of the PVN. Nissl-counterstaining facilitated the discrimination of magno- and parvocellular subdivisions of the PVN and helped visualize the borders of the nucleus. The sections without any pretreatment were mounted onto gelatine-coated slides, dehydrated with an ascending series of ethanol, treated with xylene for 5 min and rehydrated in a descending series of ethanol and in MilliQ water. Then, the sections were treated with 0.1% cresyl-violet solution (disolved in distilled water and acidified by 0.31% acetic acid) for 3 min followed by differentiation in acetic acid in 100% ethanol (at 1:50,000 dilution) for 5 sec [217]. Following dehydration in an ascending series of ethanol, the sections were treated with xylene and coverslipped using DPX Mounting medium.

2.2. Methods to identify the route of T3 transport between the thyroid hormone activating tanycytes and the hypophysiotropic TRH neurons

2.2.1. Tissue preparation and single-labeling immunocytochemistry for brightfield microscopical detection of MCT8 in the median meninence

Deeply anasthesized mice (n=5) were transcardially perfused with 10ml PBS followed by 30ml of 4% acrolein + 2% PFA in PBS, and then 20ml 4% PFA in PBS. After that, the brains were removed and cryoprotected in 20% sucrose in PBS at 4°C overnight. 25µm-thick coronal sections were prepared from the brains with a freezing microtome (Leica Microsystems, Weltzar, Germany) and stored in cryoprotective solution. To visualize the presence of MCT8 in hypophysiotropic axon terminals of the rat hypothalamus, sections were pretreated for immuncytochemical labeling as it was described earlier in *Section 2.1.2.* The sections were then incubated in anti-MCT8 rabbit polyclonal serum (1:5,000, kind gift of Dr. TJ Visser, Rotterdam, The Netherlands). The primary antiserum was reacted with biotinylated donkey anti-rabbit IgG (1:500, Jackson ImmunoResearch Laboratories, West Grove, PA, USA) for 2 hours, followed by incubation in ABC (1:1,000) for 1 hour. The peroxidase signal was visualized using Ni-DAB developer. The resulting reaction product was silver-gold-intensified using the Gallyas method [224]. The immunostained sections were mounted onto glass slides from Elvanol, air dried, and coverslipped with DPX mounting medium (Sigma-Aldrich Inc., St. Louis, MO, USA).

2.2.2. Tissue preparation and single-labeling immunocytochemistry for electron microscopic detection of MCT8 in the median eminence

To study the cellular and subcellular distribution of MCT8 in the median eminence, rats (n=5) were perfused transcardially, first with 50 ml PBS, followed by 150ml 4% acrolein + 2% PFA in phosphate buffer (PB) and 50ml 4% PFA in PB, under deep anesthesia. The brains were removed and postfixed in 4% PFA overnight. Next day, 30-50µm-thick coronal sections were cut on a Leica VT 1000S Vibratome (Leica Microsystems, Weltzar, Germany). Free aldehyde groups and the endogenous peroxidase activity were eliminated by treatment in 1% sodium borohydride (30 min in PBS) and in 0.5% H_2O_2 (15 min in PBS), respectively. The sections were cryoprotected in 15% sucrose in PBS for 15 min, and then, in 30% sucrose in PBS for 12h at 4ºC. This was

followed by permeabilization using three sequential freeze-thaw cycles in liquid nitrogen. Finally, 2% normal horse serum (in PBS) was applied (20 min) to prevent nonspecific antibody binding. The pretreated sections were incubated in rabbit anti-MCT8 serum (1:20,000 for two days at 4°C, followed by biotinylated donkey anti-rabbit IgG (1:500, Jackcon ImmunoResearch Laboratories, USA) for 2 h and ABC complex (1:1,000) for 1.5 h. The immunoreactivity was visualized with Ni-DAB developer. Finally, the immunoreaction product was intensified using the Gallyas silver-gold method [224]. The sections were treated with 1% osmium tetroxide for 60 min. This treatment preserves the lipid membranes of the sections, and the binding of heavy metal to the lipids also facilitates the electron microscopic visualization of lipid membranes. The treatment in 2% uranyl acetate (prepared in 70% ethanol) for 40 min provides further contrast to the cell membranes. The sections were then, dehydrated in an ascending series of ethanol and propylene oxide, and flat-embedded in TAAB 812 medium epoxy resin (TAAB Laboratories Equipment Ltd., Aldermaston, United Kingdom) between a glass microscope slide and a glass coverslip precoated with liquid release agent (Electron Microscopy Sciences, Hatfield, PA, USA). The embedded sections were photographed and then, cut into ultrathin sections (50-60nm) with a Leica Ultracut UCT ultramicrotome (Leica Microsystems, Weltzar, Germany). The ultrathin sections were mounted onto formvar-coated single slot grids, and contrasted with 2% lead citrate.

2.2.3. Tissue preparation and double-immunofluorescent labeling for the detection of MCT8 and TRH in the median eminence

Double-immunofluorescent labeling was carried out on tissue sections of rat hypothalami perfused with 4% acrolein + 2% PFA as described above. To facilitate antibody penetration and decrease non-specific labeling, the same pretreatments were applied as described in *Section 2.1.2.*. The sections were incubated in the mixture of rabbit anti-MCT8 (1:1,000) and sheep anti-TRH (1:1,500, #08W2) antisera for 2 days. Then, the primary antibodies were detected with Alexa555-conjugated donkey anti-rabbit IgG (Invitrogen, Life Technologies Corp., Grand Island, NY, USA) and FITC-conjugated donkey anti-sheep IgG (Jackson ImmunoResearch Laboratories, West Grove, PA, USA) (both 1:500, for 2 hours). The sections were mounted onto glass slides from TB and coverslipped with Vectashield mounting medium.

2.3. Methods used for studies focusing on the mechanism of the melanocortin resistance of the hypophysiotropic TRH neurons during refeeding

2.3.1. Tissue preparation

Since colchicine treatment highly influences the neuronal transmission and therefore, the regulation of neuronal systems, we could not study the neuronal plasticity in the brain of colchicine treated animals. Therefore, to facilitate the visualisation of TRH expressing neurons, double-transgenic mice were used in these studies. We have crossed floxed indicator Z/EG mice (The Jackson Laboratory, Sacramento, CA, USA) that can express green fluorescent protein (GFP) only in Cre recombinase expressing cells with TRH/Cre mice (generated in our laboratory) that express Cre recombinase only in TRH neurons. The resultant double-transgenic (TRH/Cre-Z/EG) mice expressed GFP only in the TRH neurons.

The double-transgenic animals were divided into 5 groups: 1) fed with standard rodent chow (n=5) 2) fasted for two days (n=5) 3) fasted for two days and refed for 2 hours (n=3) 4) fasted for two days and refed for 24 hours (n=3) 5) Treated with leptin (12μg/day, for 2 days) using an osmotic minipump for subcutaneous infusion (1003D, Alzet Corp., Cupertino, CA, USA) during the two days of fasting (n=3). At the completition of the experiment, the mice were deply anaesthesized and perfused through the ascending aorta with 10ml PBS followed by 40ml 4% PFA in PBS. The brains were removed and postfixed for 2 hours in 4% PFA in PBS. After postfixation, the brains were cryoprotected in 20% sucrose at 4°C overnight, and then, frozen on dry ice. Twenty-five μm-thick coronal sections through the rostro-caudal extent of the PVN were cut on a freezing microtome. The sections were treated with a mixture of 0.5% TritonX-100 and 0.5% H_2O_2 in PBS for 15min. Nonspecific antibody binding was blocked with 2% normal horse serum (NHS) in PBS for 15 min.

2.3.2. Triple-labeling immunofluorescence for GFP, AGRP and α-MSH

Although the autofluorescence of the GFP expressed by the TRH neurons can be detected with confocal microscope the immunofluorescent detection of GFP was used to further facilitate the visualization of TRH neurons. The pretreated sections were incubated in a mixture of rabbit anti-AGRP (1:1,000, Phoenix Pharmaceuticals Inc.,

Burlingame, CA, USA), sheep anti-α-MSH (1:10,000, kindly provided by Jeffrey B. Tatro, Tufts Medical Center, Boston, MA, USA) and mouse anti-GFP (1:5000, Chemicon, EMD Millipore Corp., Billerica, MA, USA) antisera for 2 days at 4°C in antibody diluent. Then, the sections were incubated in the following mixture of secundary antibodies: Alexa555-conjugated anti-sheep IgG for the detection of α-MSH (1:500, Invitrogen, Life Technologies Corp., Grand Island, NY, USA), FITC-conjugated anti-mouse IgG for the intensification of GFP (1:250, Jackson ImmunoResearch Laboratories, West Grove, PA, USA) and biotin-conjugated donkey anti-rabbit IgG for the detection of AGRP (1:500, Jackson ImmunoResearch Laboratories, West Grove, PA, USA). Then, the sections were treated with ABC (1:1,000 for 1h) and BT (1:1,000 for 10 min) and finally, AGRP immunoreactivity was visualized with Cy5-conjugated streptavidin (1:250, Jackson ImmunoResearch Laboratories, West Grove, PA, USA, for 2h). The sections were mounted onto glass slides from TB and coverslipped vith Vectashield mounting medium.

2.4. Method for combined use of immunocytochemistry and Nissl-staining

To demonstrate that the refeeding-activated neurons in the ventral PVN are contacted by axons containing NPY, double-labeling immunocytochemistry combined with Nissl-staining was performed. Since the presence of the activation marker c-Fos can be observed exclusively in the nucleus of cells, the cytoplasmic staining by Nissl-dye is essential for the visualization of the contacts between the perikaryon of the activated neurons and their NPY-containing afferent axons.

2.4.1. Tissue preparation

Three male Wistar rats were fasted for 3 days, and then, refed for 2 hours before perfusion. The animals were deeply anesthesized and transcardially perfused with 20ml PBS, followed by 150ml 4%PFA in PBS. Then, 25-μm-thick coronal sections were prepared with a freezing microtome.

2.4.2. Standard double-labeling immunocytochemistry for c-Fos and NPY

The sections were treated with 0.5% Triton X-100 and 0.5% H_2O_2 in 0.01M PBS for 15 min. To reduce nonspecific antibody binding, the sections were treated with 2% normal horse serum in PBS for 15 min. Then, the sections were incubated in rabbit antiserum against c-Fos (1:30,000, Ab-5, Calbiochem, EMD Millipore Corp., Billerica, MA, USA) for 2 days at 4°C. During standard immunocytochemical procedures, all antisera were diluted in TB containing 2% normal horse serum, 0.2% Kodak Photo-Flo and 0.2% sodium-azide. After the incubation in c-Fos antiserum, the sections were washed in PBS and incubated in biotin-conjugated donkey anti-rabbit IgG (1:500, 1,5h, Jackson ImmunoResearch Laboratories, West Grove, PA, USA), followed by an incubation in ABC reagent (1:1,000 dilution in TB) for 1 hour. The signal was visualized by Ni-DAB developer which resulted in a dark blue precipitate. Then, the sections were incubated in sheep anti-NPY serum (1:100,000, gift from Dr. István Merchenthaler, University of Maryland, School of Medicine, USA) for 1 day at 4°C, rinsed in PBS and incubated in biotinylated donkey anti-sheep IgG (1:500, 2h, Jackson ImmunoResearch Laboratories, West Grove, PA, USA). This was followed by an ABC treatment step (1:1,000, 1h). The signal was visualized by 0.025% DAB/0.0036% H_2O_2 in TB. The discrimination between the dark blue Ni-DAB staining and the light brown DAB label was facilitated by the different intracellular location of the chromogens: c-Fos was detected in cell nuclei, whereas NPY was located in axons in the PVN.

2.4.3. RNase-free double-labeling immunocytochemistry for c-Fos and NPY

For RNase-free immunocytochemistry, the sections were treated very similarly than for standard immunocytochemistry, but with the following modifications. All solutions were prepared with MilliQ water treated with diethylpyrocarbonate (DEPC, 0.2µl/ml) overnight and autoclaved to destroy the potential RNase contamination. PBS stock solution was also treated with DEPC (0.2µl/ml) overnight at room temperature and autoclaved. Antibodies were dissolved in the following solutions: 1% BSA, 0.2% sodium azide and 15 U/ml heparin in 0.01M PBS or 0.01M TB. Heparin was used to inhibit the RNase activity in the antisera. The primary antibodies were used at the following dilutions: rabbit antiserum against c-Fos: 1:15,000 and sheep NPY antiserum: 1:50,000.

2.4.4. Counterstaining

Nissl-counterstaining was performed identically that was described earlier in *Section 2.1.6.*. The immunostained sections that were mounted on gelatine-coated slides were dehydrated with ascending series of ethanol, treated with xylene for 5 min and rehydrated in descending series of ethanol and in MilliQ water. Then, the sections were treated with 1% cresyl violet solution (in 0,31% acetic acid diluted in distilled water) for 3 min followed by differentiation in acetic acid in 100% ethanol (at 1:50,000 dilution) for 5 sec. Then the sections were dehydrated again with ascending series of ethanol and xylene and coverslipped with DPX mounting medium.

3. Image analyses

Table 3. summarizes the microscopic techniques used for image analysis.

Table 3. Microscopic techniques used for the analyses of immunostained sections in different experiments of the PhD thesis

Study	Experiment	Microscopic techniqe
Mapping the distribution of hypophysiotropic TRH neurons in the mouse hypothalamus	Mapping of TRH-IR neurons in the PVN	Brightfield microscopy
	Comparive analysis of the distribution of hypophysiotropic TRH neurons and vasopressin and oxytocin neurons in the PVN	Confocal and fluorescent microscopy
	Co-localization of CART and TRH in the PVN of mice	Confocal and fluorescent microscopy

Identification of the transport route between the thyroid hormone activating tanycytes and hypophysiotropic TRH neurons	Presence of MCT8 in the hypophysiotropic axon terminals in the median eminence	Brightfield- and electron microscopy
	Co-localization of MCT8 and TRH in hypophysiotropic axon terminals	Confocal microscopy
Deciphering the mechanism of the melanocortin resistance of hypophysiotropic TRH neurons during refeeding	Determination of the number of α-MSH- and AGRP-boutons in contact with TRH neurons under different metabolic conditions	Confocal microscopy
Development of an improved method for combined use of immunocytochemistry and Nissl-staining	Comparison of the effect of standard and RNase-free immunocytochemistry on Nissl-counterstaining	Brightfield microscopy

3.1. Confocal microscopy

Images were taken with a Biorad Radiance 2100 confocal laser-scanning microscope (Bio-Rad Laboratories, Hertfordshire, UK) using 20X, 40X and 60X objectives and the following laser lines: 488nm for FITC, 543nm for Cy3 and Alexa555 and 637nm for Cy5. The following dicroic/emission filters were used: 560nm/500-530nm for FITC, 650/560-625nm for Cy3 and Alexa555 and a 660nm-long pass filter for Cy5.

To study the co-localization of TRH and FluoroGold, 40x magnification images were taken with 0.5 μm Z-steps through the entire PVN. The location of TRH-, Fluoro-Gold-,

OT-NP-, AVP-NP- and CART immunoreactivities was detemined on individual optical slices with the ImageJ software (http://rsbweb.nih.gov/ij/). The maps of the localization of TRH neurons in the PVN were drawn in CorelDRAW11 software. The presence of all immunolabeled neurons in representative sections was marked on the maps. Images of the blue DAPI signal were taken with AxioImager M1 microscope (Carl Zeiss, Inc., Jena, Germany) and overlaid with the fluorescent images of the immunostainings to facilitate the differentiation between magnocellular and parvocellular divisions. The composite images were prepared with the Adobe Photoshop CS program. The borders of the divisions were drawn in CorelDRAW11 software based on DAPI-staining. The contrast and brightness weres adjusted in Adobe Photoshop CS software.

The largest perikaryon diameter of randomly selected 50 TRH- and 50 vasopressin-containing neurons and 100-100 randomly selected Nissl-stained neurons located in the compact part of the PVN or in the mid level medial part of the PVN, respectively, from each animal was measured with ImageJ software.

To determine the number of α-MSH- and AGRP-IR axon varicosities in contact with the surface of TRH neurons, one section from the mid level of the PVN was analyzed from each animal. The selected sections were matched to ensure the analysis of identical section planes. Confocal microscopic images were taken from both sides of the PVN at a 60X magnification. The images were taken using 0.5μm Z-steps. The number of AGRP- and α-MSH-IR boutons was determined on all TRH neurons on both sides of the PVN. The TRH neurons were used for the analyses only if the perikaryon was present entirely in the section.

3.2. Electron microscopy

The ultrathin sections were examined with a Jeol-100C (Jeol Ltd., Tokyo, Japan) transmission electron microscope. The brightness and contrast of the digital photographs were adjusted in Adobe Photoshop CS program.

3.3. Brightfield microscopy

Images were taken with an AxioImager M1 microscope (Carl Zeiss, Inc., Jena, Germany) using 10X, 20X and 60X objectives. Brightness and contrast were adjusted with Adobe Photoshop CS software.

4. Statistical analyses

The statistical significance of the data was analyzed using T-test, ANOVA and Neuman-Kuels analyses, using the Statistica9 software package.

5. Specificity of the primary antisera

5.1. Sheep anti-TRH serum

The sheep antiserum against TRH (# 08W2) was raised in our laboratory against TRH conjugated to BSA with acrolein [213]. The specificity of the antiserum for immunocytochemistry was tested by preabsorption with TRH (Bachem Corp., Bubendorf, Switzerland) at 80 μg/ml concentration, which treatment resulted in the complete loss of immunostaining. The distribution of the immunoreactive elements was the same as previously described [111].

5.2. Mouse monoclonal antibody against CART

CART immunoreactivity was visualized using a mouse monoclonal antibody raised against purified recombinant CART(41-89) [225]. Recombinant CART(41-89) was conjugated to ovalbumin with carbodiimide. The specificity of CART antiserum was tested by the combination of single-labeling immunocytochemistry for CART and *in situ hybridization* using antisense RNA probes directed against the rat CART cDNA (bp 226-411; GenBank accession number U10071). The distribution of CART-IR cells in colchicine-treated material matched with the *in situ* hybridization distribution, suggesting that all cells expressing CART constitutively are visualized [147].

5.3. Monoclonal antibodies produced against OT-NP or AVP-NP

For monoclonal anti-OT-NP and anti-AVP-NP antibodies, BALB/c mice were immunized intraperitoneally with acid-soluble extracts of rat neurointermediate lobes in complete Freund's adjuvant. Spleen cells of these mice were isolated and immortalized

by fusion with myeloma cells. Each clone producing monoclonal antibodies were cultured separately. The monoclonal antibodies of each clone was tested by immunohistochemistry and solid and liquid phase radioimmunoassay. With light microscopic immunohistochemistry, both anti-OT-NP and anti-AVP-NP stained exclusively the posterior pituitary, and the paraventricular and supraoptic nuclei of rat hypothalamus. The radioimmunoassay demonstrated that anti-AVP IgG (PS-41) is highly specific for the complex of AVP-NP and does not cross-react with OT-NP, whereas anti-OT-NP IgG (PS-38) reacts with OT-NP exclusively. In addition, peptides synthesized in the rat neurointermediate lobe, i.e., dynorphin A and dynorphin B (100 pmol/tube), β-endorphin (100 pmol/tube), α-MSH (1000 pmol/tube), and angiotensin II (10,000 pmol/tube), did not affect antibody binding [226].

5.4. Rabbit anti-Fluoro-Gold serum

Rabbit antiserum raised against Fluoro-Gold did not give any staining on sections originating from mice without Fluoro-Gold treatment.

5.5. Rabbit MCT8 antiserum

To test the specificity of the anti-MCT8 antibody in the examined region, hypothalamic sections of MCT8-KO mice were used as a negative control (the MCT8-KO brain was kindly provided by Dr. H. Heuer, Jena, Germany). MCT8-immunoreactivity was completely absent in the median eminence of the MCT8-KO mice [227].

5.6. Sheep anti-α-MSH serum

The specificity of the antiserum was demonstrated by the loss of immunoreactivity after preabsorption of the diluted antiserum with an excess of synthetic α-MSH (10^{-5}mol/l) peptide [228].

5.7. Rabbit anti-AGRP serum

The specificity of the polyclonal antibody was verified by preabsorbtion of the antiserum with the peptide antigen fragment AGRP (83-132)-NH_2 which resulted the complete loss of the immunolabeling [179].

5.8. Rabbit c-Fos antiserum

The polyclonal antibody developed by Calbiochem (EMD Millipore Corp., Billerica, MA, USA) against a synthetic peptide (SGFNADYEASSSRC) corresponding to amino acids 4-17 of human c-Fos. However it reacts with mouse and rat c-Fos and the retroviral v-Fos proteins. The early response transcription factor c-Jun do not affects the antibody binding. The staining capability of the antiserum was tested by the producer on sections of rat brain with induced c-Fos expression which resulted in a highly specific staining pattern.

5.9. Sheep antiserum against NPY

The specificity of immunostaining with the NPY antiserum was demonstrated by the loss of immunoreactivity after preabsorption of the diluted antiserum with an excess of synthetic NPY peptide (10^{-5}mol/l) [228].

DOI:10.14753/SE.2014.1934

VI. Results

1. Distribution of hypophysiotropic TRH neurons in the mouse hypothalamus

1.1 The organization of the PVN in mice

We observed that the organization of the mouse PVN is highly different from the organization of the PVN in rats. Therefore, instead of using the nomenclature of the mouse brain atlas by Paxinos and Franklin [223] which was adapted the rat brain nomenclature [229], we have divided the mouse PVN into five parts (Fig. 6). These parts are as follows:

- compact = a cell dense region in the midlevel of the PVN which contains both magno- and parvocellular cells (Fig. 6B)
- periventricular = 3-5 cell wide zone adjacent to the third ventricle (Fig. 6A-C)
- anterior = cranial to the compact part (Fig. 6A)
- mid level medial = located between the compact part and the periventricular zone at the midlevel of the PVN (Fig. 6B)
- posterior = located caudal to the compact part (Fig. 6C)

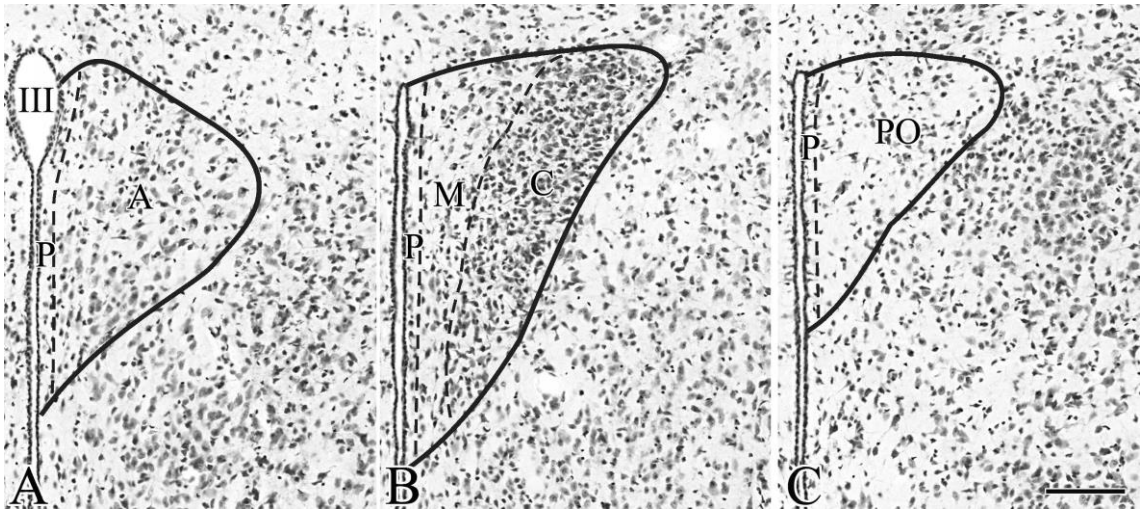

Figure 6. Illustration of the nomenclature used to define the parts of the mouse PVN. Borders of the parts of the mouse PVN are labeled on images of Nissl-stained preparations. A-C represents three anterio-posterior levels of the PVN. III, Third ventricle; A, anterior part; C, compact part; M, mid level medial part; P, periventricular zone; PO, posterior part; Scale bar=100µm;

DOI:10.14753/SE.2014.1934

1.2. Distribution of TRH-IR neurons in the PVN

TRH-IR neurons were observed in all parts of the PVN, except the periventricular zone (Fig. 7). Moving from rostral to caudal portions of the PVN, TRH-containing neurons were observed in all three levels (anterior, mid and posterior levels), but the density of these cells was the highest at the anterior and mid levels (Fig. 7A, C). The largest number of the TRH neurons was observed in the compact part of the PVN (Fig. 7C). The shape and size of the TRH neurons located in the compact and in the other parts of the PVN were similar (size of TRH neurons in mid level medial part of the PVN *vs.* compact part (μm): 12.15 ± 0.05 *vs.* 12.26 ± 0.02; P=0.31).

1.3. Distribution of hypophysiotropic TRH neurons in the PVN

Fluoro-Gold accumulation in neuronal perikarya was readily visualized and had an inhomogeneous and punctate appearance (Fig. 8B). Although the anterior part of the PVN contained a large number of TRH neurons, only very few were co-labeled with Fluoro-Gold (Fig. 8C; 9A; 10A). Similarly, none of the TRH neurons in the posterior part of the PVN contained Fluro-Gold (Fig. 8D; 9G; 10G). Most double-labeled neurons were located in the compact part of the PVN (Fig. 8A, B; 9B-F; 10B-F).

DOI:10.14753/SE.2014.1934

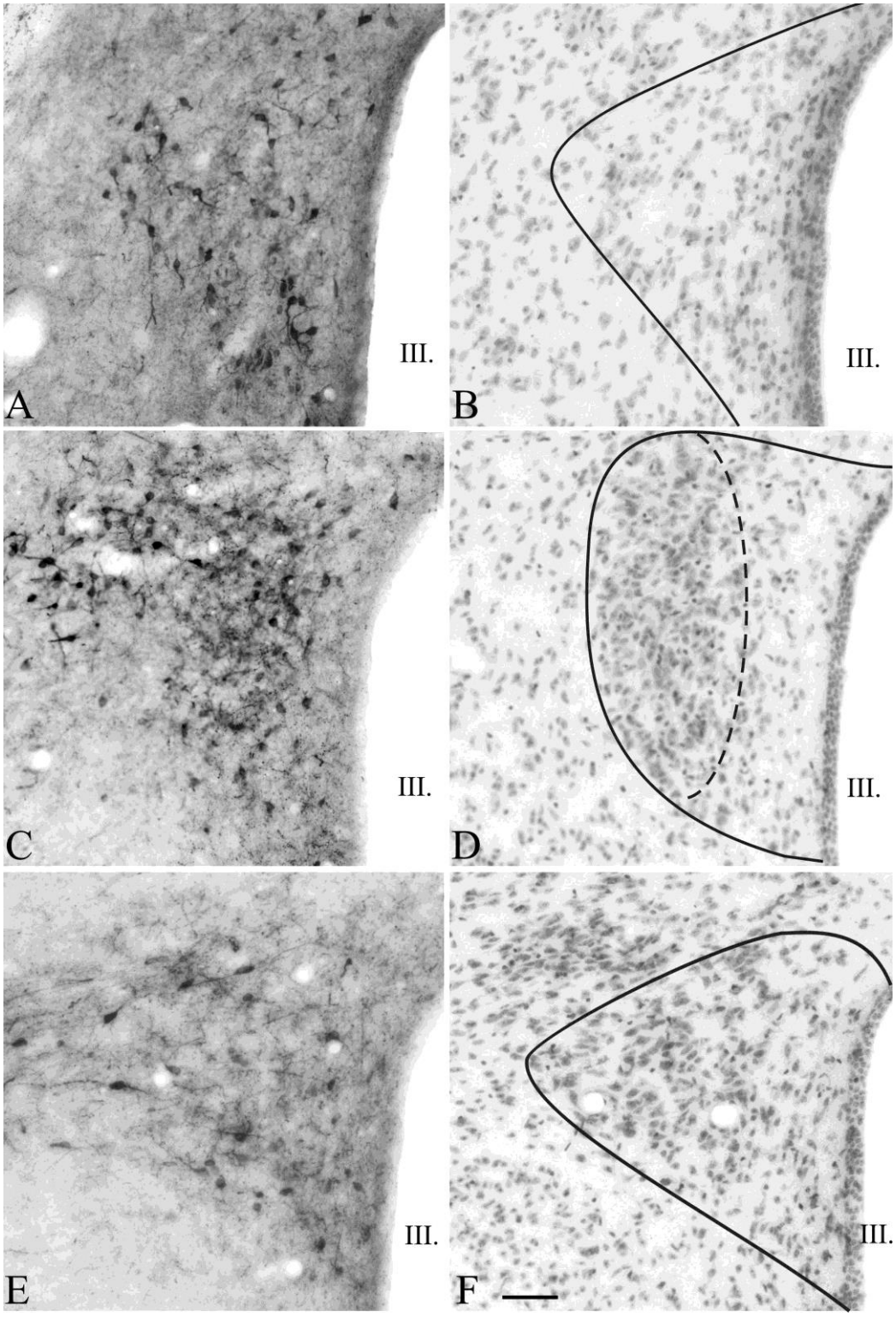

Figure 7. Distribution of TRH neurons in the PVN of mice.

Low magnification images illustrate TRH-IR neurons at three, antero-posterior levels of the PVN (A, C, E). The borders of the PVN and the localization of the compact part are illustrated on neighboring cresyl-violet stained sections (B, D, F). Scale bar = 50 μm

DOI:10.14753/SE.2014.1934

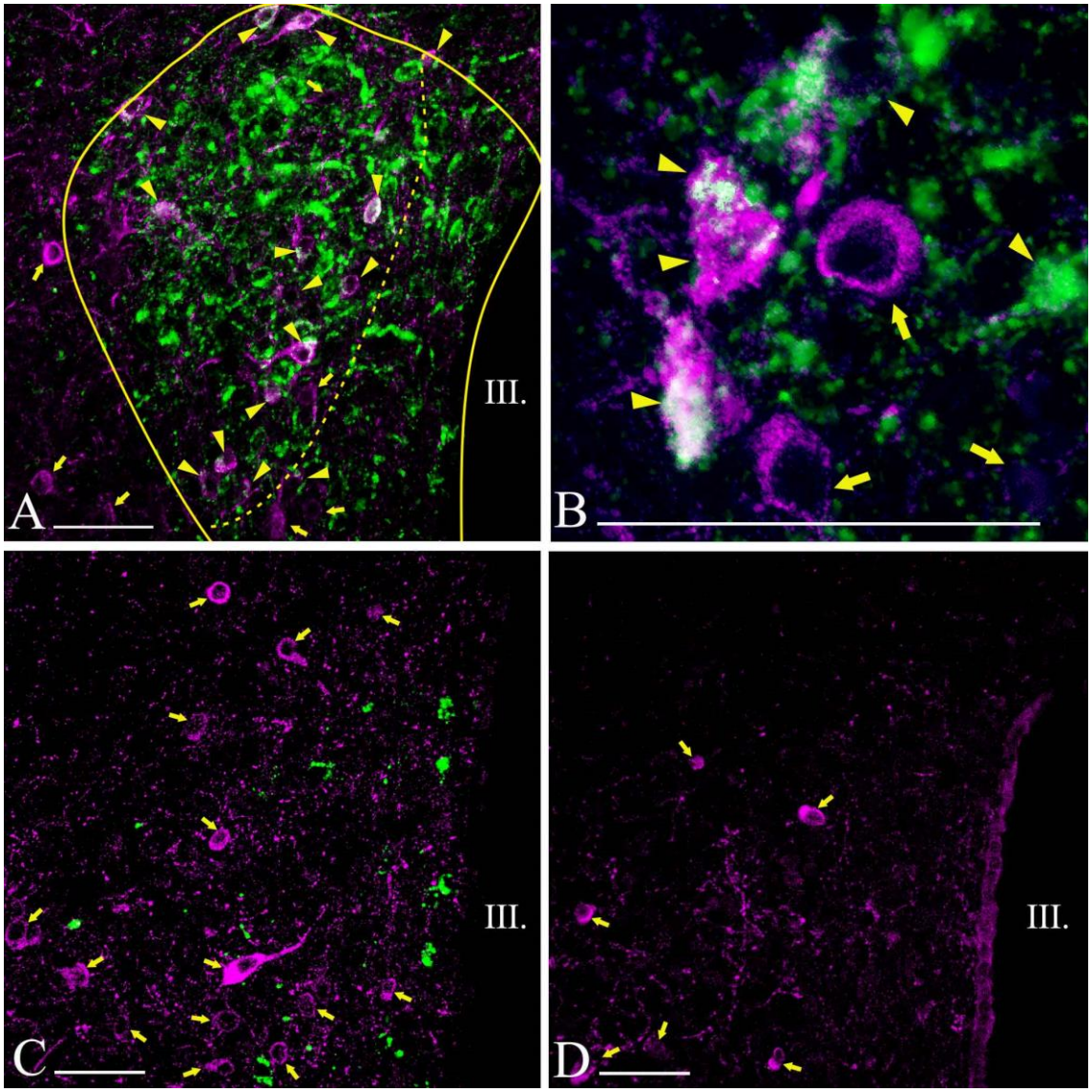

Figure 8. Distribution of hypophysiotropic TRH neurons in the PVN of mice.
The hypophysiotropic TRH neurons containing both TRH- (magenta) and Fluoro-Gold-immunoreactivity (green) can be observed at the mid level of PVN (A, B). Arrowheads point to double-labeled neurons, whereas arrows point to single-labeled non-hypophysiotropic TRH neurons. Most of the hypophysiotropic TRH neurons are located in the compact part demarcated by a broken line (A). High magnification image (B) illustrates the Fluoro-Gold immunoreactivity (green) in the TRH neurons (magenta) in the compact part of the PVN. Fluoro-Gold immunoreactivity was absent from TRH neurons in the anterior (C) and posterior parts of the PVN (D). Each image represents single optical slices. The thickness of optical slice is 1 μm in B-D and 2 μm in A.
III, third ventricle; Scale bars on A-D = 50μm.

1.4. Comparative localization of hypophysiotropic TRH neurons and vasopressin and oxytocin neurons in the PVN

AVP and OT neurons were observed primarily in the compact part of the PVN, although scattered cells were also observed in the mid level medial part of PVN (Figs. 9-11). The size of magnocellular AVP neurons (16.4 ± 0.1 μm) was significantly larger than the size of the TRH neurons ($p<0.001$). Hypophysiotropic TRH neurons containing both Fluoro-Gold- and TRH immunoreactivity were also observed primarily in the compact part of the PVN where they intermingled with AVP and OT neurons (Fig. 9-11). No co-localization of TRH and AVP or OT was observed in this region (Fig. 9-11). In addition, no co-localization was observed in any other region of the PVN where OT and AVP were identified.

To further clarify the presence of magnocellular and parvocellular cells in the compact and mid level medial parts of the PVN, histograms of the cell sizes were created using the following criteria: magnocellular neurons: ≥ 14 μm; parvocellular neurons: < 14 μm. In the compact part, an approximately equal number of cells had a diameter lower (49.3 ± 0.9%) and higher (50.7 ± 0.9%) than 14μm. In the mid level medial part of PVN, the vast majority of cells were smaller than 14 μm (96.0 ± 1.2%) and only scattered cells had a diameter equal to or above 14 μm (4.4 ± 1.2%). The distribution of the cell size of neurons located in the mid level medial part of the PVN and at the compact part of the PVN is illustrated in Fig 12.

DOI:10.14753/SE.2014.1934

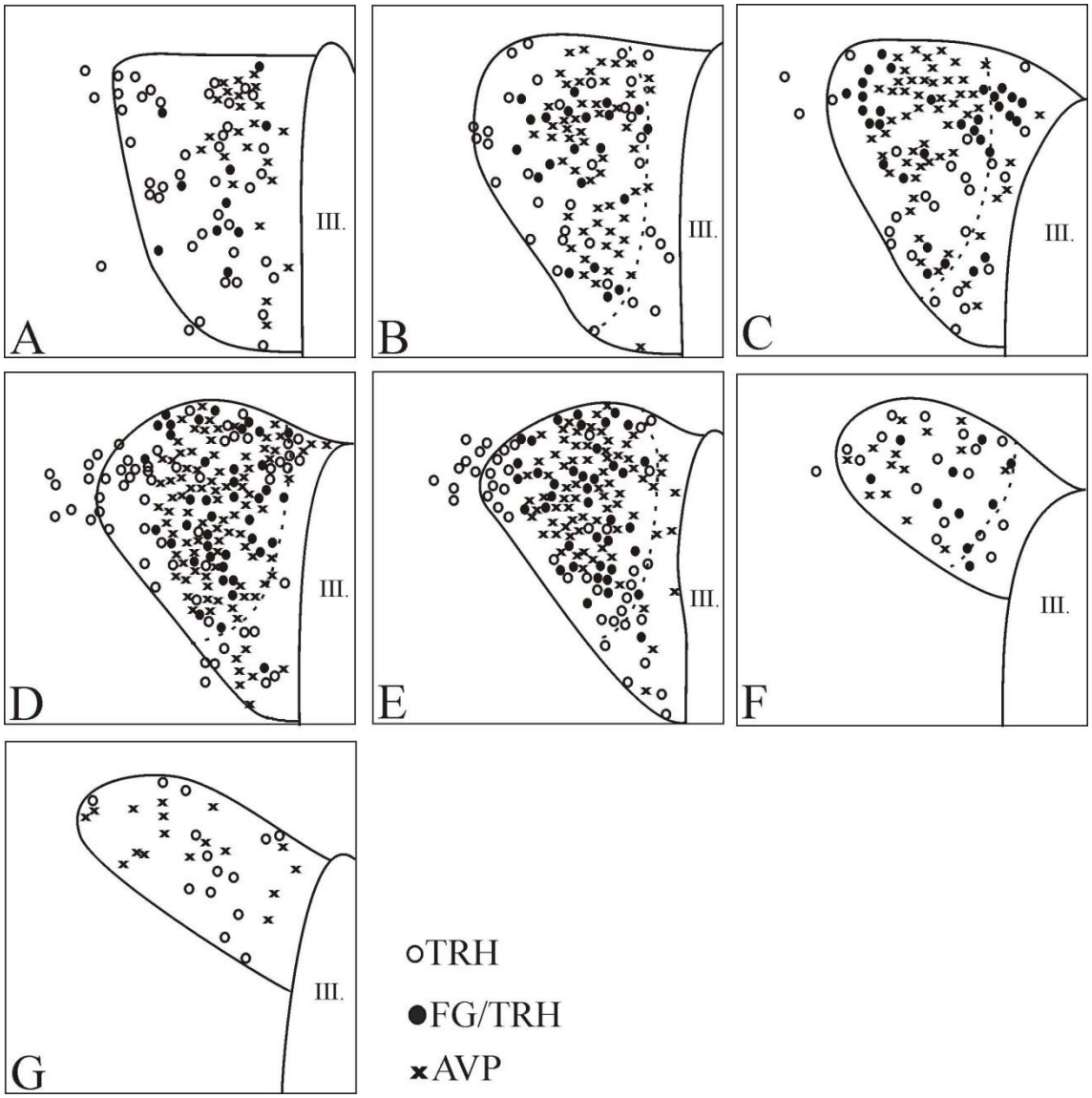

Figure 9. Schematic drawings illustrate the distribution of hypophysiotropic TRH and AVP neurons at different antero-posterior levels of the PVN.

Open circles denote single-labeled TRH neurons; filled circles denote double-labeled TRH/FG neurons; crosses denote AVP neurons. The borders of the compact part are labeled with broken lines. III, third ventricle.

DOI:10.14753/SE.2014.1934

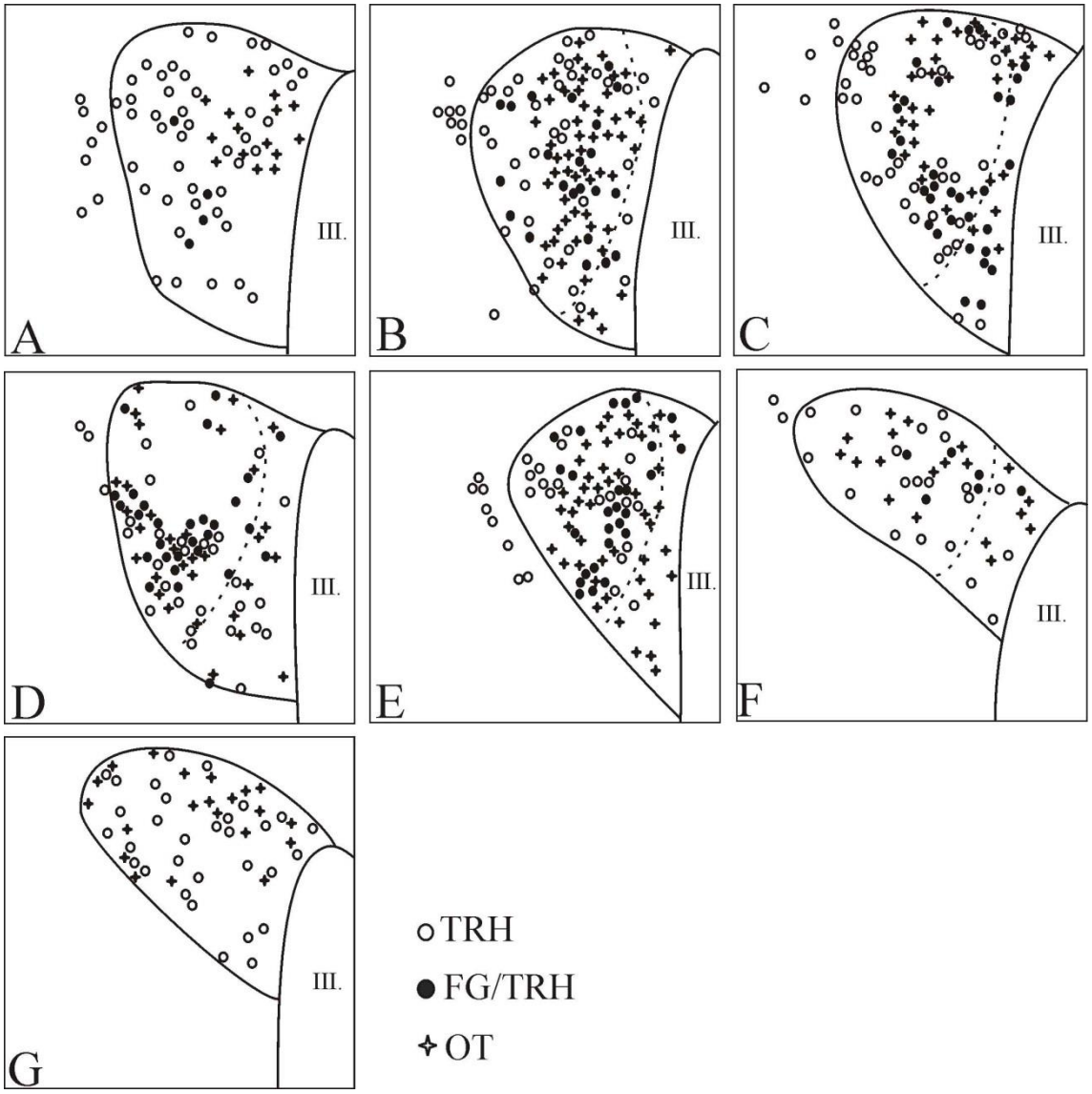

Figure 10. Schematic drawings illustrate the distribution of hypophysiotropic TRH and OT neurons at different antero-posterior levels of the PVN.

Open circles denote single-labeled TRH neurons; filled circles denote double-labeled TRH/FG neurons; crosses denote OT neurons. III, third ventricle.

DOI:10.14753/SE.2014.1934

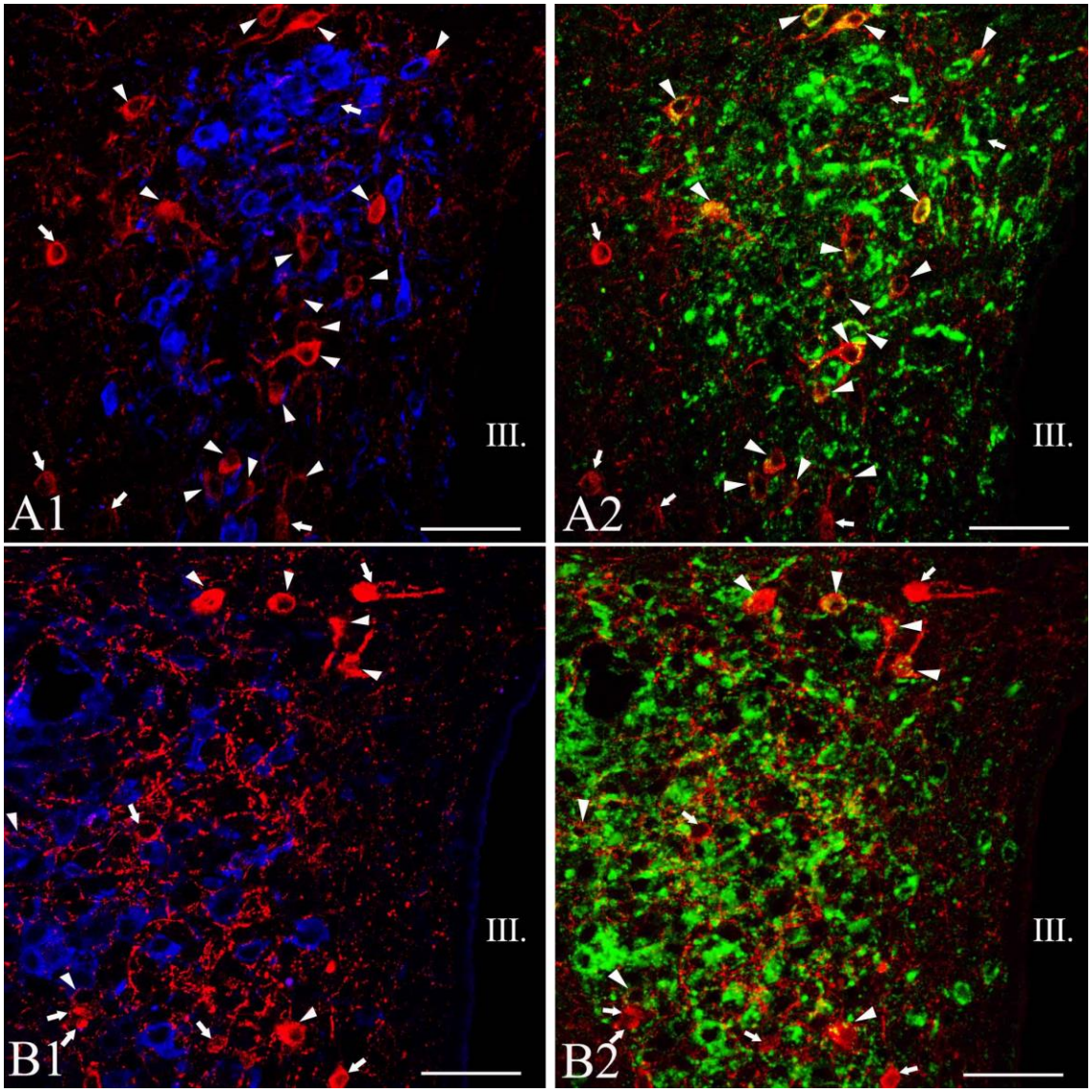

Figure 11. Simultaneous localization of TRH with oxytocin (OT) and vasopressin (AVP) in the PVN of mice.

Medium-magnification confocal images illustrate the distribution of the TRH- (red), AVP- (blue, A1), OT- (blue, B2) and Fluoro-Gold-IR (green) cells at the mid level of the PVN. A1-2 or B1-2 images represents the same field. Note that TRH is not colocalized with the magnocellular peptides. While arrows point to single-labeled TRH neurons, arrowheads label the hypophysiotropic TRH neurons. Each image represents a 1 μm thick optical slice. III, third ventricle, Scale bar = 50 μm.

DOI:10.14753/SE.2014.1934

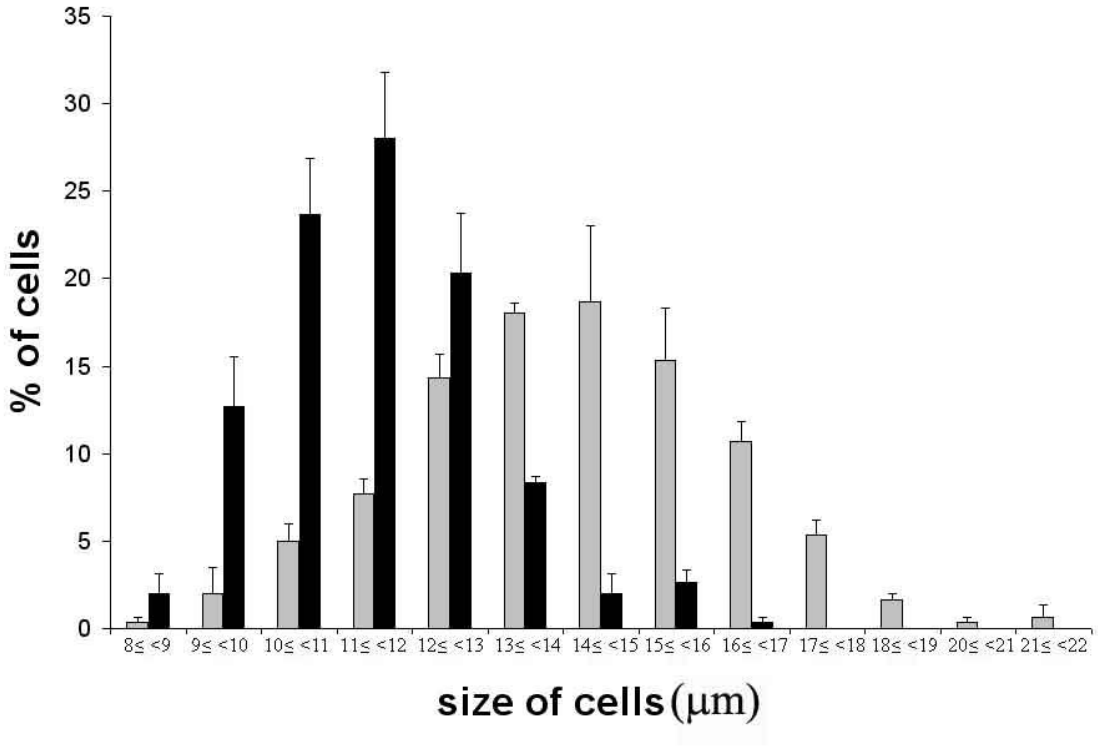

Figure 12. Distribution of cell size in the mid level medial part of the PVN (black bars) and in the compact part of the PVN (gray bars).

1.5. Co-localization of CART and TRH in the neurons of the PVN

The localization of neurons co-synthesizng CART and TRH in the PVN of mice was similar to that of the TRH neurons accumulating Fluoro-Gold. Numerous CART-TRH double-labeled neurons were observed at the mid level of PVN in the compact part (Fig. 13B-F; 14A, B). Co-localization of CART and TRH was not detected in the posterior part of PVN, and only a few double-labeled cells were present in the anterior part (Fig. 13A, G). Co-localization of the two peptides was also detected in the axon terminals of the median eminence (Fig. 14C).

DOI:10.14753/SE.2014.1934

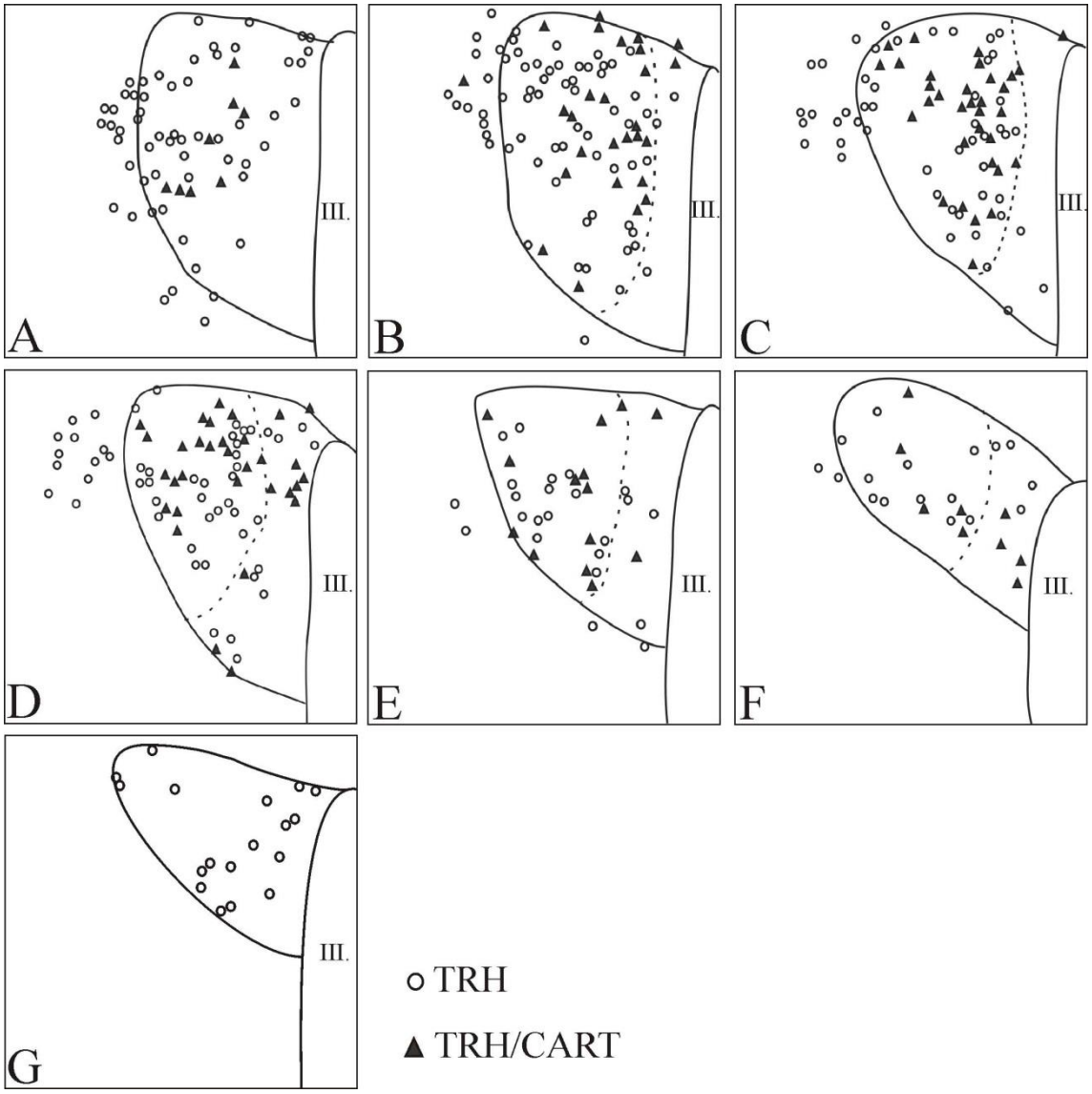

Figure 13. Schematic drawings illustrating co-localization of TRH and CART at different antero-posterior levels of the PVN.

Open circles represent single-labeled TRH neurons; filled triangles indicate double-labeled TRH/CART neurons. The borders of the compact part are labeled with broken lines. III, third ventricle.

DOI:10.14753/SE.2014.1934

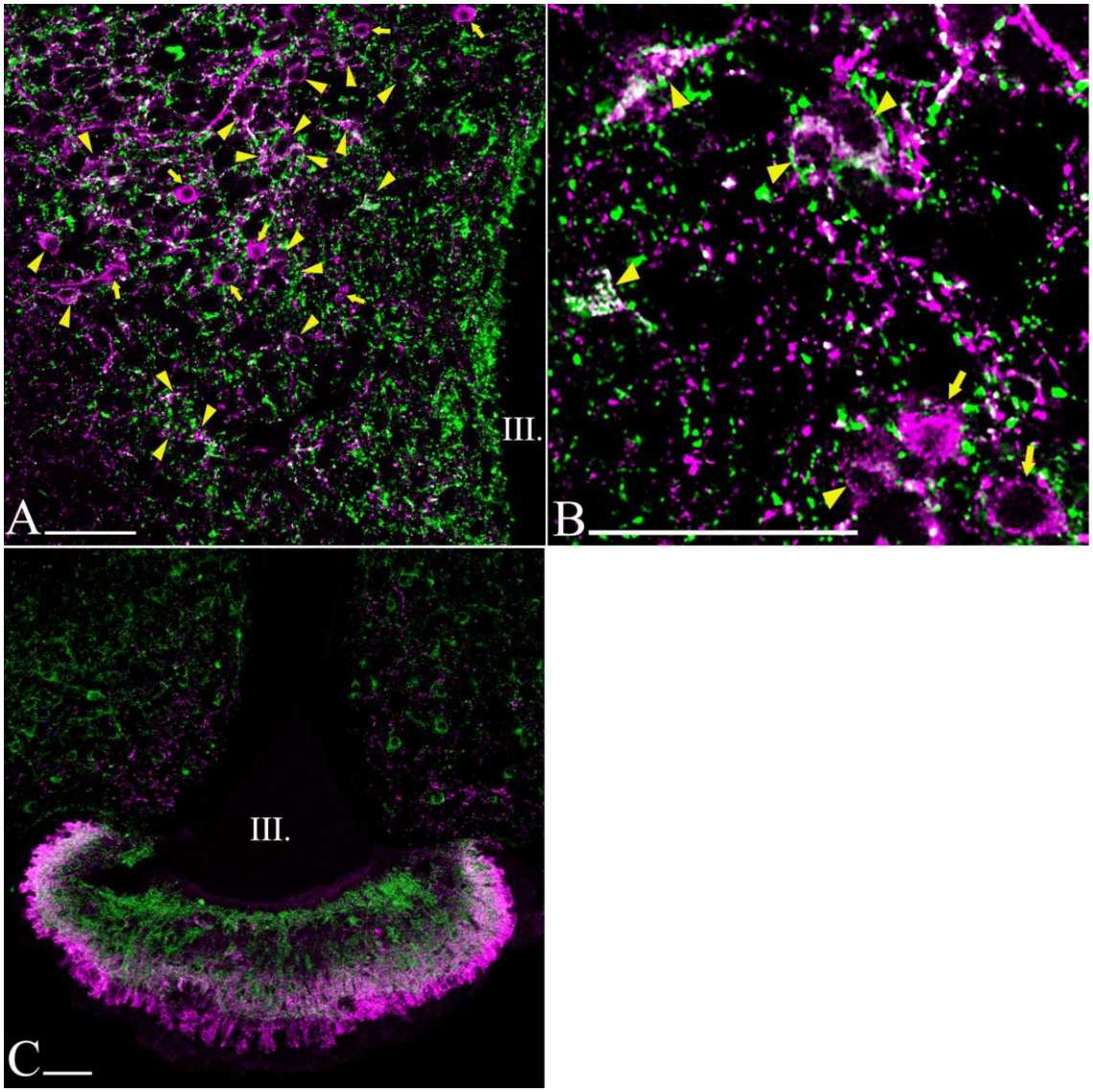

Figure 14. Co-localization of TRH with CART in the PVN and median eminence of mice. Low (A)- and high (B)-power images show co-localization of TRH (magenta) and CART (green) in the compact part of the PVN. Arrowheads indicate the double-labeled neurons, whereas arrows point to single-labeled TRH neurons. Co-localization of TRH and CART is also detected in the axon terminals of the median eminence (C). The thickness of optical slice is 1 μm in B and 2 μm in A and C. III, third ventricle; Scale bar = 50μm.

DOI:10.14753/SE.2014.1934

2. Identification of the transport route the thyroid hormone activating tanycytes and hypophysiotropic TRH neurons

2.1. Presence of MCT8 in the hypophysiotropic axon terminals in the median eminence

To determine whether the hypophysiotropic terminals are capable of accumulating T3, the distribution of MCT8 immunoreactivity was studied in the median eminence. Intense and diffuse MCT8 immunoreactivity was observed in cell bodies and processes exhibiting the characteristic distribution and morphology of tanycytes (Fig. 15A, B). In addition, punctate MCT8 immunoreactivity was detected among the tanycyte processes in the external zone of the median eminence (Fig. 15C). Ultrastructural analysis of the MCT8-IR elements in the external zone of the median eminence demonstrated strong MCT8 immunoreactivity distributed uniformly in the tanycyte processes (Fig. 16A). In addition, MCT8 immunoreactivity was also observed in axon terminals, where the silver grains focally accumulated in a segment of the axon varicosities in close proximity to the plasma membrane (Fig. 16B, C).

2.2. Co-localization of MCT8 and TRH in hypophysiotropic axon terminals

A series of double immunofluorescent labeling for MCT8 and TRH demonstrated the presence of MCT8-IR puncta on the surface of the vast majority of TRH-containing axon varicosities in the external zone of the median eminence (Fig. 17).

DOI:10.14753/SE.2014.1934

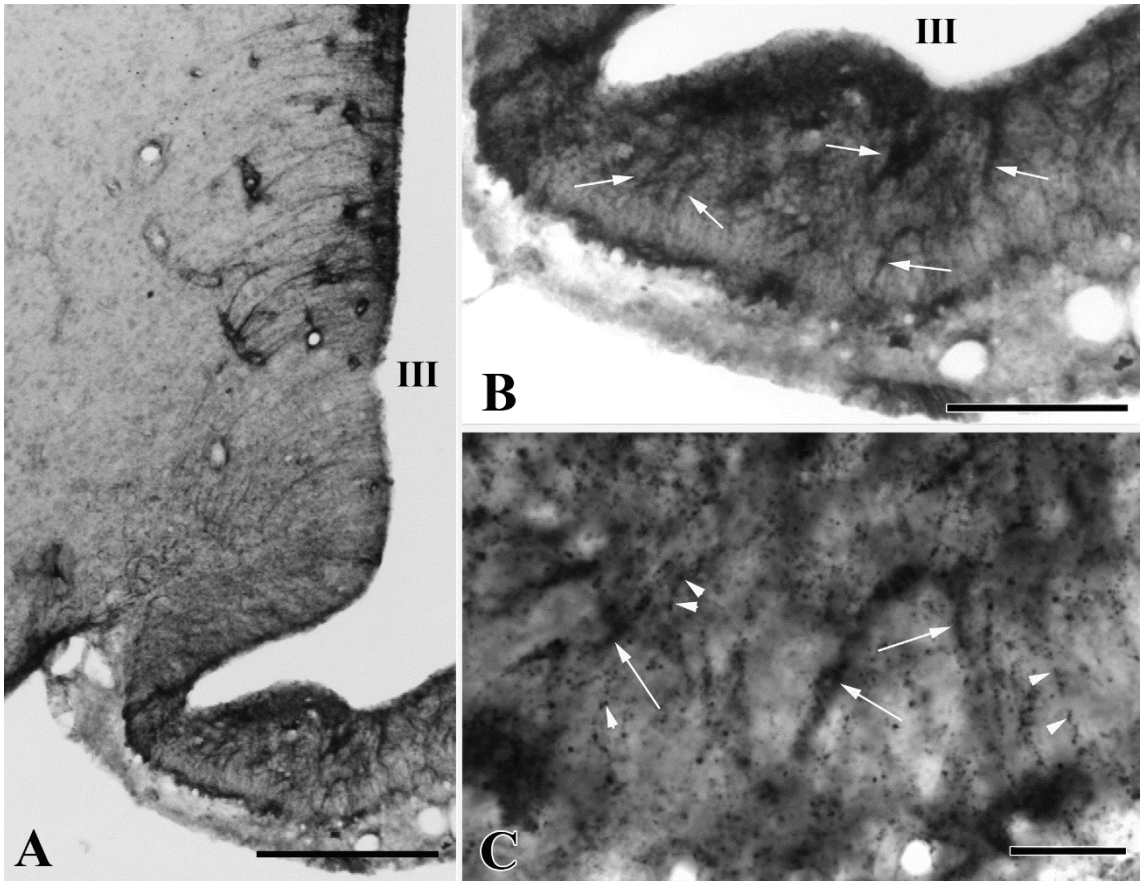

Figure 15. MCT8 immunoreactivity in the rodent mediobasal hypothalamus.
Low magnification photograph illustrates the presence of MCT8 immunoreactivity associated with tanycytes (A). In the median eminence, strong MCT8 immunoreactivity is observed in tanycyte processes (B, arrows). In addition to occurring in tanycyte processes (arrows), MCT8 immunoreactivity is also observed in small dot like structures reminiscent of axon varicosities (arrow heads) (C). III, third ventricle; Scale bars: 200 μm in A, 100 μm in B, 20 μm in C

DOI:10.14753/SE.2014.1934

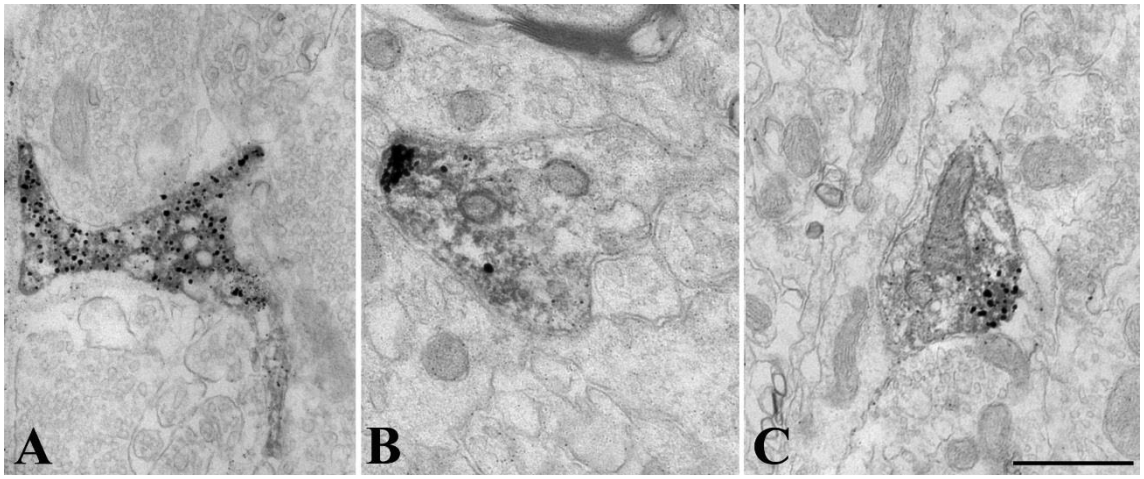

Figure 16. Ultrastructure of MCT8-IR structures in the rat median eminence.
MCT8 immunoreactivity (silver grains) is associated with tanycytes (A) and axon varicosities (B, C) in the external zone of the median eminence. In the axon varicosities, silver grains accumulate in a small region of the varicosity close to the cytoplasmic membrane (B, C). Scale bar: 500 nm.

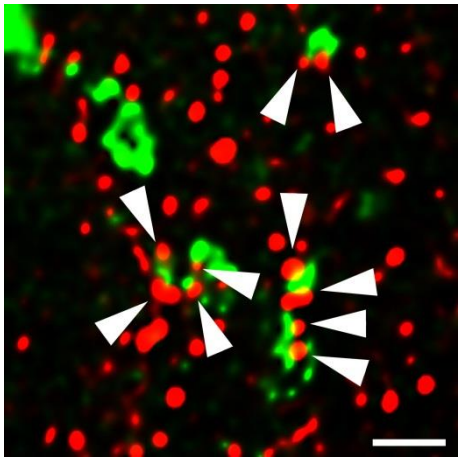

Figure 17. MCT8 immunoreactivity in axon varicosities of the rat hypophysiotropic TRH neurons.
The immunofluorescent signal for MCT8 (red) is distributed as small dots throughout the external zone of median eminence and appears (arrowheads) on the surface of TRH-immunoreactive axon varicosities (green). Scale bar: 2 μm.

3. Clarification of the mechanism causing the melanocortin resistance of hypophysiotropic TRH neurons during refeeding

3.1. AGRP- and α-MSH-IR innervation of TRH neurons

A dense network of both AGRP- and α-MSH-IR axons was observed in the PVN surrounding the TRH neurons (fig. 18A). The density of the α-MSH-containing axons was slightly higher in the rostral part of PVN, whereas the network of the AGRP-IR axons seemed to be denser in the posterior level of the PVN. In the same antero-posterior level, no difference was observed in the density of the α-MSH- and AGRP-IR axons in the medial and compact part of the PVN. Large number of AGRP- and α-MSH-IR axon varicosities formed juxtaposition with the perikarya and dendrites of the TRH neurons. In the mid level of the PVN confocal microscopic analyses identified an average of 30.9 ± 0.3 AGRP-IR and 19.3 ± 0.4 α-MSH-IR axon varicosities on the surface of TRH-IR perikarya and first order dendrites (fig. 19A). Table 2. summarizes the number and the ratio of AGRP- and α-MSH-IR boutons on the surface of TRH neurons in the PVN.

3.2. The effect of fasting on the number of α-MSH- and AGRP-IR boutons on TRH neurons

Fasting caused a marked increase in the number of AGRP-immunolabelled axon varicosities on the surface of TRH neurons (fasted *vs.* fed: 44.9 ± 0.3 *vs.* 30.9 ± 0.3 axon varicosities / TRH neuron; $P<0.001$) and decrease in the number of α-MSH-IR boutons (fasted *vs.* fed: 13.6 ± 0.7 *vs.* 19.3 ± 0.4 axon varicosities / TRH neuron; $P<0.001$) in contact with the TRH neurons in the PVN (fig. 19B). Therefore, fasting resulted in a 2.07 fold increase in the ratio of AGRP- and α-MSH-IR varicosities forming contact with the TRH neurons (fasted *vs.* fed: 3.34 ± 0.2 *vs.* 1.61 ± 0.03; $P<0.001$) (fig. 18B, 19B).

3.3. Effect of 2h vs. *24h of refeeding on the number α-MSH- and AGRP-IR boutons in contact with TRH neurons*

Two hours after the start of refeeding, the number of AGRP-IR boutons on the surface of TRH neurons differed only slightly, but significantly from the fasted values (2h refed *vs.* fasted: 46.0 ± 0.3 *vs.* 44.9 ± 0.3 axon varicosities / TRH neuron; $P=0.018$). However, the number of AGRP-IR inputs to TRH neurons was markedly elevated compared to that found in the fed animals (2h refed *vs.* fed: 46.0 ± 0.3 *vs.* 30.9 ± 0.3 axon varicosities / TRH neuron; $P<0.001$). Two hours after the onset of refeeding no significant alteration

was observed in the α-MSH-innervation of TRH neurons compared to that observed in fasted animals (2h refed *vs.* fasted: 13.9 ± 0.8 *vs.* 13.6 ± 0.7 axon varicosities / TRH neuron; P=0.746) (fig 18C, 19C). At this timepoint, the ratio of AGRP and α-MSH containing boutons was unchanged when compared to the value of the fasted animals (2h refed *vs.* fasted: 3.33 ± 0.2 *vs*. 3.34 ± 0.2; P=0.967) (fig. 18B, C). In contrast, 24 hours after the start of food consumption a marked decrease was observed in the number of AGRP-IR axon varicosities on TRH neurons, when compared to fasted animals (24h refed *vs.* fasted: 34.4 ± 0.1 *vs.* 44.9 ± 0.3 axon varicosities / TRH neuron; P<0.001), although this number was still slightly higher than fed animals (24h refed *vs.* fed: 34.4 ± 0.1 *vs.* 30.9 ± 0.3 axon varicosities / TRH neuron; P<0.001) (fig. 18D). At this timepoint, the number of α-MSH-IR boutons in contact with TRH neurons was markedly increased in comparison with that of fasted animals (24h refed *vs.* fasted: 20.9 ± 0.6 *vs.* 13.6 ± 0.7 axon varicosities / TRH neuron; P<0.001) (fig. 18D) and there was no significant difference between the α-MSH-IR innervation of TRH neurons in these mice and fed animals (24h refed *vs.* fed: 20.9 ± 0.6 *vs.* 19.3 ± 0.4 axon varicosities / TRH neuron; P=0.153). The ratio of the AGRP-IR and α-MSH-IR varicosities of TRH neurons was markedly lower than in fasted mice (24h refed *vs.* fasted: 1.64 ± 0.01 *vs.* 3.34 ± 0.2; P<0.001). In addition, no significant difference was observed in the ratio of AGRP-IR and α-MSH-IR innervation of TRH neurons, when compared to the ratio of fed animals (24h refed *vs.* fed: 1.64 ± 0.01 *vs.* 1.61 ± 0.03; P=0.866) (fig.18D, 19D).

3.4. The effect of leptin treatment on the fasting-induced rearrangement of α-MSH- and AGRP-inputs to TRH neurons

Leptin administration by subcutaneously implanted osmotic minipump completely prevented the fasting induced changes in the α-MSH-IR innervation of TRH neurons (leptin-treated fasted *vs.* fasted: 20.5 ± 0.1 *vs*. 13.6 ± 0.7 axon varicosities / TRH neuron; P<0.001; leptin-treated fasted *vs.* fed: 20.5 ± 0.1 *vs.* 19.9 ± 0.4 axon varicosities / TRH neuron; P= 0.178) and markedly attenuated the fasting induced alteration in the number of AGRP-IR boutons on the surface of these cells (leptin- treated fasted *vs.* fasted 34.4 ± 0.1 *vs.* 44.9 ± 0.3 axon varicosities / TRH neuron; P<0.001; leptin-treated fasted *vs.* fed: 34.4 ± 0.1 *vs.* 30.9 ± 0.3 axon varicosities / TRH neuron; P<0.001) (18E). This treatment also prevented the fasting-induced change in the ratio of AGRP- and α-MSH innervation

of TRH neurons (leptin-treated fasted *vs.* fasted: 1.67 ± 0.01 *vs.* 3.34 ± 0.02; P<0.001; leptin-treated fasted *vs.* fed: 1.67 ± 0.01 *vs.* 1.61 ± 0.03; P=0.939) (18A, E; 19A, E).

Table 2. Average number of α-MSH- and AGRP-IR boutons on the surface of TRH neurons.

	Control	Fasted	Refed for 2h	Refed for 24h	Fasted + leptin
AGRP	30.9 ± 0.3	44.9 ± 0.3[a]	46.0 ± 0.3[b]	34.4 ± 0.1[c]	34.4 ± 0.1 [c]
α-MSH	19.9 ± 0.4	13.6 ± 0.7[d]	13.9 ± 0.8[d]	20.9 ± 0.6[e]	20.5 ± 0.1[e]
AGRP/ α-MSH	1.61 ± 0.03	3.34 ± 0.2[d]	3.33 ± 0.2[d]	1.64 ± 0.7[e]	1.67 ± 0.01[e]

a – Significantly different from control (P<0.001), refed for 2h (P<0.05), refed for 24h (P<0.001) and leptin treated fasted (P<0.001) groups

b – Significantly different from control (P<0.001), fasted (P<0.05), refed for 24h (P<0.001) and leptin treated fasted (P<0.001) groups

c – Significantly different from control (P<0.001), fasted (P<0.001) and refed for 2h (P<0.001) groups

d – Significantly different from control (P<0.001), refed for 24h r (P<0.001) and leptin treated fasted (P<0.001) groups

e – Significantly different from fasted (P<0.01) and refed for 2h (P<0.001) groups

DOI:10.14753/SE.2014.1934

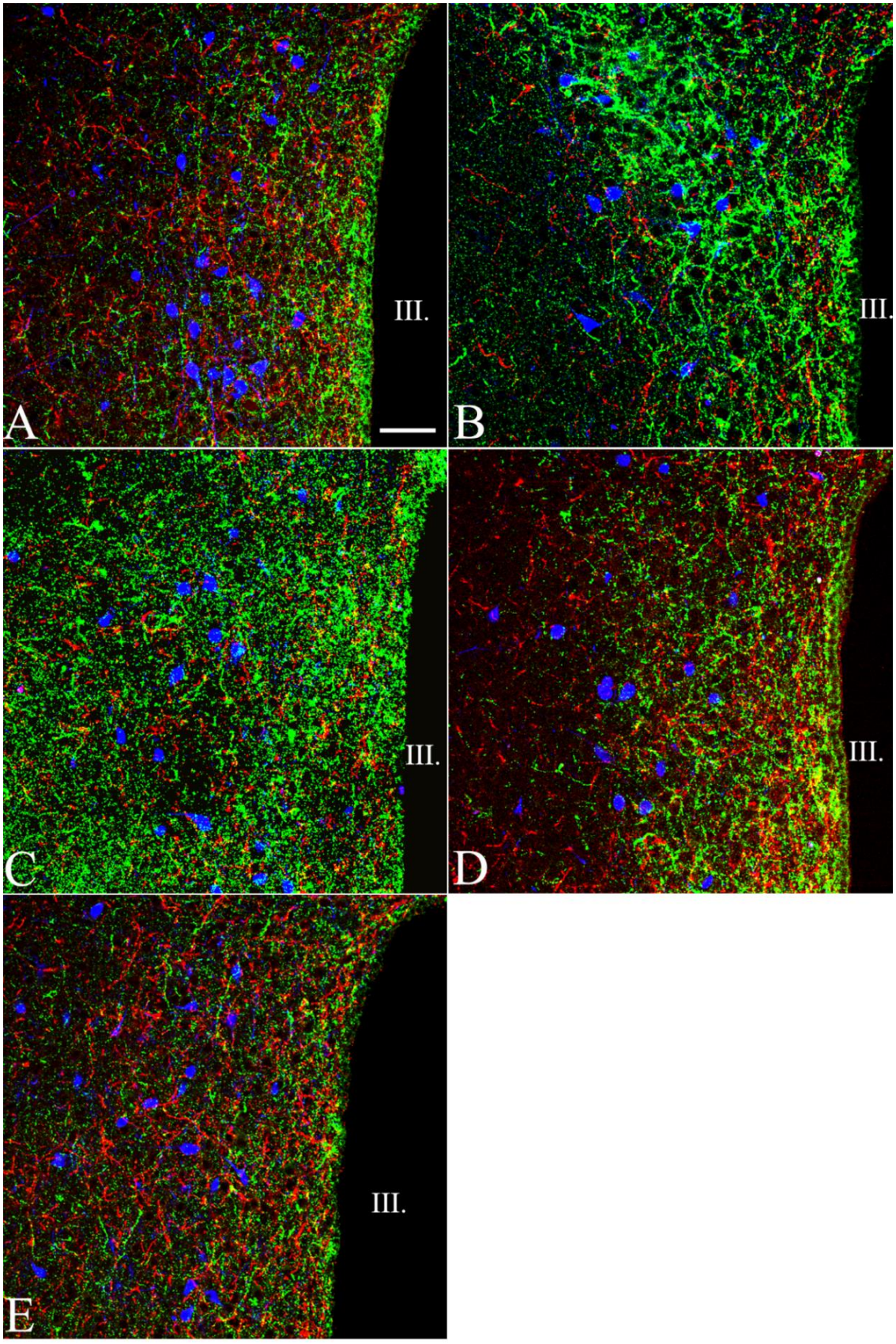

DOI:10.14753/SE.2014.1934

Figure 18. Effect of fasting and refeeding on the AGRP- (green) and α-MSH-IR (red) innervation of TRH neurons (blue) in the PVN.

Medium-power images illustrate that fasting markedly increases the density of AGRP-IR axons (green), but decreases the density of α-MSH-IR axons (red) surrounding TRH neurons (blue) in the PVN (B), compared to fed animals (A). While 2h after refeeding no remarkable change can be observed from the fasted mice (C), 24h after refeeding the axon densities are similar to those observed in the PVN of fed animals (D). Subcutaneous leptin infusion prevents the fasting-induced changes in the innervation of the PVN (E). The thickness of optical slice is 2μm. III, third ventricle. Scale bar: 50μm

DOI:10.14753/SE.2014.1934

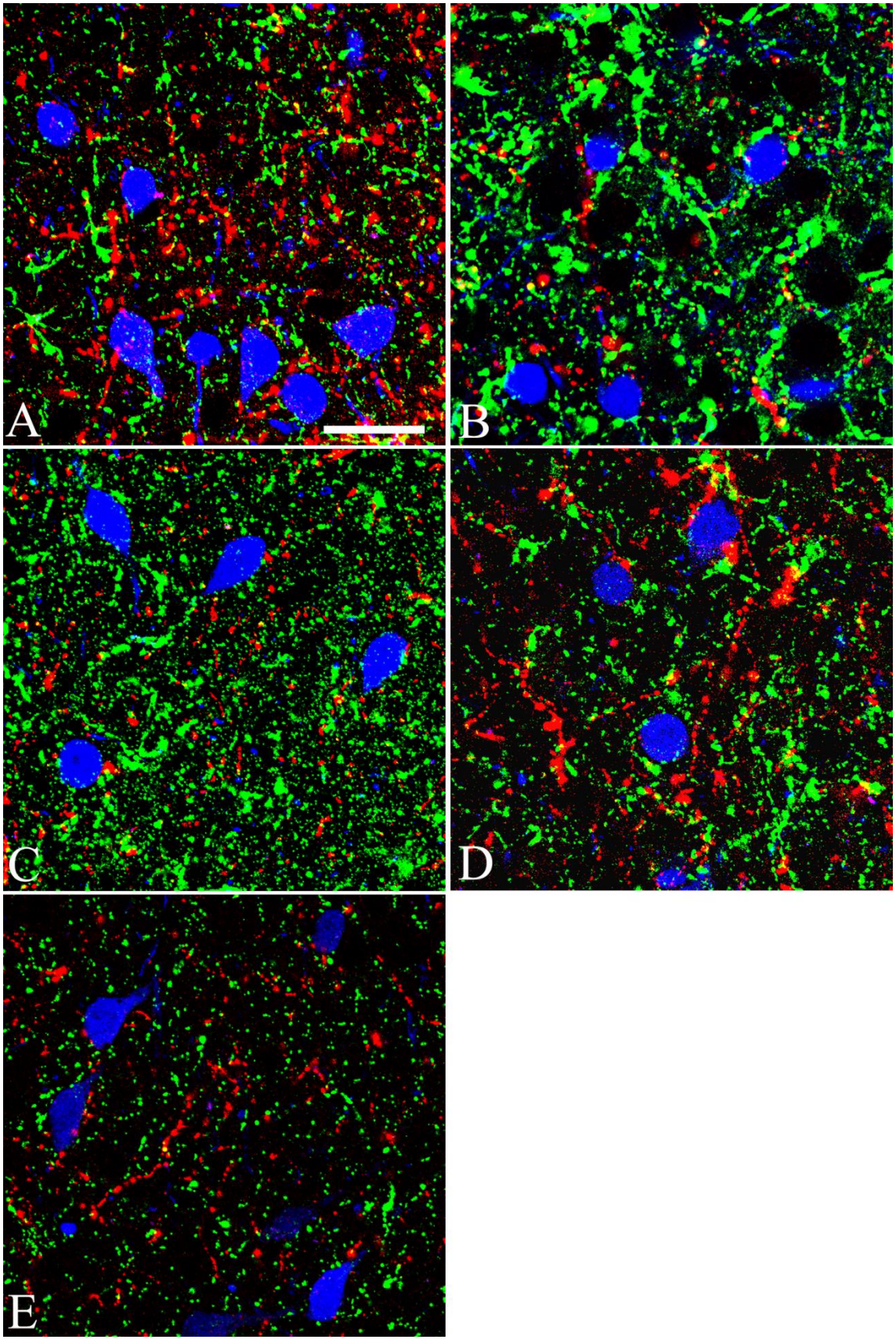

DOI:10.14753/SE.2014.1934

Figure 19. AGRP- and α-MSH-containing axon varicosities on the surface of TRH-neurons in PVN.

High magnification images demonstrate that fasting (B) resulted in an increase in the number of AGRP-IR boutons (green) on the surface of TRH neurons (blue), but decreased the number of α-MSH-IR boutons (red) compared to the values of fed animals (A). 2 h after refeeding (C) no major change was observed compared to fasted animals. 24 h after refeeding (D) the AGRP-IR innervation of TRH neurons decreased, whereas the α-MSH-IR innervation increased, in comparison with those of fasted animals. In leptin-treated mice, no fasting induced alteration was observed (E). Each optical slice represents 0.5μm thickness. Scale bar: 25μm

DOI:10.14753/SE.2014.1934

4. Development of an improved method to combinate immunocytochemistry with Nissl-staining

4.1. Effects of RNase-free immunocytochemical method on immunostaining

Two hours after refeeding, the hypothalamic nuclei including the ventral parvocellular subdivision of the ventral PVN (vPVN) showed the same distribution pattern of c-Fos-IR neurons as it was described earlier [200].

The RNase-free immunohistochemical procedure did not influence the detectability of c-Fos-IR neurons (Fig. 20A-D).

4.2. Analysis of the juxtaposition of varicosities and neurons using standard immunocytochemical method combined with Nissl-counterstaining

After standard immunocytochemistry, Nissl-counterstaining resulted in sufficient labeling of the cell nuclei, but stained the neuronal perikarya only very faintly (Fig. 20A, C, E). Numerous NPY-IR fibers were detected in the vPVN around the c-Fos containing neurons (Fig. 20A, C, E). However, due to the very faint cytoplasmic staining, the outlines of cytoplasm were not clearly visible (Fig. 20C, E). Therefore, it was not possible to safely estimate the number of c-Fos-IR neurons contacted by NPY-IR varicosities.

4.3. Analysis of the juxtaposition of varicosities and neurons in the vPVN after refeeding using RNase-free immunocytochemical method combined with Nissl-counterstaining

After RNase-free immunocytochemistry, the cresyl-violet dye stained not only the cell nuclei but also labeled the cytoplasm of neurons (Fig. 20.B, D, F). This cytoplasmic staining facilitated the identification of the different subdivisions of the PVN and the correct localization of the c-Fos-IR cell populations (Fig. 20B). In addition, the clear labeling of cytoplasm made the cell borders visible (Fig. 20F). c-Fos-IR neurons in the vPVN were contacted by numerous NPY-IR fibers (Fig. 20D, F). By quantification of the contacts, we could determine that 84.99 ± 2.35% of c-Fos-IR neurons were contacted by NPY-IR varicosities.

DOI:10.14753/SE.2014.1934

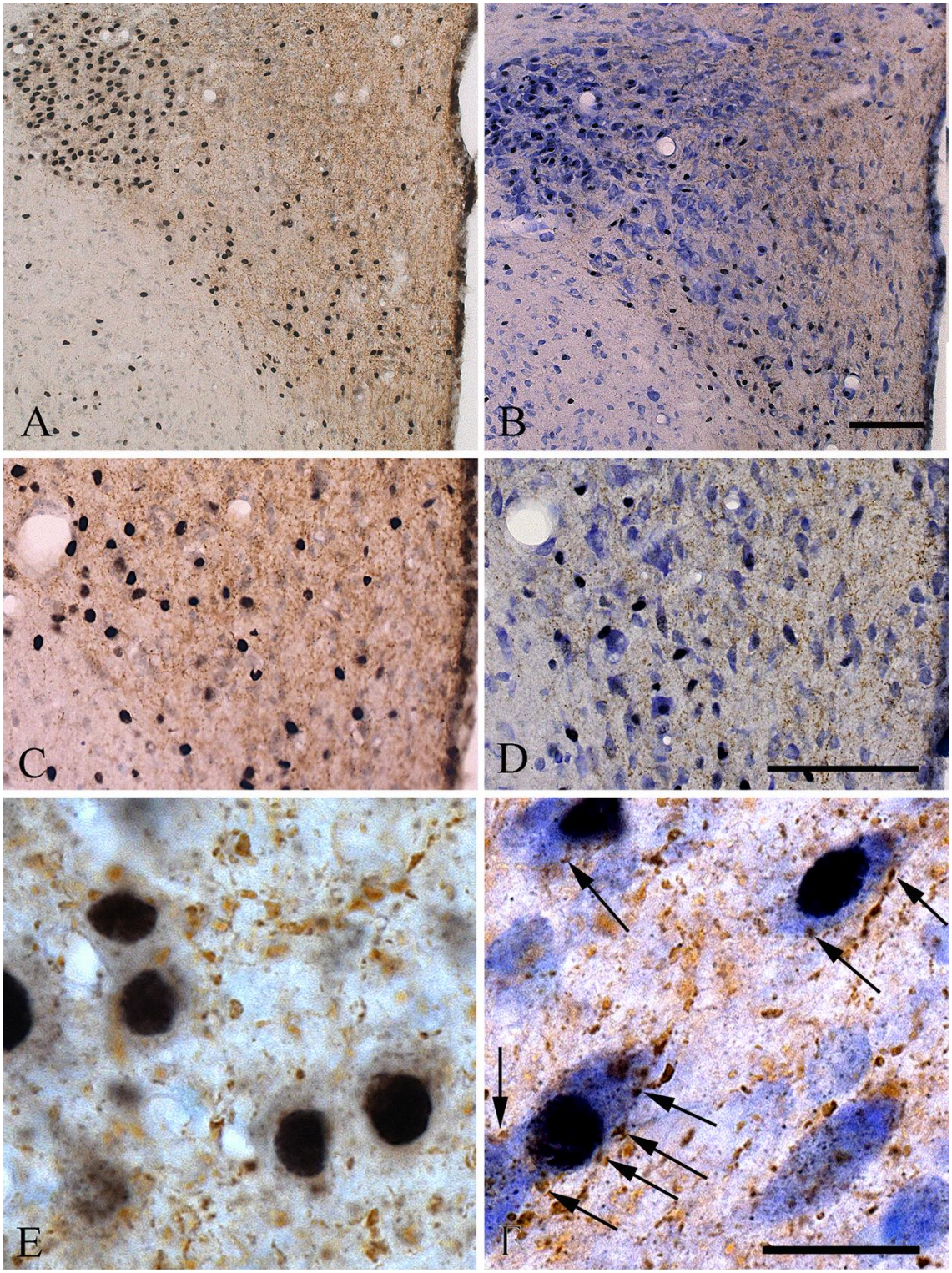

DOI:10.14753/SE.2014.1934

Figure 20. Combination of double-labeling immunocytochemistry for NPY (brown) and c-Fos (black) with Nissl-staining (violet) using standard (A, C, E) and RNase-free (B, D, F) immunocytochemical techniques on sections containing the hypothalamic paraventricular nucleus (PVN).

Rats used for this experiment were fasted for 3 days and then, refed for 2h. Low and medium power micrographs illustrate the distribution of NPY and c-Fos-IR elements in the PVN (A, B) and in the ventral parvocellular part of the PVN (C–F), respectively. The distribution of the immunocytochemical signals is identical on section immunostained with standard (A, C) or RNase-free (B, D) method. However, the Nissl-staining resulted in dominantly nuclear, and no or very weak cytoplasmic labeling using standard immunocytochemistry (A, C). In contrast, strong cytoplasmic Nissl-staining is observed after RNase-free immunocytochemistry (B, D). High-power micrographs (E, F) illustrate the relationship of NPY-IR varicosities and the c-Fos-IR neurons in the ventral parvocellular subdivision of the PVN. Note that although NPY-IR varicosities surround the c-Fos-IR neurons in both images (E, F), the cytoplasmic border of c-Fos-IR neurons and the juxtaposition of NPY-IR varicosities (arrows) to c-Fos-IR neurons can be recognized only in preparations stained with RNase-free immunocytochemistry (F). Scale bar in B = 100 μm corresponds to A and B, scale bar in D = 100 μm corresponds to C and D, scale bar ion F = 20 μm corresponds to E and F

DOI:10.14753/SE.2014.1934

VII. Discussion

1. Distribution of hypophysiotropic TRH neurons in the mouse PVN

TRH neurons were detected in all parts of the PVN of mice except the periventricular zone. This distribution markedly differs from that observed in the rat brain in which only a few TRH neurons can be identified in the magnocellular division [111]. In addition, TRH neurons are completely absent from the periventricular zone in mice, where numerous TRH neurons reside in the rat PVN [111].

The predominant localization of TRH neurons in the compact part of the PVN in mice raised the question whether these neurons have parvocellular or magnocellular phenotype. To address this issue, the co-localization of the peptides of the magnocellular neurons, the vasopressin and oxytocin, with TRH was studied by fluorescent immunocytochemistry. Although TRH-IR neurons were intermingled with vasopressin- and oxytocin-IR neurons in the compact part of the PVN, co-localization of TRH with either one of these two magnocellular peptides was not observed. In accordance with this finding, morphometric analysis of TRH- and vasopressin-IR neurons demonstrated that TRH neurons located in the magnocellular division are significantly smaller than the magnocellular, vasopressin producing neurons and not significantly different in size from TRH neurons residing in other parts of the PVN. This analysis indicates that TRH neurons in all regions of the PVN have a parvocellular phenotype. As these parvocellular neurons are intermingled with magnocellular vasopressin and oxytocin neurons in the mouse brain in a region similar to the posterior magnocellular division in the rat, the structural organization of this nucleus appears to show robust species differences in rats and mice. This observation is further supported by the morphometric analyses of the Nissl-stained preparations which showed that similar number of parvo- and magnocellular cells can be found in the compact part of the mouse PVN. Therefore, we suggest that in the mouse, this part of the PVN be termed the “compact part”, based on the high density of cells, instead of using the nomenclature adopted from rat studies. The marked differences of the mouse and the rat PVN was later confirmed by the work of Biag et al [230].

The observation that Fluoro-Gold containing hypophysiotropic TRH neurons were detected only at the mid level of the PVN further demonstrate the difference between the

PVN of the two rodent species. In particular, TRH neurons in the posterior part of the PVN that are distinctly hypophysiotropic in the rat [3, 4, 6, 112], did not concentrate Fluoro-Gold in the mouse. Furthermore, the majority of hypophysiotropic TRH neurons at the mid level of the PVN were concentrated in the compact part, with fewer neurons organized in the adjacent mid level medial part of the PVN. Similar to the rat brain [3, 4, 6, 231], however, was the absence of Fluoro-Gold in TRH neurons residing in the anterior part of the mouse PVN, establishing the non-hypophysiotropic nature of this group of neurons. In addition, similarly to observations on the rat [2], hypophysiotropic TRH neurons in the mouse also co-express CART which is present in both the perikarya in the mid level of the PVN neurons and in their axon terminals innervating the median eminence. Co-localization was only rarely observed in the anterior and posterior parts of the PVN. Similar observations were published earlier by Broberger et al. [232].

To confirm the immunocytochemical and tracing studies, we have carried out *in situ* hybridization experiments to study the effect of hypothyroidism on TRH gene expression in different subnuclei of the mouse PVN; it has been known from data obtained in rats that thyroid hormones exert negative feedback effect only on the hypophysiotropic TRH neurons. These hybridization studies on mice established that hypothyroidism only resultsin increased TRH gene expression in the compact part and in the mid level medial part of the PVN [233]. In contrast, it had no effect on TRH gene expression in the anterior and posterior parts of the PVN. It is worth emphasizing, that this observation is definitely different from the phenomenon seen in the rat in which hypothyroidism increases TRH mRNA throughout the medial and periventricular parvocellular subdivisions of the PVN with a particularly robust response in the most caudal aspect of the PVN [234].

The results of our studies indicate that the organization of the PVN and in particular, the distribution of hypophysiotropic TRH neurons, is markedly different in mice and rats. Accordingly, we propose that targeted physiological and molecular studies of hypophysiotropic TRH neurons in mice should take into consideration that these neurons are located in the compact part and in the neighboring region in the mid level of the PVN and absent from the anterior and posterior parts of the PVN.

2. A new mechanism regulating thyroid hormone availability of hypophysiotropic TRH neurons

The negative feedback effect of thyroid hormones on TRH gene expression of hypophysiotropic neurons has an essential role in the regulation of the HPT axis [112]. Studies, however, demonstrated that euthyroid concentration of peripheral T3 alone is not enough for the normal feedback regulation of the hypophysiotropic TRH neurons [136]. Conversion of T4 to T3 in the brain is also necessary for this process [136]. In the hypothalamus, the tanycytes are the primary cell type in which the conversion of T4 to T3 can be catalyzed [25]. However, tanycytes are relatively far from the PVN where the hypophysiotropic TRH neurons reside. In the median eminence, the axon terminals of the hypophysiotropic neurons and the processes of β2 tanycytes are closely associated [26].

However, it has not been clear whether or not, the axon terminals of hypophysiotropic neurons are capable of taking up thyroid hormones in the median eminence. To understand the pathway whereby T3 can reach the nuclei of hypophysiotropic TRH neurons, we studied the location and subcellular distribution of the major neuronal T3 transporter, MCT8, in hypophysiotropic neurons.

According to the literature, we have observed at light microscopic level that the tanycyte processes are highly immunoreactive for MCT8. However, we have also found punctate MCT8 immunoreactivity among the tanycyte processes in the external zone of the median eminence. Using electron microscopic examination, we have demonstrated that the punctate MCT8 immunoreactivity is associated with hypophysiotropic axon terminals. By double-labeling immunocytochemistry, we have shown that MCT8 is present in the vast majority of the TRH-containing hypophysiotropic axon terminals. This transporter is considered to be the predominant, neuronal T3 transporter, and its mutations in humans is characterized by a severe neurologic phenotype [47]. As tanycytes express MCT8, OATP1C1 thyroid hormone transporters [40, 133] and type 2 deiodinase [27, 29], they seem to be capable of accumulating T4, converting T4 to T3, and then, releasing T3 into the surrounding neuropil. As axon terminals in the external zone of the median eminence lie in close proximity to tanycyte endfeet, the observation that axon terminals of TRH neurons in the median eminence express MCT8 indicates that T3 could readily accumulate in the axon terminals of hypophysiotropic TRH neurons and then, reach the nucleus of these cells by retrograde transport. Further studies are needed to demonstrate

DOI:10.14753/SE.2014.1934

the existence of the retrograde T3 transport in the hypophysiotropic axon terminals. Of note, a very fast retrograde axonal transport of biologically active molecules, like BDNF has already been reported [235-237].

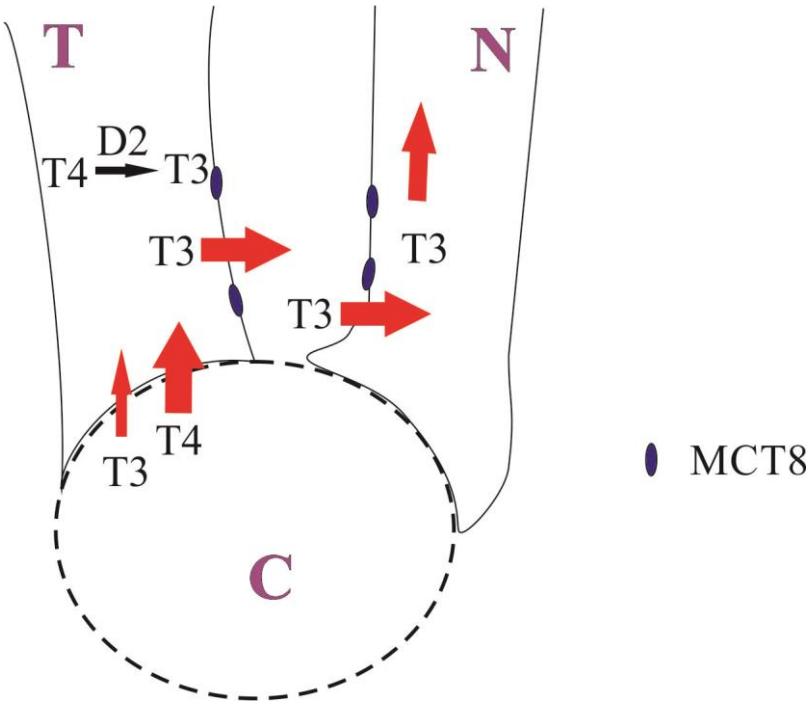

Figure 21. Schematic drawing illustrates the pathway of T3 transport from tanycytes to the hypophysiotropic TRH neurons.
Tanycytes take up T4 from the blood flow or from the CSF. Then, type 2 deiodinase, present in tanycytes converts T4 to T3. Tanycytes release this active form of THs to the surrounding neuropil. Axon terminals of the hypophysiotropic TRH neurons take up T3 with the help of an MCT8-mediated transport mechanism and allocate it by retrograde axonal transport to the perikarya of neurons located in the PVN. C=capillary, T=tanycyte, N=hypophysiotropic TRH neuron

3. Fasting-induced alterations in the α-MSH- and AGRP-IR innervation of TRH neurons: a possible mechanism of melanocortin resistance during the early phase of refeeding

Our data demonstrate that fasting results in a remarkable change in the α-MSH-IR and AGRP-IR innervation of TRH neurons. Fasting induces a significant decrease in the number of α-MSH-IR boutons on the surface of TRH neurons, and a marked increase in the innervation of these neurons by axons containing AGRP (fig. 22.)

These changes result in a two fold increase of the ratio between the inhibitory and stimulatory inputs of the TRH neurons, which may contribute to the development of fasting induced central hypothyroidism. These changes may enhance the effect of the fasting induced increase of the NPY and AGRP synthesis and the decrease of the α-MSH and CART-synthesis in the ARC neurons.

When animals are refed after fasting, the α-MSH neurons of the ARC are activated within two hours in parallel with the development of satiety after a period of vigorous food intake [200, 201]. The activation of these cells plays important role in the determination of meal size during this early period of food intake and is also critical for the refeeding-induced activation of the neurons in the ventral parvocellular subdivision of the PVN [200]. Two hours after the onset of refeeding, the pattern of the ARC input of the TRH neurons remains similar to that it is observed during fasting: increased orexigenic and decreased anorexigenic inputs. The neuropeptide content of the α-MSH-IR and AGRP-IR axons is regulated by nutritional signals. This could partly account for the differences in the immuncytochemical detection of boutons on the surface of TRH neurons under different metabolic conditions. However, while 2 hours after the onset of refeeding the α-MSH neurons are activated and the neuropeptide expression of these cells is increased [201], the number of the detected α-MSH boutons in contact with TRH neurons still remains similar as during fasting. This finding supports the concept that the observed changes of innervation pattern is due to synaptic plasticity and not to the altered peptide content of the varicosities. To provide further support to this opinion, we are currently crossing POMC-Cre mice with mice expressing miristilated GFP in Cre expressing cells. In this double transgenic mice, we can study the entire length of the axons of POMC neurons independently from the activity of cells, as the miristilated GFP labels the entire cell membrane.

After 24h of refeeding the fasting induced alterations in the AGRP- and α-MSH-IR innervation of TRH neurons become similar as observed in the fed animals. The AGRP-IR innervation of TRH neurons is decreased, whereas a marked elevation can be observed in the number of α-MSH-IR boutons on the surface of TRH neurons, compared to the early phase of refeeding.

These changes in the innervation of TRH neurons show similar timing as the changes of the TRH gene expression in the hypophysiotropic neurons [201]. While after two hours of refeeding, both the ARC input to TRH neurons and the expression of TRH in the hypophysiotropic neurons are similar to those of fasted animals, both parameters return to fed levels 24h after refeeding. Therefore, we propose that the fasting-induced alterations of the α-MSH-innervation of the TRH neurons contributes to the inability of the activated α-MSH neurons to stimulate TRH gene expression during the early phase of refeeding. Since α-MSH neurons activate the neuron population in the vPVN [200, 201] it seems that the neuron populations of the PVN involved in food intake and energy expenditure are differentially regulated by melanocortins during the early phase of refeeding. In accordance with the differential activation of these hypothalamic cell groups, food intake is inhibited 2h after the onset of refeeding, but the energy expenditure increases only after 24h [201]. Therefore the melanocortin resistance of TRH neurons during the early phase of refeeding may facilitate the restoration of depleted energy stores after fasting, while the rapid decrease of food intake after meal protects the gastrointestinal tract from overdistension.

Since leptin is the main nutritional signal that regulates the hypophysiotropic TRH neurons as well as the energy homeostasis related neuronal groups of the ARC [165], we studied whether or not leptin administration can prevent the fasting induced alteration in the AGRP-IR and α-MSH-IR innervations of TRH neurons. To prevent the fasting induced fall in circulating leptin levels, leptin was continuously administered during fasting by subcutaneously implanted osmotic minipump. Although fasting resulted in a slight, but significant increase of the number of AGRP-containing axon varicosities in contact with the surface of TRH neurons even in the leptin-treated mice, this increase was markedly attenuated compared to the effect of fasting observed in the saline-treated animals. In addition, leptin treatment completely prevented the fasting-induced decrease of the number of α-MSH-IR boutons in contact with TRH neurons. Altogether, fasting

did not alter the ratio between the AGRP-IR and the α-MSH-IR innervation of TRH neurons in leptin treated animals. These data demonstrate that leptin regulates the hypophysiotropic TRH neurons by exerting multiple effects on ARC neurons. Leptin alters the gene expression of feeding-related peptides in these cells of the ARC [165], and influences their electrophysiological activity [202], and at the same time also causes synaptic plasticity in the arcuato-paraventricular pathway [202, 203]. However, the finding that the number of AGRP-boutons in leptin treated fasted mice slightly differs from the fed values suggests that the innervation of TRH neurons by AGRP neurons might be also regulated by other signaling molecules.

The signaling pathways mediating the effects of the changes of leptin levels on the axonal sprouting and retraction are currently unknown, but one potential mediator could be the phosphatidylinositol 3-kinase – mammalian target of rapamycin (PI3K-mTOR) pathway. Leptin is known to upregulate both PI3K and mTOR in the feeding related neurons of the ARC [238]. The critical role of the PI3K was demonstrated in the leptin induced axonal growth during development in embryonic hippocampal neurons [239]. mTOR has also been shown to stimulate axonal growth after nerve injury [239]. In contrast, the inhibition of mTOR signalization by rapamycin induces the autophagy to axons in the CNS [240]. During fasting the fall in circulating levels of leptin may induce autophagy in POMC neurons by the inhibition of PI3K-mTOR pathway, whereas the increase in the leptin level during refeeding activates the PI3K-mTOR pathway in α-MSH synthesizing neurons [241] to contribute to the regrowth of axons in the PVN. Since leptin similarly regulates the PI3K-mTOR pathway in the AGRP/NPY and the α-MSH/CART neurons [241, 242], but has opposite effect on the axonal growth of these cells [203], it is likely that the leptin-mediated synaptic plasticity in the AGRP/NPY neurons are regulated by different intracellular pathways.

DOI:10.14753/SE.2014.1934

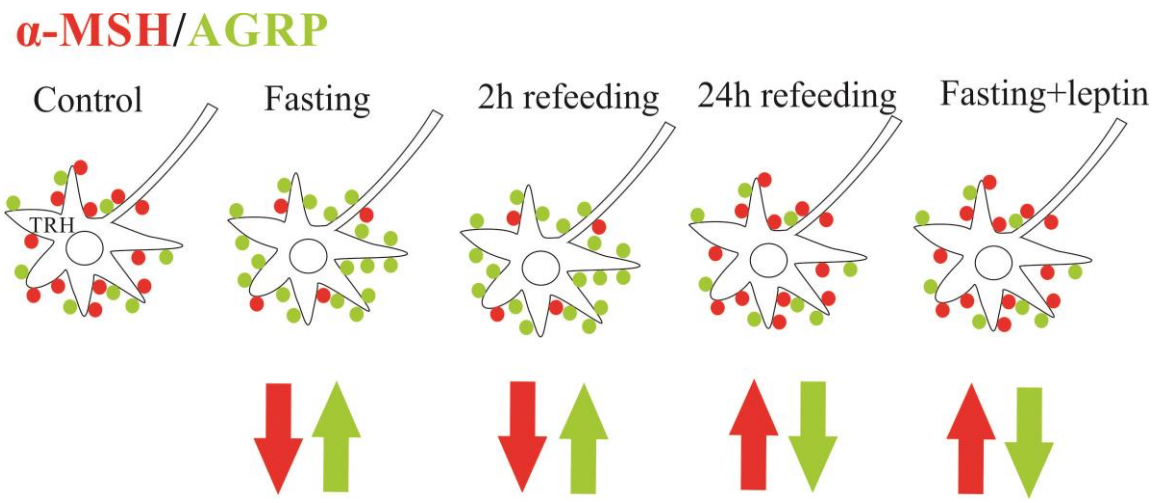

Figure 22. Schematic drawing illustrates the reorganization of the α-MSH- and AGRP-innervation of TRH neurons in different metabolic stages.
Fasting induces an increase in the number of AGRP-IR axon varicosities on the surface of TRH neurons and decreases the number of α-MSH-containing boutons in contact with these neurons. The fasting-induced alteration in the AGRP- and α-MSH-innervation of TRH neurons lasts at least 2h after the start of refeeding. 24h after the start of refeeding a dramatic decrease can be observed in the number of AGRP-boutons on the surface of TRH neurons, whereas the number of α-MSH boutons on TRH neurons is increased. Leptin markedly decreases the number of AGRP-IR axon varicosities in contact with TRH neurons and completely prevents the fasting induce fall in the α-MSH innervation of TRH neurons.

4. The effect of RNase-free immunocytochemical treatment on the cytoplasmic staining with Nissl-dyes

The Nissl-staining combined with immunocytochemistry could be a very useful histological method for the identification of the connections between neuronal perikarya and chemically identified axon varicosities. Unfortunately, Nissl-dyes tend to stain primarily the cell nuclei with only faint labeling of the cytoplasm of the neurons after immunocytochemical detection of antigens. Since the basic dyes bind to the nucleic acid content of cells and RNase treatment during the posthybridization step of *in situ* hybridization also results in the loss of the cytoplasmic staining with the basic dyes [243], we hypothesized that the RNasee contamination of the solutions used for

immunocytochemistry may be the reason for the lack of the labeling of Nissl bodies with basic dyes. This hypothesis is also supported by data showing that immunocytochemistry results in damage of RNA in samples processed for microarray analyses [244]. To test this hypothesis, we have used DEPC-treated, autoclaved buffers and RNase-free glassware for all steps of immunocytochemistry. To further prevent the potential RNase contaminations, the RNase inhibitor heparin was added to all antibody containing solutions. The RNase-free conditions slightly decreased the sensitivity of the immunocytochemistry, but it could be compensated for by using an increased primary antibody concentration. This effect of RNase-free conditions is probably due to the protease activity of heparin. The distribution of the immunoreaction products was not influenced by the treatment. The RNase-free conditions, however, markedly changed the result of the counterstaining. The Nissl-staining strongly labeled the cytoplasm of the neurons and also resulted in a slightly more intense nuclear labeling. The combination of RNase-free immunocytochemistry and Nissl-staining can be a very useful approach when precise localization of immunostained neuronal elements is necessary: mapping the localization of new peptides, proteins, identifying regions where anterogradely or retrogradely-labeled structures can be found [245] or mapping the localization of activated neurons using c-Fos as a marker [246]. In addition, the strong cytoplasmic labeling of neurons with Nissl-staining can be helpful, when the innervation of a cell group is studied at light microscopic level and the neuronal population is identified based on a marker that is localized in the nucleus of cells, like nuclear receptors and transcription factors. As an example, we show that it is very difficult to determine at light microscopic level whether the NPY-IR varicosities are juxtaposed to the surface of the c-Fos-IR neurons in the ventral parvocellular subdivision of the PVN when the cytoplasm of cells is not or very faintly stained. Due to the lack of the cytoplasmic staining, the borders of the c-Fos expressing cells can not be visualized. In contrast, when RNase-free double-labeling immunocytochemistry is combined with Nissl-staining, the brown DAB, the dark blue Ni-DAB and the purple Nissl-staining that strongly labels the cytoplasm of neurons can be easily distinguished. Therefore, the juxtaposition of NPY-IR varicosities to the c-Fos-IR neurons in the vPVN can be easily detected and quantified. Using this method we observed that in the vPVN 84.99 ± 2.35% of the c-Fos expressing neurons are contacted by NPY-IR fibers. In summary, we conclude that when standard immunocytochemistry

DOI:10.14753/SE.2014.1934

is combined with Nissl-staining, the loss of the cytoplasmic RNA content of neurons results in the lack of cytoplasmic labeling with the Nissl-staining. In contrast, combination of RNase-free immunocytochemistry with Nissl-staining preserves the RNA content of neurons and results in a strong cytoplasmic counterstaining that can facilitate mapping of immunostained neurons or the light microscopic examination of the innervation of cells characterized by their nuclear protein content.

DOI:10.14753/SE.2014.1934

VIII. Conclusions

In summary, the organization of the PVN in mice is markedly different from that observed in rats. The so called magnocellular part of this nucleus contains approximately equal numbers of parvo- and magnocellular neurons. Therefore, we suggest to call this part of the PVN compact part based on the high concentration of neurons in this division. The distribution of hypophysiotropic TRH neurons is also different in mice than in rats. These neurons are located exclusively in the mid level of PVN. Only a few hypophysiotropic TRH neurons were found in the anterior level of PVN, whereas this neuron type was absent from the posterior level of the nucleus. Interestingly, no hypophysiotropic TRH neuron was found in the periventricular zone of PVN of mice though numerous hypophysiotropic TRH neurons are located in this zone of PVN in rats. In mice, most of the hypophysiotropic TRH neurons are located in the compact part intermingled with magnocellular neurons, but no co-localization of TRH and AVP or OT was observed. Based on their size, all hypophysiotropic TRH neurons are parvocellular cells. The distribution of the hypophysiotropic and CART expressing TRH neurons overlap, suggesting that hypophysiotropic TRH neurons express CART in mice similarly to the observations in rats.

The presence of MCT8 thyroid hormone transporter on the terminals of hypophysiotropic TRH neurons in the median eminence suggests that these terminals can take up T3 from the extracellular space of the median eminence and likely transport it to the nucleus of hypophysiotropic TRH neurons. As the median eminence is located outside of the BBB and contains D2 expressing tanycytes, the origin of the T3 content of this brain region is unique: it derives from both the peripheral blood and the tanycytes. Therefore, the hypophysiotropic TRH neurons can be directly influenced by the changes of peripheral T3 concentration, but also by the activity of tanycytes. This gives high flexibility to the feedback regulation of TRH neurons.

In addition to the effects of fasting and leptin on the activity of the feeding related neurons of the ARC, the nutritional signals may also influence the hypophysiotropic TRH neurons by inducing synaptic plasticity in the arcuato-paraventricular pathway. The fasting induced increase of the AGRP- and decrease of the α-MSH-innervation of TRH neurons may facilitate the fasting induced inhibition of the hypophysiotropic TRH neurons. Since

DOI:10.14753/SE.2014.1934

this change of the innervation pattern lasts at least 2 hours after the onset of refeeding, it may contribute to the melanocortin resistance of TRH neurons during this early phase of refeeding. 24 hours after the start of refeeding the ratio between the AGRP- and α-MSH-innervation of TRH neurons reverts to fed level coincidently with the normalization of TRH expression. Leptin administration prevents the fasting-induced changes in the ratio between AGRP- and α-MSH-innervation of TRH neurons, suggesting that leptin is the main factor that regulates the plasticity of the synaptic input of TRH neurons.

Our data demonstrate that the RNase contamination of materials used for immunocytochemistry contributes to the decrease of cytoplasmic labeling of neurons with basic dyes when Nissl-staining is combined with immunocytochemistry. The application of RNase-free techniques, therefore, can highly assist the detection of the cytoplasm with Nissl-staining and facilitate the examination of the neuronal inputs of neurons identified by their nuclear protein content.

DOI:10.14753/SE.2014.1934

IX. Summary

Since the exact location of hypophysiotropic TRH neurons within the PVN of mice was unknown we have mapped the location of these cells. Hypophysiotropic TRH neurons were observed mainly at the mid level of the PVN, primarily in the compact part. In this part of the PVN, TRH-neurons were mixed with oxytocin and vasopressin neurons, but based on their size, the TRH neurons were parvocellular and did not contain magnocellular neuropeptides. Co-localization of TRH and CART were observed only in areas where hypophysiotropic TRH neurons were located. These data demonstrate that the localization of hypophysiotropic TRH neurons is highly different, while their peptide content is similar in mice and rats. Thyroid hormones have negative feedback effect on the TRH expression of hypophysiotropic neurons, but the route by which T3 can reach the TRH neurons was unknown. By immunocytochemistry, we have detected the presence of MCT8 in the hypophysiotropic TRH-containing axon terminals in the median eminence (ME) that suggests that T3 released by tanycytes or originating from the peripheral circulation may be taken up by axons of the hypophysiotropic TRH neurons in the ME and transported retrogradely to the perykarya in the PVN. For the identification of fasting- and refeeding-induced synaptic plasticity of the input of TRH neurons, the number of AGRP- and α-MSH-IR boutons on the surface of TRH neurons was studied by immunocytochemistry in different metabolic stages. Since AGRP acts as a melanocortin antagonist, the ratio between AGRP and α-MSH may has critical role in the regulation of TRH expression. Fasting resulted a dramatic increase in this ratio that was still high 2 hours following the start of refeeding. This alteration in the innervation of TRH neurons may contribute to the melanocortin resistance of these neurons during the early phase of refeeding. 24 hours after the the start of refeeding the ratio of AGRP- and α-MSH-innervation of TRH neurons reaches the fed value coincidently with the activation of TRH neurons. Leptin administration prevented the fasting-induced alteration of the ratio of AGRP- and α-MSH-innervation of TRH neurons.

To facilitate the identification of neuronal networks the method of Nissl-staining combined with immunocytochemistry was improved. The lack of cytoplasmic staining by Nissl-dyes after standard immunocytochemistry was completely prevented by RNase-free conditions of immunocytochemistry.

DOI:10.14753/SE.2014.1934

X. Összefoglalás

Mivel a hipofiziotróf TRH-idegsejtek pontos elhelyezkedése az egér hypothalamusban eddig nem volt ismert, feltérképeztük-e sejtek megoszlását e fajban. Hipofiziotróf TRH idegsejteket elsősorban a PVN középső síkjának kompakt részén figyeltünk meg, ahol e sejtek oxitocin- és vazopresszin-idegsejtekkel keveredve fordultak elő. Ugyanakkor e TRH-idegsejtek mérete a parvocelluláris tartományba esett és a magnocelluláris neuropeptidek sem voltak bennük jelen. A CART és TRH ko-lokalizációja a hipofiziotróf TRH-idegsejtekével elhelyezkedésével mutatott hasonló megoszlást. Adataink arra utalnak, hogy a hipofiziotróf TRH idegsejtek megoszlása jelentősen eltér, de peptid tartalma hasonló egérben és patkányban. Noha a T3 ismerten negatív visszacsatolással hat a TRH expresszióra, eddig az útvonal, melyen keresztül a T3 eljut a TRH-idegsejtekhez ismeretlen volt. Immuncitokémia segítségével kimutattuk, hogy a hipofiziotróf TRH-idegsejtek eminencia mediánában (ME) elhelyezkedő axonvégződései tartalmazzák a T3 fő neuronális transzporter molekuláját, az MCT8-at, ami arra utal, hogy a taniciták által felszabadított és a keringésből az ME-be jutó T3-at is képesek a hipofiziotróf TRH-idegsejtek axonvégződései felvenni, majd valószínűleg retrográd transzporttal e sejtek sejttestébe eljuttatni. Az éhezés és újratáplálás hatására létrejövő szinaptikus átrendeződések megfigyelése érdekében megvizsgáltuk a TRH-idegsejtek felszínén elhelyezkedő AGRP- és α-MSH-IR boutonok számát különböző tápláltsági állapotokban. Mivel az AGRP az α-MSH antagonistájaként hat, e két beidegzés aránya kulcsfontosságú lehet a TRH expresszió szabályozásában. Ez az arány éhezés hatására jelentősen megnőtt és magas maradt még két órával az úratáplálás megkezdését követően is, ami magyarázhatja ezen időszakban a TRH sejtek melanokortinnal szembeni rezisztenciáját. 24 óra elteltével, mikorra a TRH-idegsejtek aktiválódnak az AGRP- és α-MSH-beidegzésük aránya normalizálódott. A TRH-idegsejtek beidegzésének éhezésbeli változása leptin adásával kivédhető volt.

Továbbá, az ideghálózatok feltérképezésének megkönnyítése érdekében kidolgoztuk az immuncitokémiával kombinált Nissl-festés olyan változatát, melyben az RNáz-mentes körülmények közt végzett immuncitokémiai eljárással kiküszöböltük a citoplazmatikus festődés hiányát, mely a hagyományos immuncitokémia után általánosan előforduló jelenség.

XI. References

1. Reichlin, S. (1989) TRH: historical aspects, *Annals of the New York Academy of Sciences.* **553**, 1-6.

2. Fekete, C., Mihaly, E., Luo, L. G., Kelly, J., Clausen, J. T., Mao, Q., Rand, W. M., Moss, L. G., Kuhar, M., Emerson, C. H., Jackson, I. M. & Lechan, R. M. (2000) Association of cocaine- and amphetamine-regulated transcript-immunoreactive elements with thyrotropin-releasing hormone-synthesizing neurons in the hypothalamic paraventricular nucleus and its role in the regulation of the hypothalamic-pituitary-thyroid axis during fasting, *The Journal of neuroscience : the official journal of the Society for Neuroscience.* **20**, 9224-34.

3. Merchenthaler, I. & Liposits, Z. (1994) Mapping of thyrotropin-releasing hormone (TRH) neuronal systems of rat forebrain projecting to the median eminence and the OVLT. Immunocytochemistry combined with retrograde labeling at the light and electron microscopic levels, *Acta biologica Hungarica.* **45**, 361-74.

4. Simmons, D. M. & Swanson, L. W. (2009) Comparison of the spatial distribution of seven types of neuroendocrine neurons in the rat paraventricular nucleus: toward a global 3D model, *The Journal of comparative neurology.* **516**, 423-41.

5. Lechan, R. M. & Fekete, C. (2006) The TRH neuron: a hypothalamic integrator of energy metabolism, *Progress in brain research.* **153**, 209-35.

6. Ishikawa, K., Taniguchi, Y., Inoue, K., Kurosumi, K. & Suzuki, M. (1988) Immunocytochemical delineation of thyrotrophic area: origin of thyrotropin-releasing hormone in the median eminence, *Neuroendocrinology.* **47**, 384-8.

7. Bernal, J., Guadano-Ferraz, A. & Morte, B. (2003) Perspectives in the study of thyroid hormone action on brain development and function, *Thyroid : official journal of the American Thyroid Association.* **13**, 1005-12.

8. Cannon, B. & Nedergaard, J. (2004) Brown adipose tissue: function and physiological significance, *Physiological reviews.* **84**, 277-359.

9. Luo, L. & MacLean, D. B. (2003) Effects of thyroid hormone on food intake, hypothalamic Na/K ATPase activity and ATP content, *Brain research.* **973**, 233-9.

10. Silva, J. E. (2003) The thermogenic effect of thyroid hormone and its clinical implications, *Annals of internal medicine.* **139**, 205-13.

11. Williams, G. R. (2008) Neurodevelopmental and neurophysiological actions of thyroid hormone, *Journal of neuroendocrinology.* **20**, 784-94.

12. Dunn, J. T. (1995) Thyroglobulin, hormone synthesis and thyroid disease, *European journal of endocrinology / European Federation of Endocrine Societies.* **132**, 603-4.

13. Gereben, B., Zavacki, A. M., Ribich, S., Kim, B. W., Huang, S. A., Simonides, W. S., Zeold, A. & Bianco, A. C. (2008) Cellular and molecular basis of deiodinase-regulated thyroid hormone signaling, *Endocrine reviews.* **29**, 898-938.

14. Lechan, R. M. & Fekete, C. (2005) Role of thyroid hormone deiodination in the hypothalamus, *Thyroid : official journal of the American Thyroid Association.* **15**, 883-97.

15. Gereben, B., Zeold, A., Dentice, M., Salvatore, D. & Bianco, A. C. (2008) Activation and inactivation of thyroid hormone by deiodinases: local action with general consequences, *Cellular and molecular life sciences : CMLS.* **65**, 570-90.

16. Bianco, A. C., Salvatore, D., Gereben, B., Berry, M. J. & Larsen, P. R. (2002) Biochemistry, cellular and molecular biology, and physiological roles of the iodothyronine selenodeiodinases, *Endocrine reviews.* **23**, 38-89.

17. Kohrle, J. (1999) Local activation and inactivation of thyroid hormones: the deiodinase family, *Molecular and cellular endocrinology.* **151**, 103-19.

18. Arrojo, E. D. R. & Bianco, A. C. (2011) Type 2 deiodinase at the crossroads of thyroid hormone action, *The international journal of biochemistry & cell biology.* **43**, 1432-41.

19. Schneider, M. J., Fiering, S. N., Thai, B., Wu, S. Y., St Germain, E., Parlow, A. F., St Germain, D. L. & Galton, V. A. (2006) Targeted disruption of the type 1 selenodeiodinase gene (Dio1) results in marked changes in thyroid hormone economy in mice, *Endocrinology.* **147**, 580-9.

20. St Germain, D. L. & Galton, V. A. (1997) The deiodinase family of selenoproteins, *Thyroid : official journal of the American Thyroid Association.* **7**, 655-68.

21. Campos-Barros, A., Hoell, T., Musa, A., Sampaolo, S., Stoltenburg, G., Pinna, G., Eravci, M., Meinhold, H. & Baumgartner, A. (1996) Phenolic and tyrosyl ring iodothyronine deiodination and thyroid hormone concentrations in the human central nervous system, *The Journal of clinical endocrinology and metabolism.* **81**, 2179-85.

22. Visser, T. J., Leonard, J. L., Kaplan, M. M. & Larsen, P. R. (1982) Kinetic evidence suggesting two mechanisms for iodothyronine 5'-deiodination in rat cerebral cortex, *Proceedings of the National Academy of Sciences of the United States of America.* **79**, 5080-4.

23. Banks, W. A., Kastin, A. J. & Michals, E. A. (1985) Transport of thyroxine across the blood-brain barrier is directed primarily from brain to blood in the mouse, *Life sciences.* **37**, 2407-14.

24. Crantz, F. R., Silva, J. E. & Larsen, P. R. (1982) An analysis of the sources and quantity of 3,5,3'-triiodothyronine specifically bound to nuclear receptors in rat cerebral cortex and cerebellum, *Endocrinology.* **110**, 367-75.

25. Fonseca, T. L., Correa-Medina, M., Campos, M. P., Wittmann, G., Werneck-de-Castro, J. P., Arrojo e Drigo, R., Mora-Garzon, M., Ueta, C. B., Caicedo, A., Fekete, C., Gereben, B., Lechan, R. M. & Bianco, A. C. (2013) Coordination of hypothalamic and pituitary T3 production regulates TSH expression, *The Journal of clinical investigation.* **123**, 1492-500.

26. Rodriguez, E. M., Blazquez, J. L., Pastor, F. E., Pelaez, B., Pena, P., Peruzzo, B. & Amat, P. (2005) Hypothalamic tanycytes: a key component of brain-endocrine interaction, *International review of cytology.* **247**, 89-164.

27. Tu, H. M., Kim, S. W., Salvatore, D., Bartha, T., Legradi, G., Larsen, P. R. & Lechan, R. M. (1997) Regional distribution of type 2 thyroxine deiodinase messenger ribonucleic acid in rat hypothalamus and pituitary and its regulation by thyroid hormone, *Endocrinology.* **138**, 3359-68.

28. Guadano-Ferraz, A., Escamez, M. J., Rausell, E. & Bernal, J. (1999) Expression of type 2 iodothyronine deiodinase in hypothyroid rat brain indicates an important role of thyroid hormone in the development of specific primary sensory systems, *The Journal of neuroscience : the official journal of the Society for Neuroscience.* **19**, 3430-9.

29. Guadano-Ferraz, A., Obregon, M. J., St Germain, D. L. & Bernal, J. (1997) The type 2 iodothyronine deiodinase is expressed primarily in glial cells in the neonatal rat brain, *Proceedings of the National Academy of Sciences of the United States of America.* **94**, 10391-6.

30. Bianco, A. C. (2011) Minireview: cracking the metabolic code for thyroid hormone signaling, *Endocrinology.* **152**, 3306-11.

31. Tu, H. M., Legradi, G., Bartha, T., Salvatore, D., Lechan, R. M. & Larsen, P. R. (1999) Regional expression of the type 3 iodothyronine deiodinase messenger ribonucleic acid in the rat central nervous system and its regulation by thyroid hormone, *Endocrinology.* **140**, 784-90.

32. Huang, S. A., Dorfman, D. M., Genest, D. R., Salvatore, D. & Larsen, P. R. (2003) Type 3 iodothyronine deiodinase is highly expressed in the human uteroplacental unit and in fetal epithelium, *The Journal of clinical endocrinology and metabolism.* **88**, 1384-8.

33. Hennemann, G., Docter, R., Friesema, E. C., de Jong, M., Krenning, E. P. & Visser, T. J. (2001) Plasma membrane transport of thyroid hormones and its role in thyroid hormone metabolism and bioavailability, *Endocrine reviews.* **22**, 451-76.

34. Visser, W. E., Friesema, E. C. & Visser, T. J. (2011) Minireview: thyroid hormone transporters: the knowns and the unknowns, *Molecular endocrinology.* **25**, 1-14.

35. Hagenbuch, B. (2007) Cellular entry of thyroid hormones by organic anion transporting polypeptides, *Best practice & research Clinical endocrinology & metabolism.* **21**, 209-21.

36. van der Deure, W. M., Hansen, P. S., Peeters, R. P., Kyvik, K. O., Friesema, E. C., Hegedus, L. & Visser, T. J. (2008) Thyroid hormone transport and metabolism by organic anion transporter 1C1 and consequences of genetic variation, *Endocrinology.* **149**, 5307-14.

37. Chu, C., Li, J. Y., Boado, R. J. & Pardridge, W. M. (2008) Blood-brain barrier genomics and cloning of a novel organic anion transporter, *Journal of cerebral blood flow and metabolism : official journal of the International Society of Cerebral Blood Flow and Metabolism.* **28**, 291-301.

38. Sugiyama, D., Kusuhara, H., Taniguchi, H., Ishikawa, S., Nozaki, Y., Aburatani, H. & Sugiyama, Y. (2003) Functional characterization of rat brain-specific organic anion transporter (Oatp14) at the blood-brain barrier: high affinity transporter for thyroxine, *The Journal of biological chemistry.* **278**, 43489-95.

39. Tohyama, K., Kusuhara, H. & Sugiyama, Y. (2004) Involvement of multispecific organic anion transporter, Oatp14 (Slc21a14), in the transport of thyroxine across the blood-brain barrier, *Endocrinology.* **145**, 4384-91.

40. Roberts, L. M., Woodford, K., Zhou, M., Black, D. S., Haggerty, J. E., Tate, E. H., Grindstaff, K. K., Mengesha, W., Raman, C. & Zerangue, N. (2008) Expression of the

thyroid hormone transporters monocarboxylate transporter-8 (SLC16A2) and organic ion transporter-14 (SLCO1C1) at the blood-brain barrier, *Endocrinology.* **149**, 6251-61.

41. Friesema, E. C., Ganguly, S., Abdalla, A., Manning Fox, J. E., Halestrap, A. P. & Visser, T. J. (2003) Identification of monocarboxylate transporter 8 as a specific thyroid hormone transporter, *The Journal of biological chemistry.* **278**, 40128-35.

42. Nishimura, M. & Naito, S. (2008) Tissue-specific mRNA expression profiles of human solute carrier transporter superfamilies, *Drug metabolism and pharmacokinetics.* **23**, 22-44.

43. Price, N. T., Jackson, V. N. & Halestrap, A. P. (1998) Cloning and sequencing of four new mammalian monocarboxylate transporter (MCT) homologues confirms the existence of a transporter family with an ancient past, *The Biochemical journal.* **329 (Pt 2)**, 321-8.

44. Ceballos, A., Belinchon, M. M., Sanchez-Mendoza, E., Grijota-Martinez, C., Dumitrescu, A. M., Refetoff, S., Morte, B. & Bernal, J. (2009) Importance of monocarboxylate transporter 8 for the blood-brain barrier-dependent availability of 3,5,3'-triiodo-L-thyronine, *Endocrinology.* **150**, 2491-6.

45. Heuer, H., Maier, M. K., Iden, S., Mittag, J., Friesema, E. C., Visser, T. J. & Bauer, K. (2005) The monocarboxylate transporter 8 linked to human psychomotor retardation is highly expressed in thyroid hormone-sensitive neuron populations, *Endocrinology.* **146**, 1701-6.

46. Wirth, E. K., Roth, S., Blechschmidt, C., Holter, S. M., Becker, L., Racz, I., Zimmer, A., Klopstock, T., Gailus-Durner, V., Fuchs, H., Wurst, W., Naumann, T., Brauer, A., de Angelis, M. H., Kohrle, J., Gruters, A. & Schweizer, U. (2009) Neuronal 3',3,5-triiodothyronine (T3) uptake and behavioral phenotype of mice deficient in Mct8, the neuronal T3 transporter mutated in Allan-Herndon-Dudley syndrome, *The Journal of neuroscience : the official journal of the Society for Neuroscience.* **29**, 9439-49.

47. Dumitrescu, A. M., Liao, X. H., Best, T. B., Brockmann, K. & Refetoff, S. (2004) A novel syndrome combining thyroid and neurological abnormalities is associated with mutations in a monocarboxylate transporter gene, *American journal of human genetics.* **74**, 168-75.

48. Friesema, E. C., Grueters, A., Biebermann, H., Krude, H., von Moers, A., Reeser, M., Barrett, T. G., Mancilla, E. E., Svensson, J., Kester, M. H., Kuiper, G. G., Balkassmi,

S., Uitterlinden, A. G., Koehrle, J., Rodien, P., Halestrap, A. P. & Visser, T. J. (2004) Association between mutations in a thyroid hormone transporter and severe X-linked psychomotor retardation, *Lancet.* **364**, 1435-7.

49. Schwartz, C. E. & Stevenson, R. E. (2007) The MCT8 thyroid hormone transporter and Allan-Herndon-Dudley syndrome, *Best practice & research Clinical endocrinology & metabolism.* **21**, 307-21.

50. Dumitrescu, A. M., Liao, X. H., Weiss, R. E., Millen, K. & Refetoff, S. (2006) Tissue-specific thyroid hormone deprivation and excess in monocarboxylate transporter (mct) 8-deficient mice, *Endocrinology.* **147**, 4036-43.

51. Trajkovic, M., Visser, T. J., Mittag, J., Horn, S., Lukas, J., Darras, V. M., Raivich, G., Bauer, K. & Heuer, H. (2007) Abnormal thyroid hormone metabolism in mice lacking the monocarboxylate transporter 8, *The Journal of clinical investigation.* **117**, 627-35.

52. Friesema, E. C., Jansen, J., Jachtenberg, J. W., Visser, W. E., Kester, M. H. & Visser, T. J. (2008) Effective cellular uptake and efflux of thyroid hormone by human monocarboxylate transporter 10, *Molecular endocrinology.* **22**, 1357-69.

53. Kim, D. K., Kanai, Y., Chairoungdua, A., Matsuo, H., Cha, S. H. & Endou, H. (2001) Expression cloning of a Na+-independent aromatic amino acid transporter with structural similarity to H+/monocarboxylate transporters, *The Journal of biological chemistry.* **276**, 17221-8.

54. Kim, D. K., Kanai, Y., Matsuo, H., Kim, J. Y., Chairoungdua, A., Kobayashi, Y., Enomoto, A., Cha, S. H., Goya, T. & Endou, H. (2002) The human T-type amino acid transporter-1: characterization, gene organization, and chromosomal location, *Genomics.* **79**, 95-103.

55. Ramadan, T., Camargo, S. M., Summa, V., Hunziker, P., Chesnov, S., Pos, K. M. & Verrey, F. (2006) Basolateral aromatic amino acid transporter TAT1 (Slc16a10) functions as an efflux pathway, *Journal of cellular physiology.* **206**, 771-9.

56. Ritchie, J. W. & Taylor, P. M. (2010) Tryptophan and iodothyronine transport interactions in HepG2 human hepatoma cells, *Amino acids.* **38**, 1361-7.

57. Gagne, R., Green, J. R., Dong, H., Wade, M. G. & Yauk, C. L. (2013) Identification of thyroid hormone receptor binding sites in developing mouse cerebellum, *BMC genomics.* **14**, 341.

58. Williams, G. R. & Bassett, J. H. (2011) Deiodinases: the balance of thyroid hormone: local control of thyroid hormone action: role of type 2 deiodinase, *The Journal of endocrinology.* **209**, 261-72.

59. Harvey, C. B. & Williams, G. R. (2002) Mechanism of thyroid hormone action, *Thyroid : official journal of the American Thyroid Association.* **12**, 441-6.

60. Costa-e-Sousa, R. H. & Hollenberg, A. N. (2012) Minireview: The neural regulation of the hypothalamic-pituitary-thyroid axis, *Endocrinology.* **153**, 4128-35.

61. Hodin, R. A., Lazar, M. A., Wintman, B. I., Darling, D. S., Koenig, R. J., Larsen, P. R., Moore, D. D. & Chin, W. W. (1989) Identification of a thyroid hormone receptor that is pituitary-specific, *Science.* **244**, 76-9.

62. Lechan, R. M., Qi, Y., Jackson, I. M. & Mahdavi, V. (1994) Identification of thyroid hormone receptor isoforms in thyrotropin-releasing hormone neurons of the hypothalamic paraventricular nucleus, *Endocrinology.* **135**, 92-100.

63. Wood, W. M., Ocran, K. W., Gordon, D. F. & Ridgway, E. C. (1991) Isolation and characterization of mouse complementary DNAs encoding alpha and beta thyroid hormone receptors from thyrotrope cells: the mouse pituitary-specific beta 2 isoform differs at the amino terminus from the corresponding species from rat pituitary tumor cells, *Molecular endocrinology.* **5**, 1049-61.

64. Abel, E. D., Ahima, R. S., Boers, M. E., Elmquist, J. K. & Wondisford, F. E. (2001) Critical role for thyroid hormone receptor beta2 in the regulation of paraventricular thyrotropin-releasing hormone neurons, *The Journal of clinical investigation.* **107**, 1017-23.

65. Dupre, S. M., Guissouma, H., Flamant, F., Seugnet, I., Scanlan, T. S., Baxter, J. D., Samarut, J., Demeneix, B. A. & Becker, N. (2004) Both thyroid hormone receptor (TR)beta 1 and TR beta 2 isoforms contribute to the regulation of hypothalamic thyrotropin-releasing hormone, *Endocrinology.* **145**, 2337-45.

66. Hashimoto, K. & Mori, M. (2011) Crosstalk of thyroid hormone receptor and liver X receptor in lipid metabolism and beyond [Review], *Endocrine journal.* **58**, 921-30.

67. Castillo, A. I., Sanchez-Martinez, R., Moreno, J. L., Martinez-Iglesias, O. A., Palacios, D. & Aranda, A. (2004) A permissive retinoid X receptor/thyroid hormone receptor heterodimer allows stimulation of prolactin gene transcription by thyroid hormone and 9-cis-retinoic acid, *Molecular and cellular biology.* **24**, 502-13.

68. Chassande, O. (2003) Do unliganded thyroid hormone receptors have physiological functions?, *Journal of molecular endocrinology.* **31**, 9-20.

69. Hashimoto, K., Curty, F. H., Borges, P. P., Lee, C. E., Abel, E. D., Elmquist, J. K., Cohen, R. N. & Wondisford, F. E. (2001) An unliganded thyroid hormone receptor causes severe neurological dysfunction, *Proceedings of the National Academy of Sciences of the United States of America.* **98**, 3998-4003.

70. Guissouma, H., Ghorbel, M. T., Seugnet, I., Ouatas, T. & Demeneix, B. A. (1998) Physiological regulation of hypothalamic TRH transcription in vivo is T3 receptor isoform specific, *FASEB journal : official publication of the Federation of American Societies for Experimental Biology.* **12**, 1755-64.

71. Hollenberg, A. N., Monden, T., Flynn, T. R., Boers, M. E., Cohen, O. & Wondisford, F. E. (1995) The human thyrotropin-releasing hormone gene is regulated by thyroid hormone through two distinct classes of negative thyroid hormone response elements, *Molecular endocrinology.* **9**, 540-50.

72. Langlois, M. F., Zanger, K., Monden, T., Safer, J. D., Hollenberg, A. N. & Wondisford, F. E. (1997) A unique role of the beta-2 thyroid hormone receptor isoform in negative regulation by thyroid hormone. Mapping of a novel amino-terminal domain important for ligand-independent activation, *The Journal of biological chemistry.* **272**, 24927-33.

73. Ortiga-Carvalho, T. M., Shibusawa, N., Nikrodhanond, A., Oliveira, K. J., Machado, D. S., Liao, X. H., Cohen, R. N., Refetoff, S. & Wondisford, F. E. (2005) Negative regulation by thyroid hormone receptor requires an intact coactivator-binding surface, *The Journal of clinical investigation.* **115**, 2517-23.

74. Astapova, I., Vella, K. R., Ramadoss, P., Holtz, K. A., Rodwin, B. A., Liao, X. H., Weiss, R. E., Rosenberg, M. A., Rosenzweig, A. & Hollenberg, A. N. (2011) The nuclear receptor corepressor (NCoR) controls thyroid hormone sensitivity and the set point of the hypothalamic-pituitary-thyroid axis, *Molecular endocrinology.* **25**, 212-24.

75. Fozzatti, L., Lu, C., Kim, D. W., Park, J. W., Astapova, I., Gavrilova, O., Willingham, M. C., Hollenberg, A. N. & Cheng, S. Y. (2011) Resistance to thyroid hormone is modulated in vivo by the nuclear receptor corepressor (NCOR1), *Proceedings of the National Academy of Sciences of the United States of America.* **108**, 17462-7.

76. Berbel, P., Auso, E., Garcia-Velasco, J. V., Molina, M. L. & Camacho, M. (2001) Role of thyroid hormones in the maturation and organisation of rat barrel cortex, *Neuroscience.* **107**, 383-94.

77. Berbel, P., Guadano-Ferraz, A., Angulo, A. & Ramon Cerezo, J. (1994) Role of thyroid hormones in the maturation of interhemispheric connections in rats, *Behavioural brain research.* **64**, 9-14.

78. Ruiz-Marcos, A., Sanchez-Toscano, F., Escobar del Rey, F. & Morreale de Escobar, G. (1980) Reversible morphological alterations of cortical neurons in juvenile and adult hypothyroidism in the rat, *Brain research.* **185**, 91-102.

79. Ruiz-Marcos, A., Sanchez-Toscano, F., Obregon, M. J., Escobar del Rey, F. & Morreale de Escobar, G. (1982) Thyroxine treatment and recovery of hypothyroidism-induced pyramidal cell damage, *Brain research.* **239**, 559-74.

80. Ambrogini, P., Cuppini, R., Ferri, P., Mancini, C., Ciaroni, S., Voci, A., Gerdoni, E. & Gallo, G. (2005) Thyroid hormones affect neurogenesis in the dentate gyrus of adult rat, *Neuroendocrinology.* **81**, 244-53.

81. Desouza, L. A., Ladiwala, U., Daniel, S. M., Agashe, S., Vaidya, R. A. & Vaidya, V. A. (2005) Thyroid hormone regulates hippocampal neurogenesis in the adult rat brain, *Molecular and cellular neurosciences.* **29**, 414-26.

82. Montero-Pedrazuela, A., Venero, C., Lavado-Autric, R., Fernandez-Lamo, I., Garcia-Verdugo, J. M., Bernal, J. & Guadano-Ferraz, A. (2006) Modulation of adult hippocampal neurogenesis by thyroid hormones: implications in depressive-like behavior, *Molecular psychiatry.* **11**, 361-71.

83. Dusart, I. & Flamant, F. (2012) Profound morphological and functional changes of rodent Purkinje cells between the first and the second postnatal weeks: a metamorphosis?, *Frontiers in neuroanatomy.* **6**, 11.

84. Kimura-Kuroda, J., Nagata, I., Negishi-Kato, M. & Kuroda, Y. (2002) Thyroid hormone-dependent development of mouse cerebellar Purkinje cells in vitro, *Brain research Developmental brain research.* **137**, 55-65.

85. Wei, W., Wang, Y., Wang, Y., Dong, J., Min, H., Song, B., Teng, W., Xi, Q. & Chen, J. (2013) Developmental hypothyroxinaemia induced by maternal mild iodine deficiency delays hippocampal axonal growth in the rat offspring, *Journal of neuroendocrinology.* **25**, 852-62.

86. Heuer, H. & Mason, C. A. (2003) Thyroid hormone induces cerebellar Purkinje cell dendritic development via the thyroid hormone receptor alpha1, *The Journal of neuroscience : the official journal of the Society for Neuroscience.* **23**, 10604-12.

87. Wang, Y., Wang, Y., Dong, J., Wei, W., Song, B., Min, H., Teng, W. & Chen, J. (2013) Developmental Hypothyroxinemia and Hypothyroidism Limit Dendritic Growth of Cerebellar Purkinje Cells in Rat Offspring: Involvement of MAP2 and Stathmin, *Neuropathology and applied neurobiology*.

88. Gine, E., Echeverry-Alzate, V., Lopez-Moreno, J. A., Lopez-Jimenez, A., Torres-Romero, D., Perez-Castillo, A. & Santos, A. (2013) Developmentally-induced hypothyroidism alters the expression of Egr-1 and Arc genes and the sensitivity to cannabinoid agonists in the hippocampus. Possible implications for memory and learning, *Molecular and cellular endocrinology.* **365**, 119-28.

89. Wilcoxon, J. S., Nadolski, G. J., Samarut, J., Chassande, O. & Redei, E. E. (2007) Behavioral inhibition and impaired spatial learning and memory in hypothyroid mice lacking thyroid hormone receptor alpha, *Behavioural brain research.* **177**, 109-16.

90. Rastogi, M. V. & LaFranchi, S. H. (2010) Congenital hypothyroidism, *Orphanet journal of rare diseases.* **5**, 17.

91. Basraon, S. & Costantine, M. M. (2011) Mood disorders in pregnant women with thyroid dysfunction, *Clinical obstetrics and gynecology.* **54**, 506-14.

92. Gabarrou, J. F., Duchamp, C., Williams, J. & Geraert, P. A. (1997) A role for thyroid hormones in the regulation of diet-induced thermogenesis in birds, *The British journal of nutrition.* **78**, 963-73.

93. Hall, J. A., Ribich, S., Christoffolete, M. A., Simovic, G., Correa-Medina, M., Patti, M. E. & Bianco, A. C. (2010) Absence of thyroid hormone activation during development underlies a permanent defect in adaptive thermogenesis, *Endocrinology.* **151**, 4573-82.

94. Bianco, A. C., Carvalho, S. D., Carvalho, C. R., Rabelo, R. & Moriscot, A. S. (1998) Thyroxine 5'-deiodination mediates norepinephrine-induced lipogenesis in dispersed brown adipocytes, *Endocrinology.* **139**, 571-8.

95. Oppenheimer, J. H., Schwartz, H. L., Lane, J. T. & Thompson, M. P. (1991) Functional relationship of thyroid hormone-induced lipogenesis, lipolysis, and thermogenesis in the rat, *The Journal of clinical investigation.* **87**, 125-32.

96. Nussey SS, W. S. (2001) The Thyroid Gland, *Endocrinology: An Integrated Approach BIOS Scientific Publishers Limited, Oxford, UK*, 71-115.

97. Brooks, S. L., Rothwell, N. J., Stock, M. J., Goodbody, A. E. & Trayhurn, P. (1980) Increased proton conductance pathway in brown adipose tissue mitochondria of rats exhibiting diet-induced thermogenesis, *Nature.* **286**, 274-6.

98. Rothwell, N. J. & Stock, M. J. (1979) A role for brown adipose tissue in diet-induced thermogenesis, *Nature.* **281**, 31-5.

99. de Jesus, L. A., Carvalho, S. D., Ribeiro, M. O., Schneider, M., Kim, S. W., Harney, J. W., Larsen, P. R. & Bianco, A. C. (2001) The type 2 iodothyronine deiodinase is essential for adaptive thermogenesis in brown adipose tissue, *The Journal of clinical investigation.* **108**, 1379-85.

100. Ribeiro, M. O., Carvalho, S. D., Schultz, J. J., Chiellini, G., Scanlan, T. S., Bianco, A. C. & Brent, G. A. (2001) Thyroid hormone--sympathetic interaction and adaptive thermogenesis are thyroid hormone receptor isoform--specific, *The Journal of clinical investigation.* **108**, 97-105.

101. Hinkle, P. M., Gehret, A. U. & Jones, B. W. (2012) Desensitization, trafficking, and resensitization of the pituitary thyrotropin-releasing hormone receptor, *Frontiers in neuroscience.* **6**, 180.

102. Magner, J. A., Kane, J. & Chou, E. T. (1992) Intravenous thyrotropin (TSH)-releasing hormone releases human TSH that is structurally different from basal TSH, *The Journal of clinical endocrinology and metabolism.* **74**, 1306-11.

103. Persani, L. (1998) Hypothalamic thyrotropin-releasing hormone and thyrotropin biological activity, *Thyroid : official journal of the American Thyroid Association.* **8**, 941-6.

104. Kohrle, J. (1990) Thyrotropin (TSH) action on thyroid hormone deiodination and secretion: one aspect of thyrotropin regulation of thyroid cell biology, *Hormone and metabolic research Supplement series.* **23**, 18-28.

105. Fraser, H. M. & McNeilly, A. S. (1982) Effect of chronic immunoneutralization of thyrotropin-releasing hormone on the hypothalamic-pituitary-thyroid axis, prolactin, and reproductive function in the ewe, *Endocrinology.* **111**, 1964-73.

106. Mori, M., Kobayashi, I. & Wakabayashi, K. (1978) Suppression of serum thyrotropin (TSH) concentrations following thyroidectomy and cold exposure by passive

immunization with antiserum to thyrotropin-releasing hormone (TRH) in rats, *Metabolism: clinical and experimental.* **27**, 1485-90.

107. Shibusawa, N., Yamada, M., Hirato, J., Monden, T., Satoh, T. & Mori, M. (2000) Requirement of thyrotropin-releasing hormone for the postnatal functions of pituitary thyrotrophs: ontogeny study of congenital tertiary hypothyroidism in mice, *Molecular endocrinology.* **14**, 137-46.

108. Yamada, M., Satoh, T. & Mori, M. (2003) Mice lacking the thyrotropin-releasing hormone gene: what do they tell us?, *Thyroid : official journal of the American Thyroid Association.* **13**, 1111-21.

109. Beck-Peccoz, P., Amr, S., Menezes-Ferreira, M. M., Faglia, G. & Weintraub, B. D. (1985) Decreased receptor binding of biologically inactive thyrotropin in central hypothyroidism. Effect of treatment with thyrotropin-releasing hormone, *The New England journal of medicine.* **312**, 1085-90.

110. Swanson, L. W. & Kuypers, H. G. (1980) The paraventricular nucleus of the hypothalamus: cytoarchitectonic subdivisions and organization of projections to the pituitary, dorsal vagal complex, and spinal cord as demonstrated by retrograde fluorescence double-labeling methods, *The Journal of comparative neurology.* **194**, 555-70.

111. Lechan, R. M. & Jackson, I. M. (1982) Immunohistochemical localization of thyrotropin-releasing hormone in the rat hypothalamus and pituitary, *Endocrinology.* **111**, 55-65.

112. Fekete, C. & Lechan, R. M. (2007) Negative feedback regulation of hypophysiotropic thyrotropin-releasing hormone (TRH) synthesizing neurons: role of neuronal afferents and type 2 deiodinase, *Frontiers in neuroendocrinology.* **28**, 97-114.

113. Segerson, T. P., Kauer, J., Wolfe, H. C., Mobtaker, H., Wu, P., Jackson, I. M. & Lechan, R. M. (1987) Thyroid hormone regulates TRH biosynthesis in the paraventricular nucleus of the rat hypothalamus, *Science.* **238**, 78-80.

114. Dyess, E. M., Segerson, T. P., Liposits, Z., Paull, W. K., Kaplan, M. M., Wu, P., Jackson, I. M. & Lechan, R. M. (1988) Triiodothyronine exerts direct cell-specific regulation of thyrotropin-releasing hormone gene expression in the hypothalamic paraventricular nucleus, *Endocrinology.* **123**, 2291-7.

115. Guissouma, H., Froidevaux, M. S., Hassani, Z. & Demeneix, B. A. (2006) In vivo siRNA delivery to the mouse hypothalamus confirms distinct roles of TR beta isoforms in regulating TRH transcription, *Neuroscience letters.* **406**, 240-3.

116. Carreon-Rodriguez, A., Charli, J. L. & Perez-Martinez, L. (2009) T3 differentially regulates TRH expression in developing hypothalamic neurons in vitro, *Brain research.* **1305**, 20-30.

117. Perello, M., Friedman, T., Paez-Espinosa, V., Shen, X., Stuart, R. C. & Nillni, E. A. (2006) Thyroid hormones selectively regulate the posttranslational processing of prothyrotropin-releasing hormone in the paraventricular nucleus of the hypothalamus, *Endocrinology.* **147**, 2705-16.

118. Reichlin, S. (1989) Neuroendocrinology of the pituitary gland, *Toxicologic pathology.* **17**, 250-5.

119. Kobayashi, T., Yamamoto, K., Kaibara, M. & Ajika, K. (1968) Electron microscopic observation on the hypothalamo-hypophyseal system in rats. IV. Ultrafine structure of the developing median eminence, *Endocrinologia japonica.* **15**, 337-63.

120. Lennard, D. E., Eckert, W. A. & Merchenthaler, I. (1993) Corticotropin-releasing hormone neurons in the paraventricular nucleus project to the external zone of the median eminence: a study combining retrograde labeling with immunocytochemistry, *Journal of neuroendocrinology.* **5**, 175-81.

121. Merchenthaler, I., Setalo, G., Csontos, C., Petrusz, P., Flerko, B. & Negro-Vilar, A. (1989) Combined retrograde tracing and immunocytochemical identification of luteinizing hormone-releasing hormone- and somatostatin-containing neurons projecting to the median eminence of the rat, *Endocrinology.* **125**, 2812-21.

122. Nillni, E. A., Steinmetz, R. & Pescovitz, O. H. (1999) Posttranslational processing of progrowth hormone-releasing hormone, *Endocrinology.* **140**, 5817-27.

123. Prevot, V., Croix, D., Bouret, S., Dutoit, S., Tramu, G., Stefano, G. B. & Beauvillain, J. C. (1999) Definitive evidence for the existence of morphological plasticity in the external zone of the median eminence during the rat estrous cycle: implication of neuro-glio-endothelial interactions in gonadotropin-releasing hormone release, *Neuroscience.* **94**, 809-19.

124. Reymond, M. J. & Porter, J. C. (1985) Involvement of hypothalamic dopamine in the regulation of prolactin secretion, *Hormone research.* **22**, 142-52.

125. Holmes, H. R. (1967) Vascular patterns in the mammalian median eminence, *The Journal of physiology.* **191**, 49P-50P.

126. Buma, P. & Nieuwenhuys, R. (1987) Ultrastructural demonstration of oxytocin and vasopressin release sites in the neural lobe and median eminence of the rat by tannic acid and immunogold methods, *Neuroscience letters.* **74**, 151-7.

127. Holmes, M. C., Antoni, F. A., Aguilera, G. & Catt, K. J. (1986) Magnocellular axons in passage through the median eminence release vasopressin, *Nature.* **319**, 326-9.

128. Lechan, R. M. & Fekete, C. (2007) Infundibular tanycytes as modulators of neuroendocrine function: hypothetical role in the regulation of the thyroid and gonadal axis, *Acta bio-medica : Atenei Parmensis.* **78 Suppl 1**, 84-98.

129. Peruzzo, B., Pastor, F. E., Blazquez, J. L., Schobitz, K., Pelaez, B., Amat, P. & Rodriguez, E. M. (2000) A second look at the barriers of the medial basal hypothalamus, *Experimental brain research Experimentelle Hirnforschung Experimentation cerebrale.* **132**, 10-26.

130. Prevot, V., Bellefontaine, N., Baroncini, M., Sharif, A., Hanchate, N. K., Parkash, J., Campagne, C. & de Seranno, S. (2010) Gonadotrophin-releasing hormone nerve terminals, tanycytes and neurohaemal junction remodelling in the adult median eminence: functional consequences for reproduction and dynamic role of vascular endothelial cells, *Journal of neuroendocrinology.* **22**, 639-49.

131. Yamamura, T., Yasuo, S., Hirunagi, K., Ebihara, S. & Yoshimura, T. (2006) T(3) implantation mimics photoperiodically reduced encasement of nerve terminals by glial processes in the median eminence of Japanese quail, *Cell and tissue research.* **324**, 175-9.

132. Lechan, R. M., Qi, Y., Berrodin, T. J., Davis, K. D., Schwartz, H. L., Strait, K. A., Oppenheimer, J. H. & Lazar, M. A. (1993) Immunocytochemical delineation of thyroid hormone receptor beta 2-like immunoreactivity in the rat central nervous system, *Endocrinology.* **132**, 2461-9.

133. Alkemade, A., Friesema, E. C., Unmehopa, U. A., Fabriek, B. O., Kuiper, G. G., Leonard, J. L., Wiersinga, W. M., Swaab, D. F., Visser, T. J. & Fliers, E. (2005) Neuroanatomical pathways for thyroid hormone feedback in the human hypothalamus, *The Journal of clinical endocrinology and metabolism.* **90**, 4322-34.

134. Diano, S., Leonard, J. L., Meli, R., Esposito, E. & Schiavo, L. (2003) Hypothalamic type II iodothyronine deiodinase: a light and electron microscopic study, *Brain research.* **976**, 130-4.

135. Fekete, C., Freitas, B. C., Zeold, A., Wittmann, G., Kadar, A., Liposits, Z., Christoffolete, M. A., Singru, P., Lechan, R. M., Bianco, A. C. & Gereben, B. (2007) Expression patterns of WSB-1 and USP-33 underlie cell-specific posttranslational control of type 2 deiodinase in the rat brain, *Endocrinology.* **148**, 4865-74.

136. Kakucska, I., Rand, W. & Lechan, R. M. (1992) Thyrotropin-releasing hormone gene expression in the hypothalamic paraventricular nucleus is dependent upon feedback regulation by both triiodothyronine and thyroxine, *Endocrinology.* **130**, 2845-50.

137. Diano, S., Naftolin, F., Goglia, F. & Horvath, T. L. (1998) Fasting-induced increase in type II iodothyronine deiodinase activity and messenger ribonucleic acid levels is not reversed by thyroxine in the rat hypothalamus, *Endocrinology.* **139**, 2879-84.

138. Shioda, S., Nakai, Y., Sato, A., Sunayama, S. & Shimoda, Y. (1986) Electron-microscopic cytochemistry of the catecholaminergic innervation of TRH neurons in the rat hypothalamus, *Cell and tissue research.* **245**, 247-52.

139. Liposits, Z. (1993) Ultrastructure of hypothalamic paraventricular neurons, *Critical reviews in neurobiology.* **7**, 89-162.

140. Fuzesi, T., Wittmann, G., Lechan, R. M., Liposits, Z. & Fekete, C. (2009) Noradrenergic innervation of hypophysiotropic thyrotropin-releasing hormone-synthesizing neurons in rats, *Brain research.* **1294**, 38-44.

141. Sawchenko, P. E., Swanson, L. W., Grzanna, R., Howe, P. R., Bloom, S. R. & Polak, J. M. (1985) Colocalization of neuropeptide Y immunoreactivity in brainstem catecholaminergic neurons that project to the paraventricular nucleus of the hypothalamus, *The Journal of comparative neurology.* **241**, 138-53.

142. Zoeller, R. T., Kabeer, N. & Albers, H. E. (1990) Cold exposure elevates cellular levels of messenger ribonucleic acid encoding thyrotropin-releasing hormone in paraventricular nucleus despite elevated levels of thyroid hormones, *Endocrinology.* **127**, 2955-62.

143. Schettini, G., Quattrone, A., Di Renzo, G., Lombardi, G. & Preziosi, P. (1979) Effect of 6-hydroxydopamine treatment on TSH secretion in basal and cold-stimulated conditions in the rat, *European journal of pharmacology.* **56**, 153-7.

144. Ignar, D. M. & Kuhn, C. M. (1988) Relative ontogeny of opioid and catecholaminergic regulation of thyrotropin secretion in the rat, *Endocrinology.* **123**, 567-71.

145. Schwartz, M. W., Woods, S. C., Porte, D., Jr., Seeley, R. J. & Baskin, D. G. (2000) Central nervous system control of food intake, *Nature.* **404**, 661-71.

146. Elias, C. F., Lee, C., Kelly, J., Aschkenasi, C., Ahima, R. S., Couceyro, P. R., Kuhar, M. J., Saper, C. B. & Elmquist, J. K. (1998) Leptin activates hypothalamic CART neurons projecting to the spinal cord, *Neuron.* **21**, 1375-85.

147. Vrang, N., Larsen, P. J., Clausen, J. T. & Kristensen, P. (1999) Neurochemical characterization of hypothalamic cocaine- amphetamine-regulated transcript neurons, *The Journal of neuroscience : the official journal of the Society for Neuroscience.* **19**, RC5.

148. McMinn, J. E., Wilkinson, C. W., Havel, P. J., Woods, S. C. & Schwartz, M. W. (2000) Effect of intracerebroventricular alpha-MSH on food intake, adiposity, c-Fos induction, and neuropeptide expression, *American journal of physiology Regulatory, integrative and comparative physiology.* **279**, R695-703.

149. Stanley, S. A., Small, C. J., Murphy, K. G., Rayes, E., Abbott, C. R., Seal, L. J., Morgan, D. G., Sunter, D., Dakin, C. L., Kim, M. S., Hunter, R., Kuhar, M., Ghatei, M. A. & Bloom, S. R. (2001) Actions of cocaine- and amphetamine-regulated transcript (CART) peptide on regulation of appetite and hypothalamo-pituitary axes in vitro and in vivo in male rats, *Brain research.* **893**, 186-94.

150. Begriche, K., Sutton, G. M. & Butler, A. A. (2011) Homeostastic and non-homeostatic functions of melanocortin-3 receptors in the control of energy balance and metabolism, *Physiology & behavior.* **104**, 546-54.

151. Hinney, A., Volckmar, A. L. & Knoll, N. (2013) Melanocortin-4 receptor in energy homeostasis and obesity pathogenesis, *Progress in molecular biology and translational science.* **114**, 147-91.

152. Lee, E. J., Lee, S. H., Jung, J. W., Lee, W., Kim, B. J., Park, K. W., Lim, S. K., Yoon, C. J. & Baik, J. H. (2001) Differential regulation of cAMP-mediated gene transcription and ligand selectivity by MC3R and MC4R melanocortin receptors, *European journal of biochemistry / FEBS.* **268**, 582-91.

153. Selkirk, J. V., Nottebaum, L. M., Ford, I. C., Santos, M., Malany, S., Foster, A. C. & Lechner, S. M. (2006) A novel cell-based assay for G-protein-coupled receptor-mediated cyclic adenosine monophosphate response element binding protein phosphorylation, *Journal of biomolecular screening.* **11**, 351-8.

154. Sarkar, S., Wittmann, G., Fekete, C. & Lechan, R. M. (2004) Central administration of cocaine- and amphetamine-regulated transcript increases phosphorylation of cAMP response element binding protein in corticotropin-releasing hormone-producing neurons but not in prothyrotropin-releasing hormone-producing neurons in the hypothalamic paraventricular nucleus, *Brain research.* **999**, 181-92.

155. Yermolaieva, O., Chen, J., Couceyro, P. R. & Hoshi, T. (2001) Cocaine- and amphetamine-regulated transcript peptide modulation of voltage-gated Ca2+ signaling in hippocampal neurons, *The Journal of neuroscience : the official journal of the Society for Neuroscience.* **21**, 7474-80.

156. Lakatos, A., Prinster, S., Vicentic, A., Hall, R. A. & Kuhar, M. J. (2005) Cocaine- and amphetamine-regulated transcript (CART) peptide activates the extracellular signal-regulated kinase (ERK) pathway in AtT20 cells via putative G-protein coupled receptors, *Neuroscience letters.* **384**, 198-202.

157. Lin, Y., Hall, R. A. & Kuhar, M. J. (2011) CART peptide stimulation of G protein-mediated signaling in differentiated PC12 cells: identification of PACAP 6-38 as a CART receptor antagonist, *Neuropeptides.* **45**, 351-8.

158. Coll, A. P., Farooqi, I. S., Challis, B. G., Yeo, G. S. & O'Rahilly, S. (2004) Proopiomelanocortin and energy balance: insights from human and murine genetics, *The Journal of clinical endocrinology and metabolism.* **89**, 2557-62.

159. Yaswen, L., Diehl, N., Brennan, M. B. & Hochgeschwender, U. (1999) Obesity in the mouse model of pro-opiomelanocortin deficiency responds to peripheral melanocortin, *Nature medicine.* **5**, 1066-70.

160. Krude, H., Biebermann, H., Luck, W., Horn, R., Brabant, G. & Gruters, A. (1998) Severe early-onset obesity, adrenal insufficiency and red hair pigmentation caused by POMC mutations in humans, *Nature genetics.* **19**, 155-7.

161. Butler, A. A. & Cone, R. D. (2002) The melanocortin receptors: lessons from knockout models, *Neuropeptides.* **36**, 77-84.

162. Vaisse, C., Clement, K., Durand, E., Hercberg, S., Guy-Grand, B. & Froguel, P. (2000) Melanocortin-4 receptor mutations are a frequent and heterogeneous cause of morbid obesity, *The Journal of clinical investigation.* **106**, 253-62.

163. Wierup, N., Richards, W. G., Bannon, A. W., Kuhar, M. J., Ahren, B. & Sundler, F. (2005) CART knock out mice have impaired insulin secretion and glucose intolerance, altered beta cell morphology and increased body weight, *Regulatory peptides.* **129**, 203-11.

164. Gropp, E., Shanabrough, M., Borok, E., Xu, A. W., Janoschek, R., Buch, T., Plum, L., Balthasar, N., Hampel, B., Waisman, A., Barsh, G. S., Horvath, T. L. & Bruning, J. C. (2005) Agouti-related peptide-expressing neurons are mandatory for feeding, *Nature neuroscience.* **8**, 1289-91.

165. Fekete, C., Singru, P. S., Sanchez, E., Sarkar, S., Christoffolete, M. A., Riberio, R. S., Rand, W. M., Emerson, C. H., Bianco, A. C. & Lechan, R. M. (2006) Differential effects of central leptin, insulin, or glucose administration during fasting on the hypothalamic-pituitary-thyroid axis and feeding-related neurons in the arcuate nucleus, *Endocrinology.* **147**, 520-9.

166. Fekete, C., Legradi, G., Mihaly, E., Huang, Q. H., Tatro, J. B., Rand, W. M., Emerson, C. H. & Lechan, R. M. (2000) alpha-Melanocyte-stimulating hormone is contained in nerve terminals innervating thyrotropin-releasing hormone-synthesizing neurons in the hypothalamic paraventricular nucleus and prevents fasting-induced suppression of prothyrotropin-releasing hormone gene expression, *The Journal of neuroscience : the official journal of the Society for Neuroscience.* **20**, 1550-8.

167. Kim, M. S., Small, C. J., Stanley, S. A., Morgan, D. G., Seal, L. J., Kong, W. M., Edwards, C. M., Abusnana, S., Sunter, D., Ghatei, M. A. & Bloom, S. R. (2000) The central melanocortin system affects the hypothalamo-pituitary thyroid axis and may mediate the effect of leptin, *The Journal of clinical investigation.* **105**, 1005-11.

168. Kim, M. S., Small, C. J., Russell, S. H., Morgan, D. G., Abbott, C. R., alAhmed, S. H., Hay, D. L., Ghatei, M. A., Smith, D. M. & Bloom, S. R. (2002) Effects of melanocortin receptor ligands on thyrotropin-releasing hormone release: evidence for the differential roles of melanocortin 3 and 4 receptors, *Journal of neuroendocrinology.* **14**, 276-82.

169. Sarkar, S., Legradi, G. & Lechan, R. M. (2002) Intracerebroventricular administration of alpha-melanocyte stimulating hormone increases phosphorylation of CREB in TRH- and CRH-producing neurons of the hypothalamic paraventricular nucleus, *Brain research.* **945**, 50-9.

170. Chiappini, F., Ramadoss, P., Vella, K. R., Cunha, L. L., Ye, F. D., Stuart, R. C., Nillni, E. A. & Hollenberg, A. N. (2013) Family members CREB and CREM control thyrotropin-releasing hormone (TRH) expression in the hypothalamus, *Molecular and cellular endocrinology.* **365**, 84-94.

171. Semjonous, N. M., Smith, K. L., Parkinson, J. R., Gunner, D. J., Liu, Y. L., Murphy, K. G., Ghatei, M. A., Bloom, S. R. & Small, C. J. (2009) Coordinated changes in energy intake and expenditure following hypothalamic administration of neuropeptides involved in energy balance, *International journal of obesity.* **33**, 775-85.

172. Nguyen, A. D., Mitchell, N. F., Lin, S., Macia, L., Yulyaningsih, E., Baldock, P. A., Enriquez, R. F., Zhang, L., Shi, Y. C., Zolotukhin, S., Herzog, H. & Sainsbury, A. (2012) Y1 and Y5 receptors are both required for the regulation of food intake and energy homeostasis in mice, *PloS one.* **7**, e40191.

173. Michel, M. C., Beck-Sickinger, A., Cox, H., Doods, H. N., Herzog, H., Larhammar, D., Quirion, R., Schwartz, T. & Westfall, T. (1998) XVI. International Union of Pharmacology recommendations for the nomenclature of neuropeptide Y, peptide YY, and pancreatic polypeptide receptors, *Pharmacological reviews.* **50**, 143-50.

174. Fong, T. M., Mao, C., MacNeil, T., Kalyani, R., Smith, T., Weinberg, D., Tota, M. R. & Van der Ploeg, L. H. (1997) ART (protein product of agouti-related transcript) as an antagonist of MC-3 and MC-4 receptors, *Biochemical and biophysical research communications.* **237**, 629-31.

175. Ollmann, M. M., Wilson, B. D., Yang, Y. K., Kerns, J. A., Chen, Y., Gantz, I. & Barsh, G. S. (1997) Antagonism of central melanocortin receptors in vitro and in vivo by agouti-related protein, *Science.* **278**, 135-8.

176. Luquet, S., Perez, F. A., Hnasko, T. S. & Palmiter, R. D. (2005) NPY/AgRP neurons are essential for feeding in adult mice but can be ablated in neonates, *Science.* **310**, 683-5.

177. Qian, S., Chen, H., Weingarth, D., Trumbauer, M. E., Novi, D. E., Guan, X., Yu, H., Shen, Z., Feng, Y., Frazier, E., Chen, A., Camacho, R. E., Shearman, L. P., Gopal-

Truter, S., MacNeil, D. J., Van der Ploeg, L. H. & Marsh, D. J. (2002) Neither agouti-related protein nor neuropeptide Y is critically required for the regulation of energy homeostasis in mice, *Molecular and cellular biology.* **22**, 5027-35.

178. Bannon, A. W., Seda, J., Carmouche, M., Francis, J. M., Norman, M. H., Karbon, B. & McCaleb, M. L. (2000) Behavioral characterization of neuropeptide Y knockout mice, *Brain research.* **868**, 79-87.

179. Legradi, G. & Lechan, R. M. (1999) Agouti-related protein containing nerve terminals innervate thyrotropin-releasing hormone neurons in the hypothalamic paraventricular nucleus, *Endocrinology.* **140**, 3643-52.

180. Fekete, C., Kelly, J., Mihaly, E., Sarkar, S., Rand, W. M., Legradi, G., Emerson, C. H. & Lechan, R. M. (2001) Neuropeptide Y has a central inhibitory action on the hypothalamic-pituitary-thyroid axis, *Endocrinology.* **142**, 2606-13.

181. Fekete, C., Sarkar, S., Rand, W. M., Harney, J. W., Emerson, C. H., Bianco, A. C. & Lechan, R. M. (2002) Agouti-related protein (AGRP) has a central inhibitory action on the hypothalamic-pituitary-thyroid (HPT) axis; comparisons between the effect of AGRP and neuropeptide Y on energy homeostasis and the HPT axis, *Endocrinology.* **143**, 3846-53.

182. Fekete, C., Marks, D. L., Sarkar, S., Emerson, C. H., Rand, W. M., Cone, R. D. & Lechan, R. M. (2004) Effect of Agouti-related protein in regulation of the hypothalamic-pituitary-thyroid axis in the melanocortin 4 receptor knockout mouse, *Endocrinology.* **145**, 4816-21.

183. Fekete, C., Sarkar, S., Rand, W. M., Harney, J. W., Emerson, C. H., Bianco, A. C., Beck-Sickinger, A. & Lechan, R. M. (2002) Neuropeptide Y1 and Y5 receptors mediate the effects of neuropeptide Y on the hypothalamic-pituitary-thyroid axis, *Endocrinology.* **143**, 4513-9.

184. Mihaly, E., Fekete, C., Legradi, G. & Lechan, R. M. (2001) Hypothalamic dorsomedial nucleus neurons innervate thyrotropin-releasing hormone-synthesizing neurons in the paraventricular nucleus, *Brain research.* **891**, 20-31.

185. Bellinger, L. L. & Bernardis, L. L. (2002) The dorsomedial hypothalamic nucleus and its role in ingestive behavior and body weight regulation: lessons learned from lesioning studies, *Physiology & behavior.* **76**, 431-42.

186. Scott, M. M., Lachey, J. L., Sternson, S. M., Lee, C. E., Elias, C. F., Friedman, J. M. & Elmquist, J. K. (2009) Leptin targets in the mouse brain, *The Journal of comparative neurology.* **514**, 518-32.

187. Wilcox, B. J., Corp, E. S., Dorsa, D. M., Figlewicz, D. P., Greenwood, M. R., Woods, S. C. & Baskin, D. G. (1989) Insulin binding in the hypothalamus of lean and genetically obese Zucker rats, *Peptides.* **10**, 1159-64.

188. Zigman, J. M., Jones, J. E., Lee, C. E., Saper, C. B. & Elmquist, J. K. (2006) Expression of ghrelin receptor mRNA in the rat and the mouse brain, *The Journal of comparative neurology.* **494**, 528-48.

189. Broberger, C., Johansen, J., Johansson, C., Schalling, M. & Hokfelt, T. (1998) The neuropeptide Y/agouti gene-related protein (AGRP) brain circuitry in normal, anorectic, and monosodium glutamate-treated mice, *Proceedings of the National Academy of Sciences of the United States of America.* **95**, 15043-8.

190. Singru, P. S., Fekete, C. & Lechan, R. M. (2005) Neuroanatomical evidence for participation of the hypothalamic dorsomedial nucleus (DMN) in regulation of the hypothalamic paraventricular nucleus (PVN) by alpha-melanocyte stimulating hormone, *Brain research.* **1064**, 42-51.

191. Legradi, G., Emerson, C. H., Ahima, R. S., Rand, W. M., Flier, J. S. & Lechan, R. M. (1998) Arcuate nucleus ablation prevents fasting-induced suppression of ProTRH mRNA in the hypothalamic paraventricular nucleus, *Neuroendocrinology.* **68**, 89-97.

192. Chou, T. C., Scammell, T. E., Gooley, J. J., Gaus, S. E., Saper, C. B. & Lu, J. (2003) Critical role of dorsomedial hypothalamic nucleus in a wide range of behavioral circadian rhythms, *The Journal of neuroscience : the official journal of the Society for Neuroscience.* **23**, 10691-702.

193. Gooley, J. J., Schomer, A. & Saper, C. B. (2006) The dorsomedial hypothalamic nucleus is critical for the expression of food-entrainable circadian rhythms, *Nature neuroscience.* **9**, 398-407.

194. Legradi, G., Emerson, C. H., Ahima, R. S., Flier, J. S. & Lechan, R. M. (1997) Leptin prevents fasting-induced suppression of prothyrotropin-releasing hormone messenger ribonucleic acid in neurons of the hypothalamic paraventricular nucleus, *Endocrinology.* **138**, 2569-76.

195. Rondeel, J. M., Heide, R., de Greef, W. J., van Toor, H., van Haasteren, G. A., Klootwijk, W. & Visser, T. J. (1992) Effect of starvation and subsequent refeeding on thyroid function and release of hypothalamic thyrotropin-releasing hormone, *Neuroendocrinology.* **56**, 348-53.

196. van Haasteren, G. A., Linkels, E., Klootwijk, W., van Toor, H., Rondeel, J. M., Themmen, A. P., de Jong, F. H., Valentijn, K., Vaudry, H., Bauer, K. & et al. (1995) Starvation-induced changes in the hypothalamic content of prothyrotrophin-releasing hormone (proTRH) mRNA and the hypothalamic release of proTRH-derived peptides: role of the adrenal gland, *The Journal of endocrinology.* **145**, 143-53.

197. Kolaczynski, J. W., Considine, R. V., Ohannesian, J., Marco, C., Opentanova, I., Nyce, M. R., Myint, M. & Caro, J. F. (1996) Responses of leptin to short-term fasting and refeeding in humans: a link with ketogenesis but not ketones themselves, *Diabetes.* **45**, 1511-5.

198. Perello, M., Stuart, R. C. & Nillni, E. A. (2006) The role of intracerebroventricular administration of leptin in the stimulation of prothyrotropin releasing hormone neurons in the hypothalamic paraventricular nucleus, *Endocrinology.* **147**, 3296-306.

199. Vella, K. R., Ramadoss, P., Lam, F. S., Harris, J. C., Ye, F. D., Same, P. D., O'Neill, N. F., Maratos-Flier, E. & Hollenberg, A. N. (2011) NPY and MC4R signaling regulate thyroid hormone levels during fasting through both central and peripheral pathways, *Cell metabolism.* **14**, 780-90.

200. Singru, P. S., Sanchez, E., Fekete, C. & Lechan, R. M. (2007) Importance of melanocortin signaling in refeeding-induced neuronal activation and satiety, *Endocrinology.* **148**, 638-46.

201. Sanchez, E., Singru, P. S., Acharya, R., Bodria, M., Fekete, C., Zavacki, A. M., Bianco, A. C. & Lechan, R. M. (2008) Differential effects of refeeding on melanocortin-responsive neurons in the hypothalamic paraventricular nucleus, *Endocrinology.* **149**, 4329-35.

202. Pinto, S., Roseberry, A. G., Liu, H., Diano, S., Shanabrough, M., Cai, X., Friedman, J. M. & Horvath, T. L. (2004) Rapid rewiring of arcuate nucleus feeding circuits by leptin, *Science.* **304**, 110-5.

203. Bouret, S. G., Draper, S. J. & Simerly, R. B. (2004) Trophic action of leptin on hypothalamic neurons that regulate feeding, *Science.* **304**, 108-10.

204. Tung, Y. C., Ma, M., Piper, S., Coll, A., O'Rahilly, S. & Yeo, G. S. (2008) Novel leptin-regulated genes revealed by transcriptional profiling of the hypothalamic paraventricular nucleus, *The Journal of neuroscience : the official journal of the Society for Neuroscience.* **28**, 12419-26.

205. Segerson, T. P., Hoefler, H., Childers, H., Wolfe, H. J., Wu, P., Jackson, I. M. & Lechan, R. M. (1987) Localization of thyrotropin-releasing hormone prohormone messenger ribonucleic acid in rat brain in situ hybridization, *Endocrinology.* **121**, 98-107.

206. Morzorati, S. & Kubek, M. J. (1993) Septal TRH in alcohol-naive P and NP rats and following alcohol challenge, *Brain research bulletin.* **31**, 301-4.

207. Ao, Y., Go, V. L., Toy, N., Li, T., Wang, Y., Song, M. K., Reeve, J. R., Jr., Liu, Y. & Yang, H. (2006) Brainstem thyrotropin-releasing hormone regulates food intake through vagal-dependent cholinergic stimulation of ghrelin secretion, *Endocrinology.* **147**, 6004-10.

208. Gutierrez-Mariscal, M., Sanchez, E., Rebolledo-Solleiro, D., Garcia-Vazquez, A. I., Cote-Velez, A., Acasuso-Rivero, C., Charli, J. L. & Joseph-Bravo, P. (2012) The acute response of the amygdalar TRH system to psychogenic stressors varies dependent on the paradigm and circadian condition, *Brain research.* **1452**, 73-84.

209. Shibusawa, N., Hashimoto, K. & Yamada, M. (2008) Thyrotropin-releasing hormone (TRH) in the cerebellum, *Cerebellum.* **7**, 84-95.

210. de Gortari, P., Mendez, M., Rodriguez-Keller, I., Perez-Martinez, L. & Joseph-Bravob, P. (2000) Acute ethanol administration induces changes in TRH and proenkephalin expression in hypothalamic and limbic regions of rat brain, *Neurochemistry international.* **37**, 483-96.

211. Merchenthaler, I., Csernus, V., Csontos, C., Petrusz, P. & Mess, B. (1988) New data on the immunocytochemical localization of thyrotropin-releasing hormone in the rat central nervous system, *The American journal of anatomy.* **181**, 359-76.

212. Wittmann, G., Fuzesi, T., Singru, P. S., Liposits, Z., Lechan, R. M. & Fekete, C. (2009) Efferent projections of thyrotropin-releasing hormone-synthesizing neurons residing in the anterior parvocellular subdivision of the hypothalamic paraventricular nucleus, *The Journal of comparative neurology.* **515**, 313-30.

213. Wittmann, G., Fuzesi, T., Liposits, Z., Lechan, R. M. & Fekete, C. (2009) Distribution and axonal projections of neurons coexpressing thyrotropin-releasing

hormone and urocortin 3 in the rat brain, *The Journal of comparative neurology.* **517**, 825-40.

214. Sharma, R. P., Martis, B., Rosen, C., Jonalagadda, J., Nemeroff, C. B. & Bissette, G. (2001) CSF thyrotropin-releasing hormone concentrations differ in patients with schizoaffective disorder from patients with schizophrenia or mood disorders, *Journal of psychiatric research.* **35**, 287-91.

215. Steward, C. A., Horan, T. L., Schuhler, S., Bennett, G. W. & Ebling, F. J. (2003) Central administration of thyrotropin releasing hormone (TRH) and related peptides inhibits feeding behavior in the Siberian hamster, *Neuroreport.* **14**, 687-91.

216. Scott, J. E. & Willett, I. H. (1966) Binding of cationic dyes to nucleic acids and ther biological polyanions, *Nature.* **209**, 985-7.

217. F, N. (1984) Ueber eine neue Untersuchungsmethode des Centralorgans zur Feststellung der Localisation der Nervenzellen, *Neurologisches Centralblatt*, 507-8.

218. Knowles, R. B., Sabry, J. H., Martone, M. E., Deerinck, T. J., Ellisman, M. H., Bassell, G. J. & Kosik, K. S. (1996) Translocation of RNA granules in living neurons, *The Journal of neuroscience : the official journal of the Society for Neuroscience.* **16**, 7812-20.

219. Kosik, K. S. & Krichevsky, A. M. (2002) The message and the messenger: delivering RNA in neurons, *Science's STKE : signal transduction knowledge environment.* **2002**, pe16.

220. Fekete, C., Wittmann, G., Liposits, Z. & Lechan, R. M. (2004) Origin of cocaine-and amphetamine-regulated transcript (CART)-immunoreactive innervation of the hypothalamic paraventricular nucleus, *The Journal of comparative neurology.* **469**, 340-50.

221. Krout, K. E., Belzer, R. E. & Loewy, A. D. (2002) Brainstem projections to midline and intralaminar thalamic nuclei of the rat, *The Journal of comparative neurology.* **448**, 53-101.

222. Lefler, Y., Arzi, A., Reiner, K., Sukhotinsky, I. & Devor, M. (2008) Bulbospinal neurons of the rat rostromedial medulla are highly collateralized, *The Journal of comparative neurology.* **506**, 960-78.

223. Paxinos G, F. K. (2001) The Mouse Brain in Stereotaxic Coordinates, *Academic Press, San Diego, CA, USA.*

224. Liposits, Z., Setalo, G. & Flerko, B. (1984) Application of the silver-gold intensified 3,3'-diaminobenzidine chromogen to the light and electron microscopic detection of the luteinizing hormone-releasing hormone system of the rat brain, *Neuroscience.* **13**, 513-25.

225. Thim, L., Nielsen, P. F., Judge, M. E., Andersen, A. S., Diers, I., Egel-Mitani, M. & Hastrup, S. (1998) Purification and characterisation of a new hypothalamic satiety peptide, cocaine and amphetamine regulated transcript (CART), produced in yeast, *FEBS letters.* **428**, 263-8.

226. Ben-Barak, Y., Russell, J. T., Whitnall, M. H., Ozato, K. & Gainer, H. (1985) Neurophysin in the hypothalamo-neurohypophysial system. I. Production and characterization of monoclonal antibodies, *The Journal of neuroscience : the official journal of the Society for Neuroscience.* **5**, 81-97.

227. Kallo, I., Mohacsik, P., Vida, B., Zeold, A., Bardoczi, Z., Zavacki, A. M., Farkas, E., Kadar, A., Hrabovszky, E., Arrojo, E. D. R., Dong, L., Barna, L., Palkovits, M., Borsay, B. A., Herczeg, L., Lechan, R. M., Bianco, A. C., Liposits, Z., Fekete, C. & Gereben, B. (2012) A novel pathway regulates thyroid hormone availability in rat and human hypothalamic neurosecretory neurons, *PloS one.* **7**, e37860.

228. Mihaly, E., Fekete, C., Tatro, J. B., Liposits, Z., Stopa, E. G. & Lechan, R. M. (2000) Hypophysiotropic thyrotropin-releasing hormone-synthesizing neurons in the human hypothalamus are innervated by neuropeptide Y, agouti-related protein, and alpha-melanocyte-stimulating hormone, *The Journal of clinical endocrinology and metabolism.* **85**, 2596-603.

229. Paxinos G, W. C. (1998) The Rat Brain in Stereotaxical Coordinates, *Academic Press, San Diego, CA, USA.*

230. Biag, J., Huang, Y., Gou, L., Hintiryan, H., Askarinam, A., Hahn, J. D., Toga, A. W. & Dong, H. W. (2012) Cyto- and chemoarchitecture of the hypothalamic paraventricular nucleus in the C57BL/6J male mouse: a study of immunostaining and multiple fluorescent tract tracing, *The Journal of comparative neurology.* **520**, 6-33.

231. Kawano, H., Tsuruo, Y., Bando, H. & Daikoku, S. (1991) Hypophysiotrophic TRH-producing neurons identified by combining immunohistochemistry for pro-TRH and retrograde tracing, *The Journal of comparative neurology.* **307**, 531-8.

232. Broberger, C. (1999) Hypothalamic cocaine- and amphetamine-regulated transcript (CART) neurons: histochemical relationship to thyrotropin-releasing hormone, melanin-concentrating hormone, orexin/hypocretin and neuropeptide Y, *Brain research.* **848**, 101-13.

233. Kadar, A., Sanchez, E., Wittmann, G., Singru, P. S., Fuzesi, T., Marsili, A., Larsen, P. R., Liposits, Z., Lechan, R. M. & Fekete, C. (2010) Distribution of hypophysiotropic thyrotropin-releasing hormone (TRH)-synthesizing neurons in the hypothalamic paraventricular nucleus of the mouse, *The Journal of comparative neurology.* **518**, 3948-61.

234. Lechan, R. M. & Kakucska, I. (1992) Feedback regulation of thyrotropin-releasing hormone gene expression by thyroid hormone in the hypothalamic paraventricular nucleus, *Ciba Foundation symposium.* **168**, 144-58; discussion 158-64.

235. Hibbert, A. P., Kramer, B. M., Miller, F. D. & Kaplan, D. R. (2006) The localization, trafficking and retrograde transport of BDNF bound to p75NTR in sympathetic neurons, *Molecular and cellular neurosciences.* **32**, 387-402.

236. Jezierski, M. K. & Sohrabji, F. (2003) Estrogen enhances retrograde transport of brain-derived neurotrophic factor in the rodent forebrain, *Endocrinology.* **144**, 5022-9.

237. Magby, J. P., Bi, C., Chen, Z. Y., Lee, F. S. & Plummer, M. R. (2006) Single-cell characterization of retrograde signaling by brain-derived neurotrophic factor, *The Journal of neuroscience : the official journal of the Society for Neuroscience.* **26**, 13531-6.

238. Varela, L., Martinez-Sanchez, N., Gallego, R., Vazquez, M. J., Roa, J., Gandara, M., Schoenmakers, E., Nogueiras, R., Chatterjee, K., Tena-Sempere, M., Dieguez, C. & Lopez, M. (2012) Hypothalamic mTOR pathway mediates thyroid hormone-induced hyperphagia in hyperthyroidism, *The Journal of pathology.* **227**, 209-22.

239. Raivich, G. (2011) Transcribing the path to neurological recovery-From early signals through transcription factors to downstream effectors of successful regeneration, *Annals of anatomy = Anatomischer Anzeiger : official organ of the Anatomische Gesellschaft.* **193**, 248-58.

240. Hernandez, D., Torres, C. A., Setlik, W., Cebrian, C., Mosharov, E. V., Tang, G., Cheng, H. C., Kholodilov, N., Yarygina, O., Burke, R. E., Gershon, M. & Sulzer, D. (2012) Regulation of presynaptic neurotransmission by macroautophagy, *Neuron.* **74**, 277-84.

241. Hill, J. W., Williams, K. W., Ye, C., Luo, J., Balthasar, N., Coppari, R., Cowley, M. A., Cantley, L. C., Lowell, B. B. & Elmquist, J. K. (2008) Acute effects of leptin require PI3K signaling in hypothalamic proopiomelanocortin neurons in mice, *The Journal of clinical investigation.* **118**, 1796-805.

242. Morrison, C. D., Morton, G. J., Niswender, K. D., Gelling, R. W. & Schwartz, M. W. (2005) Leptin inhibits hypothalamic Npy and Agrp gene expression via a mechanism that requires phosphatidylinositol 3-OH-kinase signaling, *American journal of physiology Endocrinology and metabolism.* **289**, E1051-7.

243. Kiss, J., Halasz, B., Csaki, A., Liposits, Z. & Hrabovszky, E. (2007) Vesicular glutamate transporter 2 protein and mRNA containing neurons in the hypothalamic suprachiasmatic nucleus of the rat, *Brain research bulletin.* **74**, 397-405.

244. Wang, H., Owens, J. D., Shih, J. H., Li, M. C., Bonner, R. F. & Mushinski, J. F. (2006) Histological staining methods preparatory to laser capture microdissection significantly affect the integrity of the cellular RNA, *BMC genomics.* **7**, 97.

245. Quinn, B., Toga, A. W., Motamed, S. & Merlic, C. A. (1995) Fluoro nissl green: a novel fluorescent counterstain for neuroanatomy, *Neuroscience letters.* **184**, 169-72.

246. Herrera, D. G. & Robertson, H. A. (1996) Activation of c-fos in the brain, *Progress in neurobiology.* **50**, 83-107.

DOI:10.14753/SE.2014.1934

XII. List of publications

1. List of publications underlying the thesis

1. Kádár, A., Wittmann, G., Liposits, Z., Fekete, C. (2009) Improved method for combination of immunocytochemistry and Nissl-staining, *Journal of comparative neuroscience methods*. 184: (1) pp. 115-118.

2. Kádár, A., Sanchez, E., Wittmann, G., Singru, P., Füzesi, T., Marsili, A., Larsen, R., Liposits, Z., Lechan, R., Fekete, C. (2010) Distribution of hypophysiotropic thyrotropin-releasing hormone (TRH)-synthesizing neurons in the hypothalamic paraventricular nucleus of the mouse, *Journal of comparative neurology.* 518: pp 3948-3961

3. Kalló, I., Mohácsik, P.,Vida, B., Zeöld, A., Bardóczi, Z., Zavacki, AM., Farkas, E., Kádár, A., Hrabovszky, E., Arrojo e Drigo, R., Dong, L., Barna, L., Palkovits, M., Borsay, B.A., Herczeg, L., Bianco, A.C., Liposits, Z., Fekete, C., Gereben, B. (2012) A novel pathway regulates thyroid hormone availability in rat and human hypothalamic neurosecretory neurons, *PLoS One* 7: (6) Paper e37860. 16 p.

2. List of publications related to the subject of the thesis

1. Fekete, C., Freitas, B.C., Zeöld, A., Wittmann, G., Kádár, A., Liposits, Z., Christoffolete, M.A., Singru, P., Lechan, R.M., Bianco, A.C., Gereben, B. (2007) Expression patterns of WSB-1 and USP-33 underlie cell-specific post-translational control type 2 deiodinase in rat brain, *Endocrinology* 148: pp. 4865-4874

2. Fekete, C., Zséli, G., Singru, P., Kádár, A., Wittmann, G., Füzesi, T., El-Bermani, W., Lechan, R. (2012) Activation of anorexigenic POMC neurons during refeeding is independent of vagal and brainstem inputs, *Journal of neuroendocrinology* 24: (11) pp. 1423-1431

3. Sárvári, A., Farkas, E., Kádár, A., Zséli, G., Füzesi, T., Lechan, R., Fekete, C. (2012) Thyrotropin-releasing hormone-containing axons innervate histaminergic neurons in the tuberomammillary nucleus, *Brain research* 1488: pp. 72-80

DOI:10.14753/SE.2014.1934

XIII. Acknowledgements

I express my deep gratitude to Dr. Csaba Fekete, my tutor. He devoted so much time and attention to teach me for scientific research since years I was an undergraduate student at university. I thank him that he has fully promoted my professional development.

I am very grateful to Professor Zsolt Liposits, Head of the Division of Endocrine Neurobiology, who has provided me absolute support to progress in scientific research.

My sincere thanks to Professor Ronald M. Lechan at Tufts University in Boston, for his collaborative efforts.

I wish to express my thanks to my colleagues with whom I worked together when I was an undergraduate student: Gábor Wittmann and Tamás Füzesi. They helped me a lot in every aspects of the laboratory work.

I am very thankful to the technicians who helped me a lot with their careful and precise work: Ágnes Simon and Veronika Maruzs.

Special thanks for the members of the Laboratory Integrative Neuroendocrinology: Zsuzsa Beliczai, Erzsébet Farkas, Enikő Kiss, Anett Szilvási-Szabó, Dr. Barbara Vida and Györgyi Zséli. Thank you for the successful cooperation and joyful time spent together.

I would like to thank all the members of the Laboratory of Molecular Cell Metabolism for technical supports, and for their great companionship: Péter Egri, Dr. Balázs Gereben, Andrea Juhász, Zsuzsanna Kvárta-Papp, Petra Mohácsik and Dr. Anikó Zeöld.

I am very thankful to all the members of the Laboratory of Endocrine Neurobiology for many advice and technical help and their kindliness: Balázs Barkóczi, Zsuzsanna Bardóczi, Norbertné Bekó, Dr. Imre Farkas, Dr. Erik Hrabovszky, Dr. Imre Kalló, Barna László, Csilla Molnár, Dr. Miklós Sárvári, Márta Turek, Dr. Csaba Vastagh.

I would also like to express my thanks to the members of the Medical Gene Technological Unit, especially to Dr. Ferenc Erdélyi, Head of the Unit, and to Mária Szőcs and Rozália Szafner for having always been helpful when I worked in the animal facility.